STRUCTURE-FUNCTION STUDIES OF THE CO_2 UPTAKE COMPLEX IN CYANOBACTERIA

By
JULIANA ARTIER
Bachelor of Science in Biological Science
Universidade Federal de São Carlos
São Carlos, SP, Brazil
2007

Master of Science in Genetics and Evolution
Universidade Federal de São Carlos
São Carlos, SP, Brazil
2010

Submitted to the Faculty of the
Graduate College of the
Oklahoma State University
in partial fulfillment of
the requirements for
the Degree of
DOCTOR OF PHILOSOPHY
July, 2018

STRUCTURE-FUNCTION STUDIES OF

THE CO_2 UPTAKE COMPLEX

IN CYANOBACTERIA

Dissertation Approved:

Robert L. Burnap

Dissertation Adviser

Rolf A. Prade

Marianna A. Patrauchan

Wouter D. Hoff

William J. Henley

ACKNOWLEDGEMENTS

I want to thank my advisor and mentor Robert Burnap for all the support, in the past, present, and future. I also greatly appreciate the time and efforts my committee members kindly devoted towards my academic development. I am grateful to Dean G. Price for detailed help with the C_i affinity assays and collaboration in this study. Thanks to Anthony D. Kappell and Steven Holland for contribution in the molecular design of the CCM knockout constructs. Also, I am extremely thankful to all involved in this project: Steven Holland for assistance constructing the CCM knockout mutants and with PAM analysis, Minquan Zhang for collaboration on protein expression experiments, Neil T. Miller for help with Western blots, and Prachi Zawar for collaboration in constructing the *Arthrospira* heterologous expression systems. Also, I appreciate the kind gifts of vectors: the integration vectors provided by H. Wang and Wim Vermaas; MBP containing vectors from Junpeng Deng. I want to thank the assistance of Janet Rogers and Steven Hartson for DNA sequencing and mass spectrometry analyses within the DNA/Protein Resource Facility at Oklahoma State University, supported by the NSF MRI and EPSCoR programs (award #0722494). This dissertation was only possible due to financial support by the U.S. Department of Energy (DOE), Office of Science, Basic Energy Sciences, grant no. DE-

Acknowledgements reflect the views of the author and are not endorsed by committee members or Oklahoma State University.

FG02-08ER15968. During all the years of my PhD studies, my family and friends were essential, although not directly involved in the project, but in my daily life, sharing the good and the bad. I am extremely grateful to all the emotional support and loving moments. At the Burnap lab I had the pleasure to share a great, professional and fun environment by the side of Han Bao, Steven Holland, Preston Dilbeck, Aparna Nagarajan, Neil Miller and Anton Avramov, making the daily work so much more enjoyable, and I am so grateful. Also, I am thankful to the friends I made along the way, Abhaya Ranganathan, Amanda Behar, Ruth Weidman, Rachana Rathod, Sharmily Khanam, Prachi Zawar, Shaikh Saad. I am grateful for the family environment and amazing moments shared with the Brazilian community in Stillwater, including Hevila Brognaro, Mariane Zubieta, Zeyna Abramson, with a special thanks to Beatriz Solera and family for opening their hearts and home. I am also grateful to Bruno Sauce, for pushing me towards better worlds. Special thanks to my loving and kind husband Raid Alzaher, who I met at OSU, for all the support, patience and for never letting me give up. I am grateful to my family, my brother Alexandre, aunts, uncles, grandparents, for the emotional support and understanding. I dedicate this dissertation to my parents, Marli and Irineu, who always stand by my side, even when an ocean away.

Name: JULIANA ARTIER

Date of Degree: JULY, 2018

Title of Study: STRUCTURE-FUNCTION STUDIES OF TH CO_2 UPTAKE COMPLEX IN CYANOBACTERIA

Major Field: MICROBIOLOGY & MOLECULAR BIOLOGY

Abstract: Increase of CO_2 atmospheric level has led to an intense search for solutions to mitigate the problem. A natural pathway exists in photosynthesis where CO_2 is fixed into biomass. Cyanobacteria, which constitute a large phylum of natural oxygenic photosynthetic bacteria, have a huge potential for bioengineering. This includes candidates for use in diverse CO_2 capture and storage projects and the potential to redirect its energy for the production of valuable compounds. Our aim in this project is to understand the structure-function of Cup (CO_2 uptake) proteins in the NDH-$1_{3,4}$ complex, part of the cyanobacterial CO_2 concentrating mechanism (CCM). Cyanobacteria have five CCM systems responsible for increasing inorganic carbon (C_i) concentration inside of the cell, an effort to raise CO_2 level close to Rubisco, the main enzyme responsible for carbon fixation. Among them, two CO_2 uptake systems are specialized NDH-1 complexes, NDH-1_3 (NdhF3/NdhD3/CupA/CupS) and NDH-1_4 (NdhF4/NdhD4/CupB), which have very little known about their mechanism. CO_2 is usually regulated in living organisms by carbonic anhydrases (CAs), enzymes that catalyzes the interconversion of CO_2 and HCO_3^-. The hypothesis is that Cup, in the NDH-$1_{3,4}$ complex, is involved in this (non)reversible reaction, possibly coupled with release of a proton across the membrane. We constructed a double knockout mutant, where no NDH-$1_{3,4}$ is produced by the bacteria, and introduced the whole *cupA* operon under Rubisco promoter control in *Synechocystis* 6803. Physiological analysis of C_i depleted mutants with chlorophyll fluorescence traces and O_2 evolution dependent on C_i, show a high C_i requirement feature on the double knockout mutants. However, the strain expressing constitutively NDH-1_3 lost its high CO_2-requiring phenotype, displaying restored cell CO_2 uptake. In parallel, we also analyzed *Synechococcus* 7942 mutants with no functional CO_2 uptake systems, later complemented with only *chpX* (*cupB*). These systems were used in studies directed to analyze the effect of point mutations replacing amino acids (His/Cys) of CupA/CupB proteins to evaluate their potential role on CO_2 uptake in cyanobacteria.

TABLE OF CONTENTS

Chapter Page

1 CHAPTER I 1

INTRODUCTION AND LITERATURE REVIEW 1

1.1 INTRODUCTION 1

1.2 CYANOBACTERIA, PHOTOSYNTHESIS AND CO_2 ADAPTATION 5

1.3 PHOTOSYNTHESIS AND THE PHOTOSYNTHETIC ELECTRON TRANSPORT CHAIN 7

1.4 CARBON FIXATION IN CYANOBACTERIA 15

1.5 CO_2 CONCENTRATING MECHANISMS IN CYANOBACTERIA 16

1.5.1 Carboxysome 19

1.5.2 Bicarbonate transporters: BCT1, BicA and SbtA 21

1.6 NDH-1 COMPLEX AND CUP PROTEINS 23

1.7 CARBONIC ANHYDRASES, STRUCTURE-FUNCTION OVERVIEW AND IMPORTANCE IN CYANOBACTERIA 29

1.8 QUESTIONS AND GOALS 33

2 CHAPTER II 35

EXPERIMENTAL PROCEDURES 35

2.1 MATERIALS AND METHODS 35

2.2 CULTURE AND GROWTH CONDITIONS 35

2.3 STRAINS AND MOLECULAR CONSTRUCTS 37

2.4 CELL SAMPLE PREPARATION 40

2.5 C_I AFFINITY AND OXYGEN EVOLUTION ASSAYS. 41

2.6 CHL AND NADPH FLUORESCENCE AND P700 SPECTROSCOPY 42

2.6.1 Chl and NADPH fluorescence 42

2.6.2 P700 spectroscopy *43*
2.7 SDS-PAGE AND IMMUNOBLOT ANALYSIS 44

3 CHAPTER III 47
HETEROLOGOUS EXPRESSION OF CUPA 47
3.1 INTRODUCTION 47
3.2 MATERIAL AND METHODS 48
3.2.1 Molecular Construction *48*
3.2.2 Expression of CupA protein in E. coli *49*
3.2.3 Protein purification, ... *50*
3.2.4 Antibody production *52*
3.2.5 CD spectroscopy *52*
3.2.6 Zn binding evaluation and CA activity *52*
3.3 RESULTS 53
3.3.1 Genetic systems for heterologous expression of CO_2-uptake protein CupA in E. coli. *53*
3.3.2 Analysis and immunodetection of CupA *57*
3.3.3 Investigation of protein structure-function *57*
3.4 DISCUSSION 59

4 CHAPTER IV 61
SYNTHETIC DNA SYSTEM FOR STRUCTURE-FUNCTION STUDIES OF THE HIGH AFFINITY CO_2 UPTAKE NDH-1_3 PROTEIN COMPLEX IN CYANOBACTERIA ‡ 61
4.1 INTRODUCTION 61
4.2 MATERIALS AND METHODS 66
4.2.1 Constructions of mutants *66*
4.3 RESULTS 68

4.3.1 Genetic systems for studying NDH-1 associated CO_2-uptake proteins in Synechocystis 6803 ..... *68*

4.3.2 Immunodetection of CupA shows deletion and constitutive expression phenotypes of the C2 and C2A strains *72*

4.3.3 Constitutive expression of NDH-1_3 restores ability of double mutant to grow under LC *74*

4.3.4 Restoration of high affinity inorganic carbon uptake in C2A *75*

4.3.5 The carbonic anhydrase inhibitor EZ abolishes NDH-1_3-dependent C_i uptake *80*

4.3.6 Chlorophyll fluorescence as a function of C_i availability and ethoxyzolamide inhibition. *82*

4.3.7 Interactions between C_i metabolism and electron transport in the dark *85*

4.3.8 LEF and CEF are affected by NDH-1_3 presence in HC grown cells *88*

4.4 DISCUSSION 91

4.5 CONCLUSIONS 96

5 CHAPTER V 97

MUTATIONS ON CONSERVED HISTIDINE AND CYSTEINE OF CUP PROTEINS AFFECT CELL UPTAKE OF CO_2[‡] 97

5.1 INTRODUCTION 97

5.2 MATERIALS AND METHODS 102

5.2.1 Multiple sequence alignments and phylogenetic analysis *102*

5.2.2 Cyanobacterial strains and constructions of mutants *103*

5.2.3 Isolation of thylakoid membranes *105*

5.2.4 Analysis of proteins from thylakoid membrane using PAGE *107*

5.3 RESULTS 107

5.3.1 Multiple sequence alignments show conserved amino acids that are Cup potential active site residues *107*

5.3.2 Phylogenetic studies suggest separation of Cup proteins in two clades *109*

5.3.3 Point mutations on Chp/Cup proteins affect cell CO_2 uptake 110

5.3.4 CupA constitutively expressed is bound to NDH-1_3 in C2A strains 119

5.3.5 Functional heterologous expression of an Arthrospira sp. NDH-1_3 in Synechocystis 6803. 122

5.4 DISCUSSION 123

5.5 CONCLUSION 127

6 CHAPTER VI 128

CONCLUSION 128

REFERENCES 133

APPENDICES 151

LIST OF TABLES

Table Page

Table 1: Photosynthetic O_2 evolution of HC cells in response to C_i uptake.....76

Table 2. Mutations of conserved sites in CupA (ChpY) and ChpX (CupB) used in this work, identified by multiple sequence alignment.. 111

Table 3. Photosynthetic O_2 evolution of HC cells of *Synechococcus* 7942 ChpX mutants in response to C_i uptake. 114

Table 4: Photosynthetic O_2 evolution of HC cells with point mutation in Cysteine of NDH-1_3/CupA in response to C_i uptake.....116

Table 5: Photosynthetic O_2 evolution of HC cells with point mutation in Cysteine of NDH-1_3/CupA in response to C_i uptake.....118

LIST OF FIGURES

Figures Page

Figure 1. Model of cyanobacterial photosynthetic electron transport (PSET). 13

Figure 2. Representation of Type-1 NADH dehydrogenase complexes (NDH-1) of cyanobacteria present on the thylakoid membrane, showing multiple proteins involved in the complex. 25

Figure 3. CO_2 uptake systems are specialized Type-1 NADH dehydrogenase complexes (NDH-1) present on the thylakoid membrane of cyanobacteria. 26

Figure 4. Model of the strategy used to clone *Synechocystis* 6803 CupA into *E. coli*.54

Figure 5. Heterologous expression of CupA, purification and antibody production 56

Figure 6. CD spectra of fusion protein MBP-CupA. 58

Figure 7. Schematic drawing of cyanobacterial CCM (β-type) showing the five known C_i transporters and the carboxysome (CB), which houses the carbonic anhydrase (CA) on the shell and Rubisco inside as is found in *Synechocystis* sp. PCC6803. 63

Figure 8. Construction of a genetic system to examine structure-function relationships of the CO_2 uptake dehydrogenases in cyanobacteria.....70

Figure 9. Schematic design of the construction of a genetic system to examine structure-function relationships of the CO_2 uptake dehydrogenases in cyanobacteria and segregation of mutants.....71

Figure 10. Immunodetection of CupA and SbtA in WT, C2 and C2A at different C_i availability.....73

Figure 11. Spot assays for autotrophic growth under different pH and CO_2 availability conditions on agar plates.....75

Figure 12. Assays for C_i affinity measuring photosynthetic O_2 evolution rates in *Synechocystis* 6803 strains with different CO_2 uptake system under low sodium.....78

Figure 13. Assays for C_i affinity measuring photosynthetic O_2 evolution rates in *Synechocystis* 6803 strains with different CO_2 uptake systems. 79

Figure 14. The carbonic anhydrase inhibitor ethoxyzolamide (EZ) inhibits CO_2 uptake by NHD-1_3 complexes. 81

Figure 15. Chl fluorescence of cells as a function of C_i. 83

Figure 16. Chl fluorescence of HC grown cells. 85

Figure 17. Effects of bicarbonate re-addition on the post-illumination Chl (Panels A-C) and NADPH (Panels D-F) fluorescence transients in C_i depleted cells. 87

Figure 18. Photosystem I oxidation kinetics in dark-adapted cells exposed to saturating illumination. 90

Figure 19. Hypothetical model of cyanobacterial CO_2 uptake by NDH-$1_{3,4}$. 101

Figure 20. Cyanobacterial CO_2 uptake proteins multiple sequence alignment 109

Figure 21. Unrooted maximum likelihood phylogenetic tree. 110

Figure 22. Spot assays for autotrophic growth under pH7 with different CO_2 availability conditions on agar plates 113

Figure 23. Assays for C_i affinity measuring photosynthetic O_2 evolution rates in *Synechococcus* 7942 strains with different CO_2 uptake system under low sodium. 115

Figure 24. Assays for C_i affinity measuring photosynthetic O_2 evolution rates in *Synechocystis* 6803 strains with point mutation in CupA CO_2 uptake protein under low sodium 117

Figure 25. Assays for C_i affinity measuring photosynthetic O_2 evolution rates in *Synechocystis* 6803 strains with point mutation in CupA CO_2 uptake protein under low sodium 119

Figure 26. Immunodetection of CupA and SbtA in WT and C2A at different C_i availability. 121

Figure 27. Assays for C_i affinity measuring photosynthetic O_2 evolution rates in *Synechocystis* 6803 strains with an *Arthrospira* sp. (India) *cupA* operon. 123

KEY ABBREVIATIONS

ATP = Adenosine Triphosphate

B_6f = Cytochrome B_6f complex

CA = Carbonic Anhydrase

CB = Carboxysome

CBB = Calvin-Basham-Benson

CCM = Carbon Concentration Mechanism

CEF or CET = Cyclic Electron flow/transport

C_i = Inorganic Carbon (HCO_3^- and CO_2)

Chl = Chlorophyll

Chp = CO_2 hydration protein

CO_2 = Carbon Dioxide

Cup = CO_2 uptake

Cys/C = Cysteine (amino acid)

DCMU = 3-(3,4-dichlorophenyl)-1,1dimethylurea

EZ = Ethoxyzolamide

HCO_3^- = Bicarbonate

His/H = Histidine (amino acid)

IPTG = Isopropyl-β-D-thiogalactopyranoside

αKG = Alpha Ketoglutarate

LEF or LET = Linear Electron flow/transport

MBP = maltose binding protein (*malE* = gene coding MBP)

NADPH = Nicotinamide adenine dinucleotide phosphate

NDH-1= NAD(P)H dehydrogenases type-1/Type-I NDH dehydrogenases

$NDH\text{-}1_{1\text{-}4}$ = Forms of NDH-1 complexes, $NDH\text{-}1_3$ and $NDH\text{-}1_4$ catalyze CO_2 hydration

O_2	=	Oxygen
2OG	=	2-oxoglutarate
PAM	=	Pulse-Amplitude-Modulation
PC	=	Plastocyanin
2PG	=	2-Phosphoglycolate
3PGA	=	3-Phosphoglyceric acid
pmf	=	proton motive force
PQ	=	plastoquinone/ oxidized plastoquinone
PQH_2	=	plastoquinol/ reduced plastoquinone
PS	=	Photosystem
PSET	=	Photosynthetic electron transfer
Redox	=	oxidation/reduction reactions
Rubisco	=	Ribulose 1,5-Bisphosphate Carboxylase/Oxygenase
RuBP	=	Ribulose 1,5-Bisphosphate
TCA	=	Tricarboxylic Acid or Krebs cycle

1 CHAPTER I

INTRODUCTION AND LITERATURE REVIEW

1.1 Introduction

Planet Earth is unique since it has the proper conditions that allow life to exist. One of these factors is related to the appropriate concentrations of the gaseous components of the atmosphere. The metabolic activities of living organisms, which mediate the major biogeochemical cycles, is a main factor, and sometimes the dominant factor in this balance. In this regard, oxygenic photosynthetic organisms play an essential role by balancing the global levels of carbon dioxide (CO_2) and oxygen (O_2). By the process of photosynthesis, an organism can produce biomass by absorbing and fixing inorganic substrates (e.g., water, CO_2, HCO_3^-, NO_3, SO_4,) using the energy of sunlight. This way, fixed CO_2 in the form of reduced (hydrogen-containing) carbon compounds and stored as biomass in a variety of photosynthetic organisms is a significant source of food for diverse non-photosynthetic organisms and is responsible for the existence of fossil fuel.

Understanding the mechanisms that control the light-harvesting, energy transduction, and storage into biomass has been the center of photosynthesis research for many years. Among these topics, it is essential to understand the uptake of CO_2 by photosynthetic cells and tissues. Although this gas can diffuse inside of the cell, the rate of diffusion is often not high enough to keep pace with rate of photosynthesis and keeping the appropriate internal concentrations is typically a challenge for photosynthetic organisms. This can be especially problematic for aquatic photosynthetic organisms, such as cyanobacteria. In these cases, the ambient level of CO_2 may not be sufficient to maintain an adequate internal cellular CO_2 concentration necessary for efficient carbon fixation. There are a number of reasons for this, including the fact that the diffusion rate of CO_2 is 10^4-fold slower in water compared to air. This situation is exacerbated by the low affinity of ribulose bisphosphate carboxylase/oxygenase (Rubisco) for CO_2, which is the main enzyme utilized for photosynthetic CO_2 fixation (Badger, 1980). To make the situation physiologically more challenging, Rubisco has a competing and wasteful oxygenase reaction that occurs when O_2 instead of CO_2 reacts at the active site (see review by (Hanson, 2016). Since this is a competitive reaction, high concentrations of CO_2 and low concentrations of O_2 minimize the wasteful oxygenase reaction in favor of the carboxylase reaction. Accordingly, mechanisms to actively acquire and efficiently utilize inorganic carbon (*e.g.*, dissolved CO_2; bicarbonate, HCO_3^-) from the environment have evolved in aquatic photosynthetic organisms. Generally, these are known as the CO_2-concentrating mechanisms (CCM) because they function to increase the local concentration of CO_2 in the vicinity of Rubisco

(see review by (Price, 2011). Moreover, cyanobacteria and eukaryotic algae seems to have independently evolved, what are increasingly appearing to be somewhat similar, CCMs, as discussed later in the chapter. Cyanobacteria have five systems for the acquisition of inorganic carbon (C_i) that serve as components of CCM: three bicarbonate transporter systems and two CO_2 uptake systems, which collectively function to maintain a high internal cellular HCO_3^- pool. Importantly, the cyanobacterial CCM also requires a specialized microcompartment (carboxysome, CB), which houses all of the Rubisco in the cell plus a carbonic anhydrase (CA). The carboxysome acts as the sink for the HCO_3^- that accumulates in the cytoplasm, a result of the activity of the five uptake systems. Once inside the carboxysome, the carbonic anhydrase converts the HCO_3^- to CO_2 and thereby is capable of saturating the active sites of the surrounding Rubisco (see review by (Rae *et al.*, 2013; Yeates *et al.*, 2008).

Most of the research on the C_i uptake part of the CCM has been focused on the bicarbonate uptake transporters, with fewer studies on CO_2 uptake systems. Previous studies on the CO_2 uptake systems have mostly involved investigating overall function by characterizing the physiological characteristics of CO_2 uptake using inhibitors and by examining mutants that involve the inactivation of entire genes encoding the protein involved in this uptake (reviewed by (Kaplan, 2017; Price *et al.*, 2008). Previous mutant studies have been especially informative, since they indicate the existence and operation of forms of Type-I NDH dehydrogenases (NDH-1) that are entirely unique to the cyanobacteria (reviewed by (Battchikova *et al.*, 2011a). On the other hand, little has been done to understand the

catalytic mechanism of the energized CO_2 uptake and this is the subject of my dissertation. What is the molecular mechanism of CO_2 uptake in cyanobacteria? Is one of the proteins components of the putative Type-I NDH dehydrogenases system a specialized carbonic anhydrase? To what extent do early hypotheses proposing the formation of an alkaline pocket by the proteic environment that drives the CO_2 hydration reaction far-from-equilibrium (Kaplan and Reinhold, 1999) are true or is it more likely that an alternative hypothesis invoking the redox action of a quinone associated with the putative Type-I NDH dehydrogenases is in operation (Price *et al.*, 2002). Is this process related to or dependent on electron transport such as cyclic electron flow? Given that this process is unique and well conserved in cyanobacteria, could it be interchangeable among the species? While I do not intend to answer all of these questions in this dissertation, I do hope to convince the reader that I have developed a genetic system that has the potential to address these questions, and also to provide evidence in support of a specific model that is somewhat, but not entirely different from the experimentally untested models proposed nearly 25 years ago (Price *et al.*, 2002).

Why study this problem? Cyanobacteria have been intensely targeted as subject of photosynthetic studies. It attracts great attention due to its huge potential for bioengineering. Applications include possible use in diverse CO_2 capture and storage as well as the potential to redirect photosynthetic energy for the production of valuable compounds. Hence, a complete knowledge of the structure and function of the protein modules and the mechanism used by these CO_2 uptake systems is essential and still requires

additional analysis. Perhaps, even more importantly, we are in a period of human development where the anthropogenic emission of CO_2 is leading to a potentially calamitous era of climate change due to the greenhouse properties of CO_2 and the associated rise in global temperatures (Notz and Stroeve, 2016). Understanding the catalytic mechanism of CO_2 uptake coupled to electron transfer may provide a blueprint to engineer biomimetic devices to capture CO_2 from, for example, industrial processes.

Despite the importance of CO_2 uptake in cyanobacteria, very little is known about how this process works. The purpose here was to elucidate the structure-function relationships of Cup (CO_2 uptake also known as Chp, CO_2 hydration) proteins in the NDH-1$_{3,4}$ complex, part of the cyanobacterial CCM. Regulation of internal CO_2 levels in living organisms is dependent on carbonic anhydrases enzymes that catalyzes the interconversion of CO_2 and HCO_3^-. In humans, these enzymes are present in blood, assisting in CO_2 removal process, and anomalies can cause major diseases. This process is not usually energized by coupling to other biochemical energy sources such as ATP. However, cyanobacteria have evolved a mechanism that possibly energizes this process to supercharge the uptake of CO_2 against a concentration gradient. This dissertation focus on investigating the molecular basis of the poorly understood CO_2 uptake systems activity found in cyanobacteria.

1.2 Cyanobacteria, photosynthesis and CO_2 adaptation

Earth was formed around 4.5 billion years ago, and in early times, Earth's atmospheric air had concentrations of CO_2 that were extremely high and little O_2 present (Catling and

Zahnle, 2002; Kasting *et al.*, 1984; Rosing *et al.*, 2010). Life seems to have appeared around 3.8 billion years ago by the development of anoxygenic organism, with oxygenic organisms arising later (Blankenship, 2010). It was proposed that cyanobacteria had as ancestor a non-photosynthetic chemoheterotroph, and later one class of the phylum evolved photosystems (Soo *et al.*, 2017; Soo *et al.*, 2014).

Photosynthetic organisms are present in two out of the three domains of life, after a complex evolutionary development, which involved extensive amounts of horizontal gene transfer in Bacteria, together with diverse evolutionary trajectories, forming the photosynthetic organisms that populates Earth today (Blankenship, 2010). Although the intricate evolution of these organisms, evidence suggests that cyanobacteria-like organisms were the first to perform oxygenic photosynthesis and gave origin to chloroplasts, present in photosynthetic Eukaryotes, due to endosymbiosis (Margulis, 1981) (for more information see review by (Hohmann-Marriott and Blankenship, 2011).

The appearance of oxygenic photosynthetic organisms (producing O_2), coupled with the proper geological processes and conditions, allowed O_2 to accumulate causing the ratio of atmospheric gases to change, allowing life to evolve as it is today (Buick, 2008; Dorrell and Smith, 2011; Messinger and Shevela, 2012). Cyanobacteria-like organisms were essential for this process, as potentially the first oxygenic photosynthetic organisms, followed by algae and plants, which collectively led to the decrease of CO_2, apparently with significant fluctuations, to current relatively low levels.

Besides the photosynthetic apparatus, carbon fixation pathways and later CO_2 concentrating mechanisms evolved, and probably on multiple occasions (Meyer and Griffiths, 2013). In this chapter, I will discuss the general photosynthetic mechanisms present today in oxygenic photosynthetic cyanobacteria.

1.3 Photosynthesis and the photosynthetic electron transport chain

Formerly known as blue-green algae, cyanobacteria became recognized as Bacteria in the 1970's (Stanier and Bazine, 1977). Cyanobacteria are Gram negative phototrophic bacteria (Bryant, 1994; Rippka *et al.*, 1979), often motile by gliding using Type IV *pili* with phototaxis (Schuergers *et al.*, 2017), and conducting oxygenic photosynthesis that captures energy of light and converts it into chemical energy. Most cyanobacteria possess, on their photosynthetic membrane surface, a multiprotein antenna complex, called the phycobilisomes (PBS). The PBS are mostly comprised of intensely colored soluble proteins that obtain their color by binding of light-absorbing bilin pigments. The blue phycobiliproteins, phycocyanin and allophycocyanin, have the bilin pigment named phycocyanobilin covalently attached to a cysteine side chain of the polypeptide via a thioether linkage. Correspondingly, the red phycobiliprotein, phycoerythrin, has a phycoerythrobilin molecule linked the polypeptide chain. Accordingly, the bilin pigments of the PBS give the cyanobacteria their distinctive blue color and allow cyanobacteria to harvest green and orange light that is inefficiently captured by chlorophyll (Chl) and carotenoids. The phycobiliproteins assemble into large (>10^6 Dalton) PBS complexes

situated on the membrane and physically connected to the Chl-containing reaction centers embedded within the thylakoid membrane (TM). Virtually all of the Chl in cyanobacteria is located in the membrane-bound photosynthetic reaction center complexes, Photosystem I (PSI) (Jensen *et al.*, 2007) and Photosystem II (PSII) (Umena *et al.*, 2011). Most of the Chl in these reaction centers (RC) comprise the proximal antenna, which serve to feed excitation energy to 'special pairs' of Chl at the heart of the reaction center. These 'special pairs' of Chl undergo charge separation and thereby initiate photochemistry (Golbeck, 2002). In the PSII reaction center, the special pair is known as P680, which is surrounded by proximal antenna Chl molecules that either directly absorb light or accept excitation energy from the PBS. In this case the energy rapidly migrates through the PBS and antenna components until reaching the core with the 'special pair' of Chl a P680. These are excited and undergo charge separation, where the electron is excited to a higher energetic state, forming $P680^*$. The energized electron of $P680^*$ is capable of being donated to a nearby electron acceptor, plastoquinone molecule (Q_A) with the release of some of the original energy of the excited electron as heat in the process of electron transfer. In this manner, the charge separation from P680 to Q_A is stabilized by the donation with the release of some of the energy as heat since the backreaction is less likely. This charge separation happens on the environment of the multiprotein complex PSII that together with the proximal antenna forms the RC type II. This is the initial phase of the electron route in cyanobacterial photosynthesis, a path known as the photosynthetic electron transfer (PSET, Figure 1) comprising the energetic course in the Z- scheme. After losing an electron, a 'hole' is left

on the 'special pair' forming $P680^+$, which is a strong oxidant. This electron hole is replenished with an electron from the oxidation of water at the oxygen evolving complex (OEC) is catalyzed by a manganese cluster (Mn_4CaO_5), in a series of steps, referred to as the oxidant storage cycle or, more commonly, the S-state cycle. The reaction releases protons (H^+) and produces molecular oxygen (O_2), a waste product, as shown in equation 1:

$$4\,photons + 2H_2O \rightarrow 4H^+ + O_2 + 4e^-$$

Because P680 and the WOC are located in the PSII complex near the luminal surface of the membrane (P-side), the protons from the Mn_4CaO_5 during the S-state cycle are released into the thylakoid lumen (Bao *et al.*, 2013) and contribute to the proton gradient across the thylakoid membrane that is used for ATP synthesis. In parallel, a second sequence of events on the other side of the reaction center, and therefore, on the other side of the membrane, involves the acceptor of the electrons produced during charge separation as noted above: the plastoquinone molecule Q_A bound to the D1 protein in PSII receives the electron, and soon (in the range of 300-1000 microseconds) donates the electron to a second plastoquinone at the Q_B binding pocket of PSII (Golbeck, 2002). This PQ is exchangeable with PQ molecules that form the so-called 'PQ pool' dissolved in the membrane bilayer. When the PQ at the Q_B site accepts a second electron as a result of a second P680 charge separation, the plastoquinone at the Q_B site is thus further reduced forming a plastoquinol (PQH_2). For simplicity, the plastoquinone at the Q_B site is usually referred to as 'Q_B'. With

each electron transfer to Q_B, protons are acquired from the cytosol (N-side), and the doubly reduced Q_B site thereby forms PQH_2, which exchanges Q_B site and diffuses into the surrounding membrane bilayer contributing to the overall reduction state of the pool of PQ molecules in the membrane. Since water oxidation requires four charge separations, the formation of PQH_2 occurs twice per full catalytic cycle of water oxidation giving an overall reaction summarized in equation 2:

$$4\,photons + 2H_2O + 2PQ \rightarrow O_2 + 2PQH_2$$

These reactions are unique to oxygenic photosynthesis and initiate the overall process of photosynthetic electron transfer according to the classic Z-scheme involving PSII and PSI acting in series to drive electrons from water to NADPH. The product of PSII electron transfer, PQH_2 serves as a carrier of the electrons to the downstream components of the electron transport chain. Specifically, PQH_2 is oxidized by cytochrome (cyt) b_6f, a multiprotein complex that couples the transfer of electrons from PQH_2 to plastocyanin (PC) with the pumping of protons across the membrane (Aoki and Katoh, 1982; Cramer *et al.*, 2011; Wenk *et al.*, 2005). Because cyt b_6f receives electrons from PQH_2, it serves to regenerate PQ so that it can return to the Q_B site of PSII to receive more electrons. There are typically 6-10 PQ molecules per PSII (Schuurmans *et al.*, 2014) and, thus the overall PQ pool changes its redox state according to the fraction of the pool that is either in the PQH_2 (reduced) or PQ (oxidized) form. This becomes important later in my thesis since the fluorescence techniques we use can monitor the redox state of the PQ pool, and is

informative about overall electron transfer as a function of availability of the CO_2 (Holland *et al.*, 2015; Miller *et al.*, 1988). The oxidation PQH_2 by the cyt b_6f complex and the subsequent transfer of the electron to a mobile electron acceptor, either plastocyanin (PC) or cytochrome c_{553} (cyt c_{553}), is coupled to proton transfer via the so-called Q-cycle (Baniulis *et al.*, 2008; Joliot and Joliot, 2001). Both PC and cyt c_{553} are mobile electron carrier proteins that are capable of diffusing along the lumen surface to the thylakoid membrane (TM) and shuttling electrons from cyt b_6f to Photosystem I (PSI). Whether PC or cyt c_{553} is utilized depends upon the nutritional conditions since a complex regulatory mechanism controls their alternative expression (Bryant, 1994). The PSI complex is similar to PSII in the sense that it has a proximal antenna with pigments which channel excitation energy to a 'special pair' of Chl a, named P700. However, instead of requiring four photons and four electrons per catalytic cycle as with the water oxidation mechanism of PSII, it only requires one photon to complete a catalytic cycle. Charge separation in PSI produces an electron hole (oxidant), $P700^+$, which is reduced by the mobile carrier (PC or cyt c_{553}). Toward the electron acceptor side of PSI, charge separation sends the high energy electron to a series of redox carriers, and ultimately, to the mobile single electron acceptor, ferredoxin (Fd), which is a small, soluble, low-potential iron-sulfur protein that has a docking site on the cytoplasmic side (N-side) of the photosynthetic membrane. In other words, a mobile single electron carrier, instead of water, is the donor of electrons to replenish the electron 'hole' in ($P700^+$) created by photochemical charge separation. On the acceptor side, the reduced Fd (Fd_{red}) diffuses from the PSI to carry the high energy

(relatively negative midpoint potential) electron to one of several alternative pathways. Cyanobacteria typically express multiple isoforms of Fd, with different functions, active in numerous pathways (Cassier-Chauvat and Chauvat, 2014). However, the most abundant form of Fd mediates dominant route of the transport of electrons, which is from PSI to ferredoxin-NADP reductase (FNR), an oxidoreductase enzyme with a flavin cofactor that catalyze the reduction of $NADP^+$ into NADPH. Because the full reduction of $NADP^+$ to NADPH requires two electrons, there are two Fd_{red} consumed by FNR per NADPH produced. Interestingly, two isoforms of FNR are expressed in cyanobacteria as a result of the utilization of alternative translational start sites of the *petH* gene (Thomas *et al.*, 2006). The longer isoform, FNR_L, has a domain that attaches it to the phycobilisomes and this form is involved in the reduction of $NADP^+$ to NADPH. The short form FNR_S is less well understood, may catalyzes the reduction of $NADP^+$, but also appears to enhance cyclic electron flow (discussed below). Summing up, the overall electron pathway from water to NADPH is known as linear electron flow/transport (LEF or LET) (Figure 1).

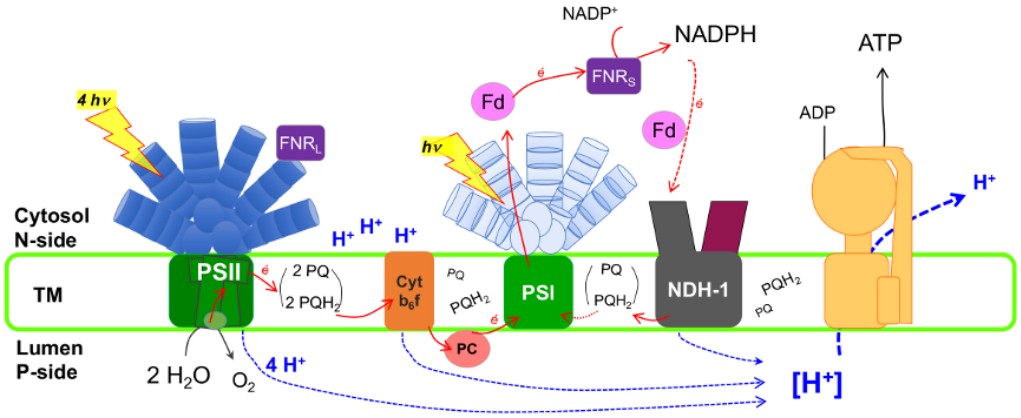

Figure 1. Model of cyanobacterial photosynthetic electron transport (PSET). Light driven energy transfer coupled with electron (e^-) transport through five protein complexes: PSII, cyt b_6f, PSI, NDH-1 and ATP synthase present in the thylakoid membrane (TM). Also shown in the scheme are the mobile electron carriers such as PQ/PQH_2, PC, Fd, FNR, NADPH and ATP. For more information see text.

The oxidation/reduction (redox) reactions of PSET are coupled with protons being translocated across the membranes (from cytosol to TM lumen, N-side to P-side), forming a proton gradient across the membrane that is strong enough to drive ATP production by ATP synthase utilizing the proton motive force (*pmf*) present in the gradient. The global PSET gain is represented in equation 3:

$$8\,photons + 2H_2O + 2NADP^+ + 3ADP \rightarrow 12H^+ + O_2 + 2NADPH + 3ATP$$

However, the cell has multiple metabolic pathways operating at once, so electrons in the mobile carriers can be deviate along different routes at any stage, or fed back to the

photosynthetic chain, as necessary. Consequently, not all the electrons are used for the net reduction of CO_2 in the downstream reactions. An important alternate pathway is the cyclic electron flow/transport (CEF/CET), necessary to increase the ratio of ATP relative to NADPH (Alric *et al.*, 2010; Joliot and Joliot, 2002; Munekage *et al.*, 2004). Among the alternative routes, Fd_{red} (and possibly, NADPH) may donate its electron to the so-called NAD(P)H dehydrogenases type-1 (NDH-1) complexes (Figure 2), eventually reducing PQ, feeding the PQH_2 pool (Bernat *et al.*, 2011; Mi *et al.*, 1992). The returned reductant can be consumed in PSET by redox reactions coupled to proton transfer, assuring extra production of ATP. It seems that this involves the shorter form of FNR, FNR_S, with no linker, but the whole mechanism is still under intense investigation. Additionally, supercomplex formation between PSI and NDH-1 may increase the efficiency of CEF (Gao *et al.*, 2016).

Overall, five protein complexes participate in cyanobacterial PSET: PSII, Cyt b_6f, PSI, NDH-1 and ATP synthase, together with mobile electron carriers such as PQ/PQH_2, PC, Fd, FNR, NADPH and ATP. Hence, the energy of PSET can produce NADPH, form a proton motive force required for synthesis of ATP, and balance ATP/NADPH through CEF. The energy produced during photosynthesis and stored as ATP and NADPH is free to be consumed in anabolic processes, of which CO_2 fixation is the dominant sink for ATP and NADPH. Reduced products of the PSET also have regulatory roles. Most notably, many enzymes involved in CO_2 fixation are regulated by thioredoxin (TX) using electrons from Fd_{red} or NADPH produced in the light reactions (Dai *et al.*, 2004; Hishiya *et al.*,

2008). These redox reactions are responsible to activate the CBB cycle (Michelet *et al.*, 2013).

1.4 Carbon fixation in cyanobacteria

Photosynthesis is used by oxygenic photoautotrophic organisms to supply the energy necessary for carbon fixation process. Cyanobacteria use the most widespread pathway, the Calvin–Benson–Bassham (CBB) cycle, found in all oxygenic photosynthetic bacteria, most purple bacteria, and all algae and plants (Blankenship, 2010). CBB is a step-wise and cyclic metabolic process, where carbon from CO_2 is assimilated into an organic molecule in a reaction catalyzed by the main enzyme CO_2-fixing enzyme Rubisco (Ribulose-1,5-bisphosphate carboxylase/oxygenase) (Tabita *et al.*, 2008).

Rubisco catalyzes the carboxylation of ribulose-1,5-bisphosphate (RuBP) with CO_2 to produce two molecules of 3PGA (3-phosphoglyceric acid). Cyanobacterial Rubisco has an optimal activity at pH 7.5 (Badger, 1980), but a low affinity to CO_2 with K_m >150 μM (Tabita *et al.*, 2008). As mentioned above, an alternative oxygenation reaction with RuBP can occur at the same catalytic site. This is a wasteful reaction in which O_2 competes for the active site with CO_2 as the second substrate to react with RuBP (Tabita *et al.*, 2008). The process where the oxygenation of RuBP produces one 3PGA and one molecule of 2-phosphoglycolate (2PG), is known as photorespiration and is considered a wasteful reaction, decreasing the efficiency of carbon provided to the cell (Burnap *et al.*, 2015; Price, 2011; Tabita *et al.*, 2008). Yet, in cyanobacteria photorespiration is kept low, 0.5-1% of

total carbon assimilation, mostly due to mechanisms to saturate Rubisco with CO_2 (Burnap *et al.*, 2015; Eisenhut *et al.*, 2008).

1.5 CO_2 concentrating mechanisms in cyanobacteria

Cyanobacteria evolved multiple mechanisms to adapt and survive the changes in CO_2 and O_2 ratios available in our atmosphere. The level of dissolved inorganic carbon is often very low in current environmental conditions for an efficient photosynthesis, with typical aquatic concentration of free CO_2 of 15 μM, despite of 1-2 mM total C_i, mostly as HCO_3^- (Price *et al.*, 2008). Equation 4 shows the forms of C_i present on water, including dissolved CO_2 (following Henry's law).

$$CO_2 + H_2O \rightleftharpoons H_2CO_3 \leftrightharpoons H^+ + HCO_3^- \rightleftharpoons 2H^+ + CO_3^{2-}$$

The concentration of the C_i species present depend strongly on the pH, and cell permeability vary for the available species (Mangan *et al.*, 2016). Dissolved CO_2 and H_2CO_3 can passively cross the outer membrane and cell wall, and across the cytoplasmic membrane into the cytoplasm, possibly via aquaporins (Ding *et al.*, 2013; Tchernov *et al.*, 2001). It is not fully understood how bicarbonate ions (HCO_3^-) cross the outer membrane, but it may pass through porins (maybe *porB*) (Woodger *et al.*, 2007). Still, cyanobacteria maintain an internal C_i pool of 20-40 mM, preferably in the form of HCO_3^-, since the ionic form has a poor permeability through the lipoproteic membrane (Kaplan and Reinhold, 1999; Price *et al.*, 2008). This internal cell concentration is only possible due to a specialized uptake system, the CO_2-concentrating mechanism (CCM). CCM comprises a

complex network of several inorganic carbon transporters falling in an array of protein families widely distributed through cyanobacteria (Price *et al.*, 2008). This includes a group of active bicarbonate transporters (using either ATP or Na^+ gradient) and CO_2 uptake systems. Additionally, a bacterial microcompartment (BMC) known as the carboxysome (CB) is part of the CCM. It is the sink for the accumulated HCO_3^- and houses Rubisco and carbonic anhydrase, such that the carboxylation efficiency of Rubisco is enhanced as discussed in the next section.

The many components of the CCM are highly conserved and this includes their regulatory properties, which typically involve a set of constitutively expressed proteins, which, in many species, are supplemented by proteins which are regulated by the availability of C_i. The part of the CCM that is constitutively expressed, includes the CB, and certain high flux and low affinity C_i uptake proteins. Other components are only induced under conditions of low ambient C_i and these typically exhibit high affinity, but comparatively low flux uptake characteristics. The genes for some of these inducible proteins appear to have been completely lost during evolution, particularly in oceanic strains where C_i levels are more stable (reviewed in (Kaplan, 2017; Price, 2011). The regulation of CCM is complex, with multiple levels of regulation guiding the expression and activity of the CCM components, including sensing metabolic changes and allosteric interactions (Orf *et al.*, 2015; Price, 2011; Wang *et al.*, 2004), also see review (Burnap *et al.*, 2015). In general, cells growing under ambient air (low C_i, LC) start accumulating intermediate molecules such as RuBP, since overall rate of the CBB decreases due to the paucity of CO_2. Simultaneously, 2PG,

levels begin to rise due to increase of photorespiration. These molecules act as co-activators of CmpR, a LysR-type transcriptional regulator (LTTR), responsible for the transcriptional activation of genes coding for BCT1, the ATP powered bicarbonate transporter (Nishimura *et al.*, 2008; Omata *et al.*, 2001). A second LTTR known as CcmR (or ndhR) acts as repressor of many components of CCM and is de-repressed under LC, being modulated by its co-repressors $NADP^+$ and α-ketoglutarate (αKG, or 2-oxoglutarate, 2OG) (Daley *et al.*, 2012). The regulatory logic is that with LC and the resultant lower rates of the CBB cycle, there is less NADPH consumption, which explain the higher ratio of NADPH/$NADP^+$ and lower flux of carbon into the TCA (Tricarboxylic acid or Krebs cycle) and its intermediates such as αKG (Burnap *et al.*, 2013). This is especially noticeable in the acclimation hours following shift from HC grown cells to LC for 24 hours (Daley *et al.*, 2012). Yet another level of regulation involves non-coding RNAs (ncRNAs) including antisense (asRNAs) and regulatory small RNAs (sRNAs), which modulated the expression of certain CCM proteins, with mechanisms still poorly understood (Georg and Hess, 2011; Mitschke *et al.*, 2011). Hence, a complex network of interactions of metabolites and sensor proteins, together with ncRNAs and still unknown regulatory mechanisms are involved in the multi-layer regulation of LC adaptation, including CCM components and its high affinity C_i transporters.

1.5.1 Carboxysome

Carboxysomes (CB) are present in all cyanobacteria and some chemoautotrophic bacteria (Cannon *et al.*, 2001). The CB was the first BMC discovered and was revealed in an electron microscopic study of the ultrastructure of the cyanobacterium *Phormidium uncinatum*. Although they have been difficult to work with biochemically due to their fragility, a CB was first isolated from the chemoautotrophic *Halothiobacillus neapolitanus* (reviewed in (Yeates *et al.*, 2010; Yeates *et al.*, 2008). Biochemical analysis of purified and intact CBs indicated a high concentration of active Rubisco (Cannon *et al.*, 2001; Cannon *et al.*, 1991). Physiological examination of cells grown under air (CO_2 about 0.04%) showed increased CB number and Rubisco activity (Cheng *et al.*, 2008). Moreover, studies of mutants with defective CB presented a high CO_2-requiring phenotype (CO_2 1-5%) (Cheng *et al.*, 2008; Price and Badger, 1991). These and other evidence suggested the currently accepted role of CB as a BMC specialized in C_i fixation (Price *et al.*, 2013).

Specifically, the CB is responsible for the second phase of the CCM, during which cyanobacteria consume the accumulated HCO_3^- by converting it to CO_2 in proximity of the Rubisco housed in the CB (Badger and Price, 2003). Cyanobacterial Type 1 Rubisco (L_8S_8) has K_m >150 μM and K_{cat} 1-13 s^{-1}, considered an enzyme with low affinity reaction (Cannon *et al.*, 2001; Cheng *et al.*, 2008; Tabita *et al.*, 2008). The level of dissolved inorganic carbon (C_i: CO_2 and HCO_3^-) is low in environmental conditions, typical aquatic [CO_2] of 15 μM (Price *et al.*, 2008). C_i is actively pumped into the cell in the first phase of

the CCM, and HCO_3^- is assumed to diffuse into CB (Yeates *et al.*, 2010). The encapsulation of Rubisco and the localization of a CB carbonic anhydrase (Price and Badger, 1991), which rapidly dehydrates the HCO_3^- to form CO_2, allows an increase in concentration of CO_2 to 20 mM near the enzyme, 1000-fold higher than environmental conditions (Price *et al.*, 2013). This is essential to overcome competition with O_2 as a substrate (photorespiration) and to enhance enzyme activity to near substrate saturation (Kerfeld *et al.*, 2010).

There are two types of CB, classified according to the type of Rubisco, protein shell, and CA (Badger and Price, 2003). The α-CB is present in (mostly oceanic) α-cyanobacteria and chemoautotrophs (*e.g. Halothiobacillus neapolitanus*), with type 1A Rubisco and genes arranged in an operon (Price *et al.*, 2008). The second class of CB is characteristic of (mostly freshwater and estuary) β-cyanobacteria (*e.g. Synechocystis* sp. PCC 6803), with type 1B RuBisCO and the genes are distributed in clusters throughout the genome (Price *et al.*, 2008). CB associated proteins include Rubisco subunits (large, RbcL; small, RbcS), shell proteins (CcmK1-4, CcmO, CcmL), plus organizational proteins (CcmM, CcmN) and a CA (CcaA or IcfA) (Kinney *et al.*, 2011). CcmL is a pentameric protein required in vertices, taking the final structural organization of an icosahedron, and may prevent CO_2 leakage (Cai *et al.*, 2009).

1.5.2 Bicarbonate transporters: BCT1, BicA and SbtA

There are three known bicarbonate transporters systems, BCT1, SbtA and BicA. BCT1, an ATP-binding cassette (ABC)-type system, is composed of four proteins whose genes are clustered under an operon, *cmp(A-D)* (Omata *et al.*, 1999). CmpA is a periplasmic lipoprotein that binds to HCO_3^- present in the periplasmic space with high affinity ($K_{0.5}$ 5-15μM) (Maeda *et al.*, 2000), transported there probably passively through porins in the outer membrane (Price, 2011). CmpB is a hydrophobic membrane protein, possibly present as dimers with a channel in between that would allow the transport of HCO_3^- coupled to ATP hydrolysis. The associated CmpC and CmpD subunits have ATP binding sites, powering the transport (Omata *et al.*, 2002). Also, the operon sometimes includes the gene *porB*, which is a putative outer membrane porin. This transport system is induced under ambient air levels of CO_2 (Wang *et al.*, 2004), with medium to low flux, and is of special use for fresh water organisms (Kaplan, 2017; Omata *et al.*, 2002; Price *et al.*, 2008; Price *et al.*, 2002).

SbtA is a protein comprised of a single polypeptide that works as a bicarbonate transporter, with high affinity (~5μM) (Shibata *et al.*, 2002) and low flux (Price *et al.*, 2004). It seems, however, that the protein forms a tetrameter (Price, 2011; Zhang *et al.*, 2004). The gene *sbtA* is usually localized with *sbtB*, of unknown function, but is in the PII-family of regulatory proteins and therefore may interact with SbtA to exert some form of regulation (Du *et al.*, 2014). Despite its subunit simplicity, SbtA seems to have a significant

importance in HCO_3^- transport in cyanobacteria. It is induced under LC conditions (Wang *et al.*, 2004), and it seems strictly dependent on the electrochemical gradient of Na^+, in fact, its function appears to be almost inexistent in the absence of Na^+, with maximal HCO_3^- uptake at 6 mM Na^+, requiring 1mM for half maximal HCO_3^- uptake (Shibata *et al.*, 2002). Therefore, SbtA can be considered a Na^+-HCO_3^- symport relying on the electrochemical gradient of Na^+, where relatively high concentrations of external Na^+ allow the inward movement of Na^+ down a concentration gradient to be obligately coupled to the parallel inward movement of HCO_3^- up a concentration gradient into the already high concentration of HCO_3^- in the cytoplasm. There appears to be considerable diversity in the SbtA family and different members exhibit different kinetic characteristics. A study of multiple cyanobacteria SbtA activity showed a wide range of affinities, $K_{0.5}$ 74-353 μM, indicating that the higher affinity modules also had lower flux (V_{max}) and *vice versa* (Price, 2011; Price *et al.*, 2004).

BicA, the most recent C_i transporter discovered, is a member of a large family of transporter (SulP-type), and has a mechanism similar to SbtA insofar as it appears to be a Na^+ symporter (Price *et al.*, 2004). The membrane protein contains multiple transmembrane alpha helices, and it utilizes a Na^+ concentration gradient, requiring 1.7 mM Na^+ for half maximal HCO_3^- uptake (Price, 2011). Accordingly, both BicA and SbtA are involved in the symport transport of Na^+ and HCO_3^- (Espie and Kandasamy, 1994; Kaplan, 2017; Price *et al.*, 2002). Notably, BicA seems to be constitutively expressed in freshwater cyanobacteria such as *Synechocystis* sp. PCC 6803 (Klähn *et al.*, 2015; Wang *et al.*, 2004),

but is inducible under LC in marine organisms, for example *Synechococcus* sp. PCC7002 (Woodger *et al.*, 2007).

These bicarbonate transporters are important for aquatic photoautotrophs, since C_i dissolved in water is four times lower in concentration than in air, is pH dependent and CO_2 diffusion is 10^4 times slower than in air (Price, 2011). In order to overcome these conditions of low C_i-availability, cyanobacteria accumulate C_i in the form of HCO_3^- (Kaplan and Reinhold, 1999; Price and Badger, 1989c; Woodger *et al.*, 2005). Later, this will be converted into CO_2 by a CA present on the interior wall of the CB (Kinney *et al.*, 2011; Price and Badger, 1991). This process is enough to ensure and enhance C_i fixation, and decrease competition with O_2 (photorespiration), by keeping near saturation CO_2 concentrations near Rubisco, boosting its carboxylation activity (Kinney *et al.*, 2011; Marcus *et al.*, 1992). However, CO2 can passively leave the cell, hence a dedicated scavenger system is required to decrease this undesirable escape of C_i in the form of CO_2.

1.6 NDH-1 complex and Cup proteins

Contrary to bicarbonate, dissolved CO_2 can passively enter/exit the cell, possibly via aquaporins (Ding *et al.*, 2013; Tchernov *et al.*, 2001). Since internal C_i is maintained primarily as the ionic species, HCO_3^-, it is not prone to leakage form the cell. However, HCO_3^- can spontaneously be converted to CO_2 or, following the action of the CB carbonic anhydrase, it may leak from the CB if it is not utilized by Rubisco. Hence, cyanobacteria evolved dedicated systems that hydrate CO_2 to form HCO_3^- for primary uptake and avoid

CO_2 leakage back to the environment, thereby maintaining the high and far from equilibrium concentrations of accumulated HCO_3^- (Burnap *et al.*, 2015; Kaplan, 2017).

The specialized CO_2 uptake systems are variations of NAD(P)H dehydrogenases type-1 (NDH-1) complexes (Figures 2 and 3), and are multiprotein systems, having Cup ($\underline{C}O_2$ $\underline{up}$take) proteins as part of the large U shaped active membrane complex (Arteni *et al.*, 2006; Battchikova *et al.*, 2011a; Folea *et al.*, 2008; Ohkawa *et al.*, 2000a; Ohkawa *et al.*, 2000b; Zhang *et al.*, 2004). These specialized forms of the NDH-1 complex catalyze the energy-requiring conversion of CO_2 into HCO_3^-, against the equilibrium $CO_2 \rightleftharpoons HCO_3^-$. In other words, the hydration reaction resembles a classical carbonic anhydrase activity, except that it may also utilize an energy source to drive the reaction far from equilibrium (very high $[HCO_3^-]/[CO_2]$ ratios) reflecting the high concentrations of HCO_3^- that are maintained in the cytoplasm. It is not clear whether these specialized CO_2 uptake forms of the NDH-1 complex are associated with recently discovered supercomplexes between NDH-1 and PSI. It was shown that a supercomplex NDH-1-PSI may be formed between these protein systems under specific conditions. Importantly, these and other forms of the NDH-1 complex appear to mediate cyclic electron flow (CEF) (Gao *et al.*, 2016). For CEF, high energy electrons in the form of Fd_{red} produced by PSI are thought to be recycled into the plastoquinone pool via the NDH-1 complex, although the details of the process and the exact polypeptides mediating it are not well-defined. Similarly, how CO_2 uptake is associated to the photosynthetic electron transport and the NDH-1 complexes, it is also not well understood. It is generally accepted that CO_2 uptake depends on the core NDH-1

proteins (Han *et al.*, 2017) and CEF (Bernat *et al.*, 2011), which would indicate an energized system using the redox energy of NADPH or Fd_{red} to power CO_2 uptake (He *et al.*, 2015) (also see review by (Battchikova *et al.*, 2011a).

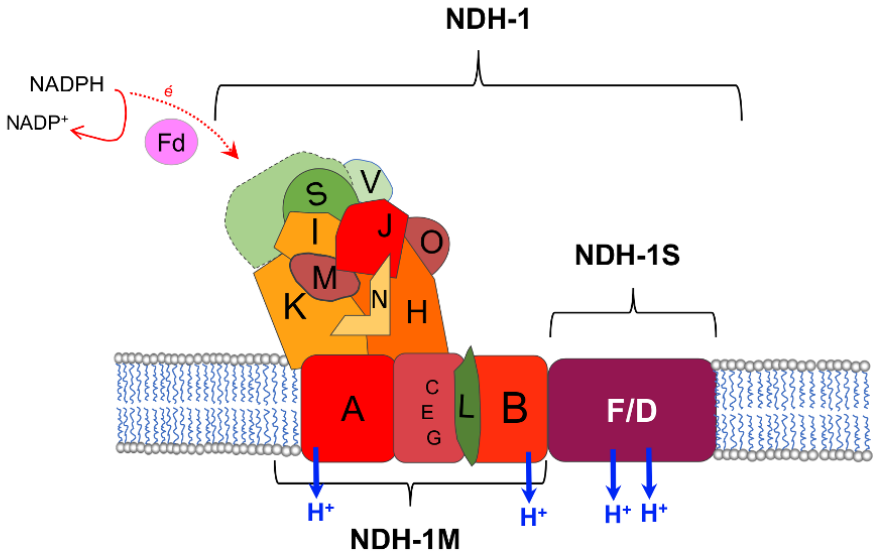

Figure 2. Representation of Type-1 NADH dehydrogenase complexes (NDH-1) of cyanobacteria present on the thylakoid membrane, showing multiple proteins involved in the complex. The core protein (NDH-1M) with L shape is highly conserved. Four variations of NDH-1_{1-4} are possible due to interchange of several homologous NdhF and NdhD subunits (NDH-1S), responsible for the complex structural and functional multiplicity. For more information, see text and review by (Battchikova *et al.*, 2011a); (He *et al.*, 2015).

Synechocystis sp. PCC6803 has four types of NDH-1 complexes (NDH-$1_{1\text{-}4}$), where two are involved in CO_2 uptake (NDH-$1_{3,4}$) (Maeda *et al.*, 2002; Shibata *et al.*, 2001). All four have a multiprotein core in a L format, with about 11 proteins homologous to Complex 1 in *Escherichia coli* (Battchikova *et al.*, 2011a). These NDH-1 complexes are modular in structure with a common core (NDH-1M) that contains the redox centers involved in electron transfer and alternative modules connected to this core. The defined function of the complexes depends on the proteins attached to the core, with the subcomplex (NDH-1S) containing one of the multiple NdhD and NdhF variants making the proper combination (Battchikova *et al.*, 2011a). Two forms, NDH-1_1 and NDH-1_2 (also known as NDH-1L/L'), function in cyanobacteria as both respiratory and photosynthetic CEF systems. The two other structures, NDH-1_3 and NDH-1_4, contain CO_2 uptake proteins (Figure 3), and are widespread in cyanobacteria (Badger *et al.*, 2006).

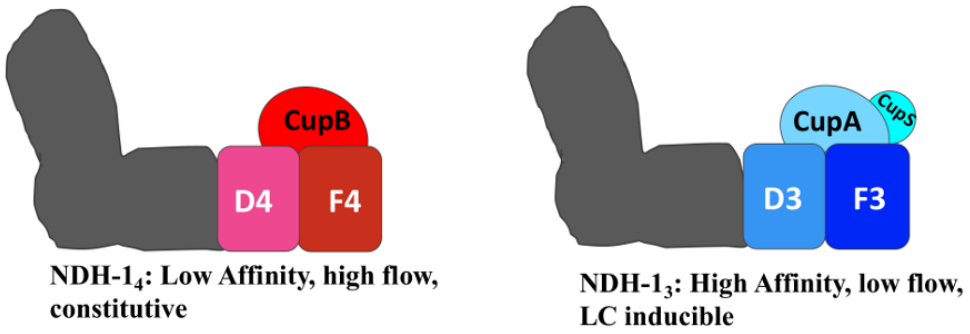

Figure 3. CO_2 uptake systems are specialized Type-1 NADH dehydrogenase complexes (NDH-1) present on the thylakoid membrane of cyanobacteria. NDH-1_4 is a constitutive CO_2 uptake system,

containing NdhF4, NdhD4 and CupB. NDH-1_3 is induced under LC growth conditions, comprising of NdhD3, NdhF3, CupA and CupS. For more information, see text and review by (Price, 2011).

NDH-1_4 (also known as NDH-1MS') is a constitutive CO_2 uptake system, composed of three proteins, NdhF4, NdhD4 and CupB (or ChpX in *Synechococcus* sp. PCC 7942) forming the subcomplex attached to the L core, giving a U shape to the structure. NDH-1_4 has a medium-low affinity ($K_{0.5}$ 10-15 μM) and high flux (190 μmol mg^{-1} Chl h^{-1}) in the organisms previously studied (Maeda *et al.*, 2002; Shibata *et al.*, 2001). Similar work showed that NDH-1_3 (also known as NDH-1MS) is induced under LC conditions, having NdhD3, NdhF3, CupA (or ChpY in *Synechococcus* sp. PCC 7942) and CupS, all expressed part of the *cupA* operon (plus a fifth ORF of unknown function). Contrary to NDH-1_4, NDH-1_3 has a high affinity ($K_{0.5}$ 1-2 μM) and low flux (90 μmol mg^{-1} Chl h^{-1}) (Maeda *et al.*, 2002; Shibata *et al.*, 2001), but seem to be missing from some cyanobacteria (Kaplan, 2017). Note that neither the NDH-1_4 nor NDH-1_3 enzyme have ever been purified to homogeneity so that the actual specific flux activity is still not known and therefore the cited values of 190 and 90 μmol mg^{-1} Chl h^{-1} are normalized to the total amount of Chl instead of a true specific activity (rate per enzyme complex). Accordingly, the number of NDH-1_4 and NDH-1_3 expressed per cell will also determine the actual measured flux activity. The high affinity system has an unique structural component, CupS as part of the U shaped complex with a specific docking site in NdhF3 (Birungi *et al.*, 2010; Korste *et al.*, 2015), although absence of CupS did not affect growth under LC (Ohkawa *et al.*,

2000b) and distinct function requires further studies. The poorly understood CO_2 hydration mechanism of NDH-$1_{3,4}$ may involve a special type of carbonic anhydrase, CupA and CupB, and proton transport (involving NdhD3F3 and NdhD4F4) as constituents (Han *et al.*, 2017; Price *et al.*, 2002). Moreover, it is known that the traditional carbonic anhydrase inhibitors, particularly ethoxyzolamide (EZ), decreases CO_2 uptake in cyanobacteria with no interference on HCO_3^- transport (Espie *et al.*, 1991; Price and Badger, 1989a; Price and Badger, 1989b). The majority of these studies are based solely on absence or presence of genes and coded proteins, yet no functional protein work or X-ray crystal structures are available, and work on the structure has been difficult since the complex is fragile, easily dissociating in two subcomplexes (the core and attached modules), plus it is generally present in low concentrations in the cell compared to the reaction centers (Battchikova *et al.*, 2011a; Zhang *et al.*, 2005). A recent near-atomic structure of cyanobacterial NDH-$1_{1,2}$ by cryo-EM single particle analysis may shine some light in the multiprotein structure (Laughlin *et al.*, 2018). However, the CO_2 hydration mechanism, involving the Cup proteins, remains enigmatic and requires further study. The CO_2 hydration mechanism has been a target of intense discussion in the literature, with two main hypotheses: 1) CO_2 hydration is solely due to an alkaline pocket formation due to the proteins environment (Kaplan and Reinhold, 1999), and 2) Cup proteins are the proteins with CA-like activity, possibly energized by CEF (Price *et al.*, 2002). This conundrum was raised over fifteen years ago, with no new insights.

The CCM function is essential for the increase of C_i inside of the cell, which is necessary for high efficiency photosynthesis (Burnap *et al.*, 2015; Price, 2011). To better understand the mechanism of the CCM, more specifically the Cup complexes, in the present study I investigated the structure-function of NDH-$1_{3,4}$, as a first step in an effort to probe the molecular mechanism using a combined molecular genetics and physiological approach. This will be further discussed in Chapters 4 and 5.

1.7 Carbonic anhydrases, structure-function overview and importance in cyanobacteria

Bicarbonate interchange into CO_2 is catalyzed by carbonic anhydrases (CAs) and is essential for metabolism hemostasis and pH control in living organisms (Kupriyanova *et al.*, 2017). CA is widespread among the three domains of life, comprising a very diverse collection of proteins with several known families of CA, α, β, γ, δ, ζ, η, ε, θ, with numerous isoforms dispersed throughout multiple kingdoms (DiMario *et al.*, 2017; Supuran, 2016). The families are phylogenetically unrelated, as they have little to no amino acid sequence or structure similarity (Supuran, 2016). Cyanobacteria, algae and plants, which evolved at distinct periods before and after the CO_2 levels drastically changed, have different families and isoforms involved in CO_2 hydration. This suggests that CAs evolved independently through the years, having a convergent evolution (DiMario *et al.*, 2017).

A common feature among CAs is an active site associated with a metal cofactor, hence they belong to the superfamily of metalloproteases. Zinc (Zn) is usually the element

present, however, some CAs may interchangeably interact with cobalt (Co^{2+} in α), cadmium (Cd^{2+} in ζ) or iron (Fe^{2+} in γ) under special conditions (reviewed in (Supuran, 2016). The metal ion coordination also may differ among classes and even isoforms (Kupriyanova *et al.*, 2017). In general, three amino acids bonds to the metal ion and a hydroxide ion as the forth ligand forming a tetrahedral shaped active site (Supuran, 2016).

The amino acids forming the catalytic site and also involved in its structure are well conserved within each CA family and some convergent evolution between CA families has been noted (Kupriyanova *et al.*, 2017). α-CA has three conserved histidine residues (His) from a single monomer coordinating Zn^{2+}, and its structure is dominated by antiparallel β-sheet (DiMario *et al.*, 2017; Liljas *et al.*, 1972). β-CA forms oligomers, usually dimers, with structure dominated by α-helices, Zn^{2+} coordinated by two cysteine (Cys) and one His, and is categorized according to its "open site" (type I) or "closed site" (type II) (Kimber and Pai, 2000). ε-CA were initially classified as an unique CA class (So *et al.*, 2004) and later identified as a highly modified β-CA (DiMario *et al.*, 2017; Sawaya *et al.*, 2006). γ-CA structure is rich in left-handed parallel β-sheet, may form a homotrimer, and have amino acids from two monomers supporting the active site, one with two His plus a third His from a second monomer (Kisker *et al.*, 1996). Interestingly, in mitochondria from plants, a γ-CA was found to be localized in the complex I, with no known function (Parisi *et al.*, 2004). ζ-CA may be monomeric enzymes, and like β-CA has two Cys and one His linked to the metal cofactor (Cd^{2+}), with an unusual sequence of three almost identical

amino acids repeats, forming a large active site with the metal at the bottom of the funnel-shaped pocket (Alterio *et al.*, 2012). δ-CAs seems to have an active site similar to α-CA with three His forming the active site (Cox *et al.*, 2000). η-CAs used to be classified as α-CA, however the active site differs in having two His and one glutamine (Gln) binding to Zn^{2+} (De Simone *et al.*, 2015). θ-CA is the newest group discovered an is still poorly studied.

All CAs have a metal in the active site, however, the metal alone is not capable of the catalytic interconversion between CO_2 and HCO_3^- (Kupriyanova *et al.*, 2017). In the first step of the process, the hydroxide group bound to metal is a strong nucleophile. A molecule of CO_2 is trapped on a hydrophobic pocket near the metal, favoring the nucleophilic attack upon the C nucleus of the CO_2 by metal-hydroxide, forming HCO_3^-. This weak binding of HCO_3^- to the metal, stabilized by a neighboring threonine (Thr), is displaced by a water molecule in the adjacent hydrophilic pocket, releasing HCO_3^- into solution (Lindskog, 1997). The rate-limiting step of the reaction is the deprotonation of the water coordinated by the metal to regenerate the metal-hydroxide species, thus a new HCO_3^- may be produced (Supuran, 2016). Thus, it is the reaction of water with the metal active site and, specifically, the deprotonation of the water that limits the rate of the reaction. The protein active site environment is again important, with titratable amino acids in the vicinity being responsible as a proton acceptor and shuttle, facilitating the deprotonation to form the metal-hydroxide and thereby enhancing efficiency and enzymatic activity (Lindskog, 1997). In many cases,

the proton shuttle residue is a His in the middle of the active site, further assisted by a cluster of His extending to the outside of the enzyme, which remove the proton, preventing the backreaction of the released proton to return to the nascent hydroxide (Aggarwal *et al.*, 2015; Supuran, 2016). Both of these steps can be partially or completely disrupted by CA inhibitors, such as the membrane permeable ethoxyzolamide (EZ) that binds to the metal cofactor replacing the hydroxide (Baranauskienė and Matulis, 2012; Supuran, 2008).

The Cup proteins from cyanobacteria have been suggested to be CA-like proteins, since they are present in the CO_2-uptake systems and are not enclosed in the membrane, which suggest they are not the main proton transfer proteins, but are essential for CO_2-hydration activity (Price *et al.*, 2002). However, cyanobacteria do not have a true CA in the cytosol, since when a human α-CA II was heterologously expressed in *Synechococcus* sp. PCC7942 the strain developed a high CO_2-requiring phenotype (Price and Badger, 1989c). This is explained as being a result of non-native CA rapidly dissipating the non-equilibrium concentrations of bicarbonate that would otherwise accumulate in the cytoplasm due to the bicarbonate and CO_2 proteins of the CCM. Thus, the Cup protein cannot be simply a CA, but must have an energy source to help sustain the non-equilibrium concentrations of bicarbonate in the cytoplasm. Consistent with this, it is noted that the Cup proteins are not classified as being part of any CA family based upon sequence analysis, and if CA-activity is confirmed it will form a new CA group (Kupriyanova *et al.*, 2017).

Since NDH-1$_{3,4}$ purification has proven challenging, there are no published structural or biochemical analyses of Cup proteins (Zhang *et al.*, 2004; Zhang *et al.*, 2005). However, in the past, when no crystal structures were available for CA families, point mutations on conserved amino acids confirmed by multiple sequence alignments have proven to be useful in characterizing the active site. Studies on spinach CA with site direct mutants altering conserved cysteine to alanine, histidine to glutamine, aspartate to asparagine and glutamates to glutamine showed severe diminished catalytic activity and that the enzyme has a Cys-His-Cys-H_2O, with the catalytic Zn being coordinated by sulfur ligands (Bracey *et al.*, 1994). In *Chlamydomonas reinhardtii,* mutation of conserved amino acids Cys and His of the N-termini of CCM1, a low CO_2 regulatory protein, led to complete loss of zinc binding, decreased the amount of the expressed protein (Kohinata *et al.*, 2008). In Chapter 4 we show the results of point mutations on conserved amino acids of CupA and CupB, and the effect on its activity.

1.8 Questions and goals

CO_2 uptake systems are essential for the survival of many cyanobacterial organism as a scavenger for CO_2 and also have an exciting biotechnological potential in crop improvement projects (Price *et al.*, 2013). However, some key understanding of their molecular mechanisms is missing, and important questions remains unresolved. Given the NDH-1$_{3,4}$ complex is involved in the uptake of CO_2 (CO_2 hydration producing HCO_3^-), would CupA/CupB be a special type of (redox coupled?) carbonic anhydrase-like protein?

(Figure 19) Could point mutations in conserved histidine and cysteine trigger changes in Cup enzymatic activity by potentially disrupting the potential active site?

Our hypothesis is that CupA/CupB is a special type of carbonic anhydrase unique in cyanobacteria. Thus, site directed mutagenesis in conserved histidine and cysteine will change the activity of Cup proteins, affecting cell CO_2 uptake.

The aims of this study were:

- Develop a strain missing functional CO_2 systems by constructing gene knockouts of the whole *cupA* operon together with the deletion of *cupB*;
- Insert a synthetic molecular construct where *cupA* operon is under the regulation of *rbcL* promoter, making the native inducible system, now constitutive;
- Use site-directed mutagenesis to introduce amino acid substitutions in the protein. This would help identify functionally important sites by targeting highly conserved amino acids in the potential active site of Cup proteins according to their impact upon CO_2 uptake activity.

2 CHAPTER II

EXPERIMENTAL PROCEDURES

2.1 Materials and methods

In general, physiological experiments were performed on at least three biological replicates, with technical replicates within each biological replicate as noted. Standard deviation (SD) was calculated, typically using Excel (Microsoft) software, and presented as error bars in the graphs. Graphs were plotted using Kaleidagraph software (Synergy).

2.2 Culture and growth conditions

Wild-type *Synechocystis* sp. PCC6803 (WT) and mutants were maintained in standard BG-11 medium (Allen, 1968), pH 8, supplemented with 10 mM HEPES-NaOH. Cells from frozen glycerol (32% v/v) stock were grown in BG-11 pH 8 supplemented with 18 mM sodium thiosulfate and 1.5% agar. These were used to inoculate 100 mL of BG-11 in 250 mL Erlenmeyer flasks, kept on shaker at 180 rpm at 30°C, with illumination of approximately 50 μmol (photons) m^{-2} s^{-1} provided by Cool White fluorescent lamps.

Plates and liquid culture were supplemented with 5% CO_2 (flowing in the headspace of the shaking 250 mL Erlenmeyer flasks or in the atmosphere for solid agar growth plates) when necessary, and if later used for experiments.

Cultures in log phase of growth, usually from shaking culture, were used to inoculate 800 mL pH 8 media in 1 L Roux bottles, continuously bubbled (approximately 150 mL min^{-1}) with 3% CO_2, at 32°C (water bath) with light intensity of approximately 70 μmol (photons) m^{-2} s^{-1}. Cells were inoculated to a starting density of 0.04-0.10 OD_{750} grown with supplementation of 3% CO_2 were considered to be in high C_i (HC) condition, since both CO_2 and HCO_3^- were expected to be abundant. Antibiotics was added for maintenance of strains and segregation, but were not added when cells were to be used in physiological experiments: spectinomycin (Sp) 20 μg mL^{-1}, chloramphenicol 5 μg mL^{-1} (Cm), kanamycin (Km) 20 μg mL^{-1}.

Evaluation of growth characteristics using agar growth plate spot assays (Shibata *et al.*, 2001) used modified BG-11 at pH 7, buffered with 40 mM HEPES-KOH and no sodium carbonate was added (Holland *et al.*, 2016; Wang *et al.*, 2004). Cells were grown in 100 mL pH 7 liquid media with 5% CO_2 (flowing in the headspace of the shaking 250 mL Erlenmeyer flasks) until late log phase, when cells were collected, washed with either pH 8 or pH 7 media, and resuspended to OD_{750} 1, with serial dilutions to 0.1, 0.01 and 0.001. Five μL of each dilution were spotted on agar plates and grown for 5 days at 30°C with light intensity of approximately 40 μmol (photons) m^{-2} s^{-1}, with no supplemented gassing

or with 5% CO_2. Agar growth plate spot assays used BG-11 with pH 8 and pH 7 (modified), with 20 mM $NaHCO_3$ added when indicated.

The low C_i pH 7 modified BG-11 was shown to be useful for modulating C_i species concentrations, since in this conditions CO_2 is favored over HCO_3^- thus making cells primarily dependent upon CO_2 uptake. Cells grown at pH 7 for 48 h with 3% CO_2 later switched to gassing with air for 20-24 h were considered low C_i (LC). This condition is known to promote the expression of the LC inducible C_i transporters (Holland *et al.*, 2016; Wang *et al.*, 2004).

The majority of CO_2-enriched gassing described in this study involved a mixing system (Qubit, Canada) with the mixed gas flow humidified by bubbling through a flask containing water and sterilized passage through a 0.2 μm filter (Whatman Polydisc TF Filter, GE Healthcare) before reaching samples. Absorbance spectra and optical density due to scattering at 750 nm were measured with a UV–Vis Scanning Spectrophotometer (UV-2101PC, Shimadzu, Japan).

2.3 Strains and molecular constructs

Details of strains constructed for each study are detailed in its chapter methods section. In general, all DNA amplifications for constructions using the polymerase chain reaction (PCR) were performed using *Herculase* II fusion DNA polymerase (Agilent) with addition of 2% DMSO (dimethyl sulfoxide), following manufacturer instructions. The Gibson DNA fragment assembly technique (Gibson *et al.*, 2009) was applied in creating molecular

constructs in this study, first with homemade kits, later replaced with commercially available kits (New England Biolabs, NEB). *Escherichia coli* (*E. coli*) DH5α (NEB) was used for general plasmid maintenance, and plasmids were extracted with *E.Z.N.A.*® *Plasmid* Mini/Midi Kit (Omega, Bio-tec). Restriction enzymes employed in plasmid digestion were used following manufacture instructions (NEB). Molecular constructions were confirmed by sequencing at DNA/Protein Resource Facility at Oklahoma State University.

Synechocystis sp. PCC6803 (here *Synechocystis* 6803, Genbank GCA_000009725.1), a naturally transformable and glucose tolerant cyanobacterium, was used as the wild-type (WT) organism of study and the background strain for mutant construction. Transformation, where foreign DNA is introduced into *Synechocystis* 6803, was performed as previously described (Eaton-Rye, 2004). 100 mL of cells (from shaker) with OD_{750} of 0.6-0.9 were centrifuged at 4000 rpm for 10 minutes (min) at room temperature (RT), and resuspended in 2 mL BG-11 by agitation on a shaker. Later, 10 μg of DNA construct (plasmid or linear DNA) was added to 500 μL of cells with OD_{750nm} of 2.5, gently mixed and incubated for 5 hours (standing, with gentle mixing at 3 hours mark), at 30°C with light intensity of approximately 40 μmol (photons) m^{-2} s^{-1}, with no supplemented gassing or with 5% CO_2. Approximately 200 μL cells were spread plated onto sterile membrane filters (MF-Millipore Mixed Cellulose Ester Membranes, 0.45μm EMD Millipore), and laid onto BG-11 with 20mM $NaHCO_3$ incubated overnight in presence of 5% CO_2. Membranes were transferred to plates with antibiotics, later gradually increasing the

concentration (2.5-20 μg mL^{-1}). Generally, in cyanobacteria, single crossover events are significantly less frequent than double recombination, especially when the plasmid is introduced via transformation (Tsinoremas *et al.*, 1994). The integration of the construct into the targeted site was confirmed by PCR of a picked colony dispersed in a PCR tube or from genomic DNA.

Genomic DNA was extracted from 100 mL of cells (from shaker) in late log phase (10-14 days old), centrifuged 5000 *x g*, 10 min, RT and resuspended in 14 mL of 5X TE (50 mM Tris-HCl, 5mM Na_2EDTA, pH 7.6). Later samples were centrifuged 5000 *x g*, 10 min, RT and the pellet resuspended in 1.5 M KCl, and heated to 65°C for 20 min to inactivate endogenous nucleases. The solution was centrifuged 5000 *x g*, 10 min, RT, and after supernatant removal, the pellet was resuspended in 14 mL of 5X TE, centrifuged 5000 *x g*, 10 min, RT. The precipitate was resuspended in 3 mL of 5X TE with lysozyme (1 mg mL^{-1}) and held at RT for 20 min. Then I added 60 μL of 20% (w/v) SDS (sodium dodecyl sulfate) and 20% (w/v) Sarkosyl, plus proteinase K (100 μg mL^{-1}, Sigma) for cell lysis, and incubated overnight at 50°C with intermittent mixing. An equal volume of phenol: chloroform (1:1) was added to the solution, vortexed and centrifuged 10000 *x g*, 5 min at RT. The aqueous top phase was transferred to a new tube and an equal volume of chloroform was added and centrifuged 10000 *x g*, 5 min, RT, and this step was repeated. The upper layer was transferred to a new tube and equal volume of isopropanol was added, then placed at -20°C for two hours. Precipitation of DNA was achieved by centrifugation

at 10000 *x g*, 10 min, RT, with pellet resuspended in 400 μL 1X TE plus 200 μg mL^{-1} DNase-free RNase incubated at 37°C for 30 min. The phenol: chloroform extraction was repeated as described before. The aqueous top phase was transferred to a new Eppendorf tube with addition of one tenth volume of 3 M sodium acetate (pH 5.2) and 2.5 volumes of 100% ethanol, then stored at -20°C overnight. Precipitation of DNA was completed by centrifugation at 10000 *x g*, 20 min, RT, washed with 70% ethanol and dried using a Speed Vac (medium speed). The dried pellet was resuspended in 100 μL of water and quantified with NanoDrop 1000 (Thermo). This typically yielded approximately 100 μg of DNA. Later, this protocol was replaced by a genomic extraction kit (Quick-DNA™ Fungal/Bacterial Miniprep Kit, Zymo research) with lower yield but much less time consuming and still with high purity.

2.4 Cell sample preparation

HC cultures with OD_{750} between 0.5 and 0.8 (approximately 36-40 h) were collected by centrifuging approximately 200-400 mL at 6000 *x g*, 10 min, RT. A modified low C_i, low sodium (approximately 0.39 μM) BG-11 pH 7 media was used for the C_i depletion assays, similar to the one mentioned above, except that buffered with 50 mM Bis-Tris-Propane (BTP) and omitting sodium nitrate and gassed with N_2/O_2 mixed gas for C_i depletion. In order to obtain a C_i depleted samples, cells grown under HC were washed in this media twice (first with 40 mL and later 2 mL media), resuspended in about 5-10 mL to a

chlorophyll (Chl) density of 50-200 μg Chl mL^{-1}, shaking at 40 rpm in darkness for about 3 hours, and purged with N_2 gas before experiments.

HC cells were instead washed with standard BG-11 pH 8 bubbled with 3% CO_2 for 2-3 h. Chl concentration was measured after extraction in methanol (20 μL sample in 1mL final volume with methanol, vortexed and centrifuged at 10000 *x g*, 5 min, 4°C) using an extinction coefficient of 12.95 at 665 nm, and all experiments were performed at a final Chl concentration of 5 μg Chl mL^{-1} (Ritchie, 2006).

2.5 C_i affinity and oxygen evolution assays.

C_i affinity assays were performed using a water jacketed Clark-type electrode (Yellow Springs Instruments, OH, USA) system at 32°C, 1.8 mL sample volume, similar to previous described (Benschop *et al.*, 2003; Price and Badger, 1989a). C_i depleted cells were acclimated and further depleted by pre-illumination for about 10 min at approximately 800 μmol (photons) m^{-2} s^{-1} or until O_2 evolution ceased. This is called the compensation point, where rates of O_2 production (evolution) and consumption are comparable since C_i is limiting (Miller *et al.*, 1990). C_i uptake was measured in light after stepwise injections of bicarbonate, and O_2 evolution rates were recorded as a function of C_i added. To evaluate the effect of primarily CO_2 uptake, potassium bicarbonate ($KHCO_3$) was added in the presence of 25 μg mL^{-1} CA (approximately 87 W-A units, CA II, Sigma, USA). To evaluate the combined CO_2 uptake and HCO_3^- uptake, sodium bicarbonate ($NaHCO_3$) was used as source of bicarbonate. Rates were obtained using a linear regression fit from 10 to 50 s (40s

total) steady state data. V_{max} was obtained as the maximum raw rate at saturation. The estimated $K_{0.5}$ was used instead of Michaelis Menten K_m since multiple C_i transporters are usually present. $K_{0.5}$ was annotated as the C_i concentration required to half saturate the maximum rate.

2.6 Chl and NADPH fluorescence and P700 spectroscopy

Analysis of changes in activity of photosystem I and II were assessed by variations on reduction and oxidation of P700 and Chl fluorescence, respectively. Assays were performed as previously described in co-authored work from our laboratory (Holland *et al.*, 2016), but with small changes as noted below.

2.6.1 Chl and NADPH fluorescence

The DUAL-PAM-100 (Walz, Germany) was used so simultaneous measurements of Chl a and NADPH fluorescence could be followed. The pulse amplitude modulated (PAM) fluorometer had attached an emitter-detection-cuvette assembly (ED-101US/MS), with the DUAL-DR mode that contains a single red (620 nm) for measuring light (ML), plus a LED Array (COB, 24 reds, 635 nm) for actinic light (AL), saturating and multiple turnover pulses (SP and MT, respectively). In front was a system that allows NADPH fluorescence to be measured, the detector 2 with the DUAL-ENADPH (emitter) with a measuring light (365nm) at a 90° angle from the DUAL-DNADPH (detector), a blue-sensitive photomultiplier (420-550 nm light), and ML intensity 8 was used for the experiments. Samples with Chl density of 5 μg Chl mL^{-1} were loaded in a glass cuvette (1 cm) and placed

in the ED-101US/MS. Dark adapted samples (4 min with stir, 1 min without) were exposed to actinic illumination (AL, 53 μmol (photons) m^{-2} s^{-1}, ML=12 μmol (photons) m^{-2} s^{-1}) with multiple turnover flashes (20,000 μmol (photons) m^{-2} s^{-1}) applied for 300 milliseconds on five minute traces (at 15, 300, and 540 seconds) or without when one minute analysis was followed. Before AL was turned on, fluorescence traces were measure for 60 or 10 seconds in dark, and post-illumination fluorescence was followed for an additional 200 or 190 seconds and the program was terminated. The short, one minute trace had samples pre-illuminated for 4 min (53 μmol (photons) m^{-2} s^{-1}) before dark adaptation. The pre-illumination causes the products of photosynthesis to accumulate enabling the detection of fluorescence transients due to reductant entering the PQ pool from cytoplasmic sources (e.g. sugar oxidation via the pentose phosphate pathway). The precise program was designed with the DUAL-PAM-100 software on trigger mode. Traces were acquired at a rate of one point per millisecond, with a total of 1024000 points collected, later smoothed with a running average of 300 points. Traces shown are typical (n= 3-8) and maximal fluorescence (F_m') was verified by the addition of 10 μM DCMU. Ethoxyzolamide (EZ) 200 μM was added when indicated.

2.6.2 P700 spectroscopy

P700 absorbance was measured with JTS-10 (LED pump-probe spectrometer, Bio-Logic, France) with 705 nm interference filters over sample and reference photodetectors. Cells were dark-adapted (4 min with stirring on and 1 min off) before measurements in a glass

cuvette (1cm). Samples with Chl density of 5 µg Chl mL^{-1} were illuminated for 5 seconds with 2050 µmol (photons) m^{-2} s^{-1} red AL (620 nm). DCMU 10 µM (3-(3,4-dichlorophenyl)-1,1-dimethylurea) was used when measuring cyclic electron flow, since it blocks the electron transfer between Q_A and Q_B sites at PSII. The program used was the 5 s illumination (excitation PSI +PSII and decay), ensuing 10 s dark for a baseline of the P700 state before 5s AL followed for 8s once light was terminated (D, detection pulse): 3(10msD)10sD2(10msD)10msG200µsD1msD1msD3msD(3ms,30,5s,D)100µsH200µsD(2ms,20,8s,D). Data analysis was done using Bio-Logic software to obtain half times of oxidation and reduction, later converted to apparent rate constants (*k*), by dividing ln2 by the half times.

2.7 SDS-PAGE and Immunoblot analysis

Approximately 400-600 mL of cell culture was harvested from HC, HC after C_i depleted treatment or LC grown cells and centrifuged at 6000 *x g* for 10 minutes, RT. Whole cells were collected, resuspended in 25 mM Tris-HCl pH 7.5 buffer and stored frozen (-80°C) until protein analysis, following established protocol (Holland *et al.*, 2016). Samples were diluted to a density of 1 mg Chl mL^{-1}, broken with 0.1 mm zirconium beads (1:1) in a Bullet Blender (Next Advance Inc., USA) (beat 1 min, intensity 5, rest 4 min on ice; repeated 1 time) in the presence of 1mM ε-aminocaproic acid, benzamidine and PMSF, at 4 ºC, to decrease protease activity. After centrifuging at 1000 *x g* for 1 minute, the supernatant was collected, adjusted to 100 µg Chl mL^{-1} , and sample was further solubilized

by addition of 2% SDS and 5 mM DTT (dithiothreitol), heated at 65°C for 10 min, and separated on SDS-PAGE (8% stacking, 12% resolving; 0.5 mm) (Laemmli, 1970). 1 µg Chl was added to 2x SDS sample buffer (125 mM Tris-HCl pH 7.5, 20% glycerol, 2% SDS, 0.02% bromophenol blue, 5% β- mercaptoethanol) and loaded in the gel. Electrophoresis was performed at 100 V for approximately 2 hours at RT.

Protein content was transferred to a PVDF membrane using a Bio-Rad semi-dry apparatus (25 V, 25 minutes) in the presence of Towbin buffer (25 mM Tris, 192 mM glycine, 20% methanol) supplemented with 0.03% SDS (w/v) and membrane was stained with 0.5% Ponceau S (Sigma) to verify equal loading. After washes with water to remove excess of dye, membranes were washed two times with 5% bovine serum albumin (BSA) in TBS (50 mM Tris-HCl, 150 mM NaCl, pH 7.5) with 0.2% Tween 20 (TBST) for 15 minutes and blocked by a 45 minute incubation with 5% BSA in TBST under gentle agitation (50 rpm) at RT. The membranes were incubated overnight in primary antibody (rabbit anti-SbtA; 1:2000 dilution, Agrisera, Sweden; or goat anti-CupA, 1:750 dilution) in 5% BSA and TBST at RT with gentle agitation. After incubation, membranes were washed three times in TBST for 15 minutes. Antibodies of anti-rabbit HRP-conjugated goat antibody (1:3000, Bio-Rad) or anti-goat HRP-conjugated rabbit antibody (1:1000, Bio-Rad) were used respectively as the secondary antibody diluted in 5% BSA and incubated for 2 hours at RT while gently shaking. After incubation, membranes were washed two times in TBS (no Tween) for 15 minutes. Development was obtained using the chromogenic substrate 4-chloro-1-naphthol (4CN, Bio-Rad) and H_2O_2 (60 mg of 4CN, 20 mL methanol, 60 µL 30%

H_2O_2, volume to 100 mL with TBS). Following color development (visible bands), it was terminated by washing with water, then membranes were dried, photographed, and stored at RT in dark.

3 CHAPTER III

HETEROLOGOUS EXPRESSION OF CupA

3.1 Introduction

Global human population has been on a steep growth curve, raising problems such as high CO_2 air levels (Farrelly *et al.*, 2013; Notz and Stroeve, 2016) and predicted future food shortage (Hibberd *et al.*, 2008; Parry and Hawkesford, 2010). Several research groups are invested in incorporating cyanobacterial components into plants in the hope to enhance crops yields (Lin *et al.*, 2014; Ort *et al.*, 2015).

Numerous plants used as food source are C3 plants, including rice, wheat, potato, oat, soybean, spinach, among others. C3 plants have high rates of photorespiration, the wasteful process where Rubisco (ribulose bisphosphate carboxylase/oxygenase) uses O_2 instead of CO_2 (Zhu *et al.*, 2010). These plants use a carbon fixation cycle similar to cyanobacteria, except lack a CO_2 concentrating mechanism (CCM) (Price *et al.*, 2013). Recently, projects are in progress investigating the possibility of introducing cyanobacterial CO_2

concentrating mechanisms into C3 plants (Long *et al.*, 2016; McGrath and Long, 2014; Price *et al.*, 2013).

Heterologous expression of CCM components in model organisms such as *Escherichia coli* (*E. coli*) is important so the systems involved can be further characterized, and feasibility of functional expression assessed before introducing in plant chloroplasts. Previous studies were successful in expressing functional bicarbonate transporters (Du *et al.*, 2014) and carboxysomes (Bonacci *et al.*, 2012) from cyanobacteria in *E. coli*. This Chapter 3 focuses on the efforts, struggles and achievements in the attempt of heterologous expression and characterization of *Synechocystis* 6803 CO_2 uptake protein CupA in *E. coli*.

3.2 Material and Methods

3.2.1 Molecular Construction

The gene *sll1734 cupA* from *Synechocystis* 6803 was amplified by PCR with Herculase II Fusion DNA Polymerase (Agilent, USA) following manufacturer's instructions. Using the Gibson Assembly technique (Gibson *et al.*, 2010) and kit (NEB, USA), the insert was assembled into a pMAL c5x vector (NEB, USA), between NotI and EcoRI sites. PCR fragment and digested plasmid were separated on 1% Agarose gels, and bands with appropriate size were extracted with QIAquick Gel Extraction Kit (Qiagen), then samples were used for Gibson Assembly. The pMAL c5x vector plasmid has a *malE* gene coding a maltose binding protein (MBP), and the *cupA* gene was inserted at the end of *malE* so that

a fusion protein with the MBP may be expressed at the N-terminus. At the end of *malE* the plasmid has an enzymatic cleavage site for factor Xa, allowing the separation of MBP and CupA. Three other similar systems were constructed using vectors kindly provided by Junpeng Deng (OSU, USA): pMBP, a pet28b vector derivative with the *malE* gene containing modifications to enhance yields and a TEV proteolytic site for between MBP and the protein of interest; W480 and W479 vectors, similar plasmids containing a few modifications, where MBP is expressed with or without a non-cleavable linker between the proteins. The latter constructions were made in duplicate, each with or without a 6x His-tag at the C-terminus of CupA. The plasmids were transformed into *E. coli* DH5α (NEB, USA), then purified using E.Z.N.A Plasmid Extraction kits (Omega Bio-tek, USA).

3.2.2 Expression of CupA protein in E. coli

Constructed plasmids were transformed into *E. coli* BL21(DE3) (NEB, USA). This strain allows the expression of MBP:CupA fusion protein under the strong promoter P_{Tac} and has the Lac operon, which allows expression induction by IPTG (Isopropyl β-D-1-thiogalactopyranoside).

Cells were stored frozen as 16% glycerol stocks at -80°C and grown in plates with LB media (tryptone, yeast extract, NaCl, 10, 5, 5% w/v, respectively) supplemented with 1.4% (w/v) agar. One colony was used to inoculate 50 mL LB media, used as the pre-inoculum culture, grown at 37°C, 250 rpm, overnight. Kanamycin (Km) or Ampicillin (Ap) were

added at final concentrations of 20 and 100 μg mL^{-1}, respectively, as needed in this 'starter culture'.

The starter culture was then used to inoculate 250 mL LB, in duplicate, containing 0.2% (w/v) glucose and appropriated antibiotic (for pMAL, Ap 100 μg mL^{-1}), with growth at 200 rpm, room temperature (RT). When OD_{600} reached 0.6, IPTG 0.3 mM and $ZnCl_2$ 10 mM were added to induce the expression and cultures were moved to 18°C, 250 rpm, overnight. The pre-inoculum culture was also used to inoculate a control, 50 mL LB media, grown similar to the induced condition, lacking just IPTG supplement to serve as an un-induced control. Cells were obtained by centrifugation (4500 *x g*, 20 min, RT), pellet was snap froze with liquid nitrogen and kept at -20°C until next step.

3.2.3 Protein purification,

Pellet obtained was shortly thawed and resuspended in 50 mL column buffer (CB) containing 20 mM Tris-HCl pH 7.4, 200 mM NaCl, 1 mM sodium azide and 10 mM β-mercaptoethanol, with 1 mM of PMSF, Benzamidine and ε- Aminocaproic acid, and sonicated (20 s pulse, amplitude 50mA). Supernatant was obtained (12500 *x g*, 25 min, 4°C) and loaded in a column containing amylose resin (NEB). After washes (8 column volumes) with CB buffer, the fusion protein was eluted elution Buffer (EB: 20 mM Tris-HCl, 200 mM NaCl, 1 mM EDTA, 1 mM sodium azide, 10 mM β- mercaptoethanol, 10 mM maltose) and cleaved with Factor Xa (NEB), in buffer (20 mM Tris-HCl pH 8.0 with 100 mM NaCl and 2 mM $CaCl_2$) incubated for 6 hours at RT, later dialyzed in buffer (20 mM

Tris-HCl, 6 M guanidine hydrochloride, pH 7.4) for 4 hours, at 4°C. This was loaded to the amylose column and flow through was concentrated in an Amicon Ultra centrifugal filter unit (Ultra-15, MWCO 30 kD, Sigma). Protein samples from each purification step were collected, then proteins concentrations were quantified using Bradford protein assay (Bio-Rad). Protein samples (non-induced, induced, after 1st column, once cleavage, after 2nd column) with ~10 μg were analyzed by 12% SDS-PAGE.

After separation of the proteins, the band ~47 kD (see Figure 5) was cut with a blade, digested with trypsin, and analyzed by LC-MS/MS. Protein band was prepared for mass spectrometry and analyzed as previously described (Voruganti *et al.*, 2013), except using a 75 min acetonitrile gradient to develop 40 cm long columns packed with 3 micron Magic AQ C18 beads (Bruker) heated to 55°C to reduce backpressure. Columns terminated with a stainless steel emitter were used to generate ions in a Nanospray Flex ion source (Thermo Fisher Scientific). Relative protein levels were quantified using intensity based absolute quantification (iBAQ) (Schaab *et al.*, 2012; Schwanhäusser *et al.*, 2011), using MaxQuant version 1.5.3.8 (Cox *et al.*, 2014; Cox and Mann, 2008) to search the raw LC-MS/MS data files including the established parameters. MaxQuant output was analyzed within the Perseus 1.2.0.16 framework (Cox and Mann, 2012; Tyanova *et al.*, 2016). The database used were *Escherichia coli* and *Synechocystis* sp. PCC 6803.

3.2.4 Antibody production

After confirming that the band with approximate 47 kD was CupA in the mass spectrometry data, polyclonal antibodies against CupA protein were obtained by immunization of a goat (Bob, Triple J Farms, Jorgensen & Son's LLC, Bellingham, WA). The proteins for the immunization were obtained from bands cut out from several 12% SDS-PAGE. Bands were homogenized in an electrically driven glass-teflon homogenizer in buffer (137 mM NaCl, 1.5 mM KH_2PO_4, 1.8 mM Na_2HPO_4, 2.7 mM KCl, pH 7.0). Approximately 100 μg of protein homogenized was injected into one goat, with booster injections repeated with three-week intervals, and a test bleed about 12 days after the third immunization. The coagulated serum from was collected by centrifugation (10,000 rpm, 10min, RT) and stored at -20°C until use.

3.2.5 CD spectroscopy

Far-UV Circular dichroism spectra was recorded on a J-815 spectropolarimeter (Jasco Inc., Easton, MD), as previous described (Adam *et al.*, 2012). The fusion protein MBP-CupA purified was measured in a buffer consisting of 20 mM potassium phosphate buffer (pH 7.0) with 150 mM NaCl. Results are an average of three measurements.

3.2.6 Zn binding evaluation and CA activity

Preliminary analysis with the fusion protein MBP-CupA purified were performed in order to investigate metal (Zn) presence following previous described protocol (Klemba and Regan, 1995). CA activity analysis was accordantly to established methods involving

spectroscopic evaluation, using an indicator dye, of pH changes associated with CO_2 hydration (Lotlikar *et al.*, 2013).

3.3 Results

3.3.1 Genetic systems for heterologous expression of CO_2-uptake protein CupA in E. coli.

Plasmids containing MBP were used to facilitate the expression of CupA, increasing protein solubility, and stability. Initially, multiple constructions were developed, and later the most promising one was used for further studies. Several attempts using different constructions were performed and different purification strategies were employed. As discussed below, the protein proved very difficult to work with unless it remained as a fusion protein with the MBP. For example, initial attempts to purify the protein using only a His-tag, a common strategy, failed since there was little accumulation of the protein either in the soluble or insoluble fractions of any of the heterologous *E. coli* expression hosts employed. Successful accumulation was only observed in the family of MBP-CupA fusion protein expression vectors that I constructed. An example of the construction procedure can be seen in Figure 4. The plasmid pMAL c5x vector (NEB, USA) has a Xa cleavage site that allows separation of the fused proteins (Figure 5A). However, since commercially available Factor Xa can be expensive, a plasmid containing the site for TEV was used (pMBP), yet the cleavage seemed to be less specific and resulting proteins yields were

suboptimal. Two systems allowing non-cleavable fusion between MBP and CupA were also constructed, with an amino acid linker AAAEF in W480 or without in W479. The W480 MBP-CupA systems showed good expression, with yields similar to the commercial vector, however due to problems characterizing the fusion proteins (discussed more below), no further studies were performed. The whole *cupA* operon or ndhF3-ndhD3-cupA components were inserted into W480 (with and without MBP fused to CupA) and also into a modified pET28b (Bose *et al.*, 2002) using a BL21 (DE3) *E. coli* expressing strain. Results showed problematic expression, so a LEMO21(DE3) *E. coli* strain optimized for the expression of membrane proteins (Schlegel *et al.*, 2012) was attempted, with little success, and heterologous studies were abandoned.

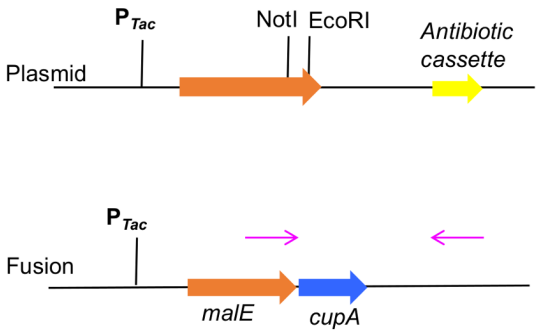

Figure 4. Model of the strategy used to clone *Synechocystis* 6803 CupA into *E. coli*. A plasmid containing the gene *malE* coding for maltose binding protein was used and *cupA* gene was introduced by Gibson assembly between the restriction endonucleases sites for NotI and EcoRI. Arrows in pink represent primers used for sequencing.

The proteins resulting from the expression of the molecular construct pMAL c5x MBP-CupA had significant yields and can be seen on Figure 5, with the fused protein presenting a voluminous band around 90 kD. However, upon cleavage of CupA from the MBP and further purification, much of the desired product compared to the fused protein decreased, as result of loss of the CupA polypeptide (not shown), possibly due to precipitation. This is not likely due to low water solubility, at least based upon consideration of the primary amino acid sequence, which predicts a highly soluble protein. Speculatively, the loss of the protein could be due to its inability to fold resulting in aggregation and/or precipitation onto the surfaces of the purification vessels. The W480 MBP-CupA system contacting a His-tag was also evaluated by further purification of CupA using size exclusion chromatography in Dr. Deng's lab (S200, not shown) showing aggregates formation, suggesting that the losses that were occurring were indeed due to aggregation. Purification of His tagged MBP-CupA, after cleavage of MBP, using nickel columns (Ni-NTA Superflow, Qiagen) was unsuccessful, with CupA being lost, even in the presence of n-Dodecyl-β-D-maltoside (DDM/DM), a maltoside based non-ionic "gentle" detergent.

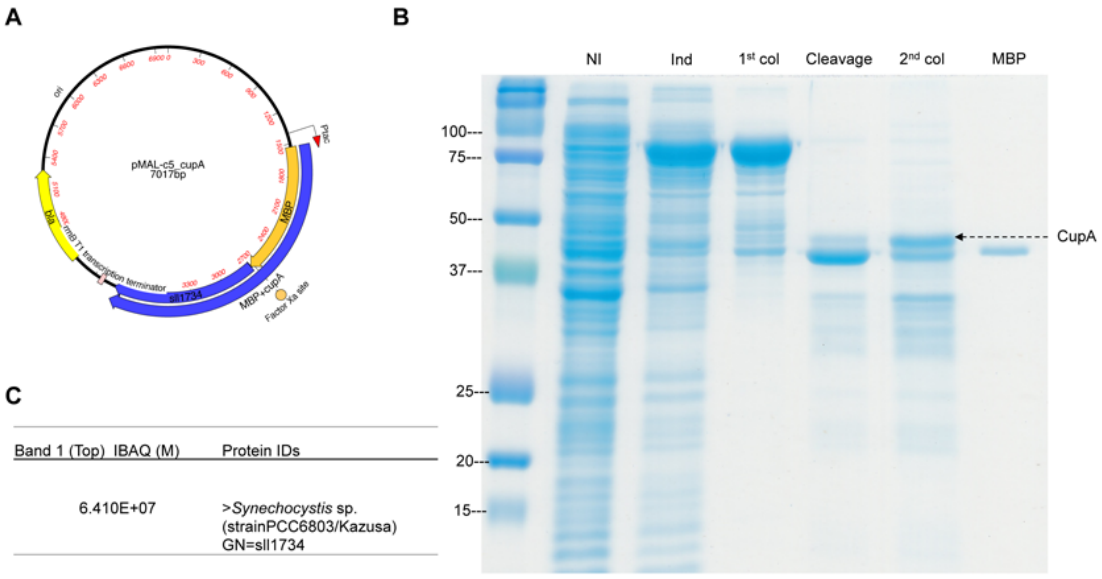

Figure 5. Heterologous expression of CupA, purification and antibody production. A) Construction of pMAL-c5_cupA, for fusion of MBP and CupA proteins. B) Gel analysis of CupA at various stages of purification (SDS-PAGE 12%). M: Marker (Precision Plus Protein Kaleidascope, Bio-Rad); NI: Non-induced cells; Ind: Induced cells; 1st col: 1st amylose column with elution buffer; Cleavage: After cleavage with Factor Xa; 2nd col: after 2nd amylose flow through; MBP: control, MBP5 (42.5 kD); fusion MBP-CupA (90 kD); CupA (~47 kD); Factor Xa (43 kD). C) Confirmation of CupA protein as component of 47 kD band by mass spectrometry analysis.

Still, we were able to collect enough purified CupA protein from excising multiple ~47 kD bands, separated in SDS-PAGE after a second amylose column purification (Figure 5B). Mass spectrometry confirmed its identity as *Synechocystis* 6803 CupA protein (Figure 5C). Several bands with the identified CupA were extracted, homogenized and used to raise antibody against CupA.

3.3.2 Analysis and immunodetection of CupA

In order to verify the presence of CupA protein from the NDH-1_3 CO_2 uptake system, we produced antibodies against the whole protein CupA, heterologously expressed in *E. coli* BL21(BE3) as a fusion with MBP at the N-terminus. The purified fused protein was proteolytically cleaved and the CupA polypeptide moiety was separated by SDS-PAGE (Figure 5B). The electrophoretic band was excised, verified by mass spectrometry of tryptic fragments, and after homogenization in Tris pH 7.5 the preparation was used for four injections in one goat (Triple J Farms, Bellingham, WA, USA). The serum was collected and used for immunoblotting, with successful visualization of a band at 47 kD (see Chapter 4, Figure 10).

This antibody was later used to evaluate and confirm the deletion and restoration of the *cupA* operon in the C2 and C2A strains, respectively, probing immunoblots of whole cell lysates (Figure 10). As shown in Figure 10A, a reaction is observed at the expected 47 kD mass of CupA in the wild-type grown under LC conditions, and CupA is expressed under both HC and LC growth, yet, no reaction was observed for C2 strain, as expected. See Chapter 4 for more discussion on these results.

3.3.3 Investigation of protein structure-function

The MBP-CupA fusion was analyzed with Far-UV CD spectroscopy to investigate the secondary structure. The resulting graph (Figure 6) indicate that the fusion contains a

significant proportion of α-helical structure. However, analysis of the secondary structure ratios showed that about 26 ±5 % was "disordered", that is, no detectable structure.

The detection of zinc in the fusion MBP-CupA was also explored following previous protocol (Klemba and Regan, 1995), but no signal was detectable (data not shown). Additionally, carbonic anhydrase activity was surveyed with a traditional pH change technique. Bovine αCA II (Sigma) was used as control, and a signal was noted. However, no indication of CO_2 hydration was observed for the heterologous expressed MBP-CupA fusion (data not shown).

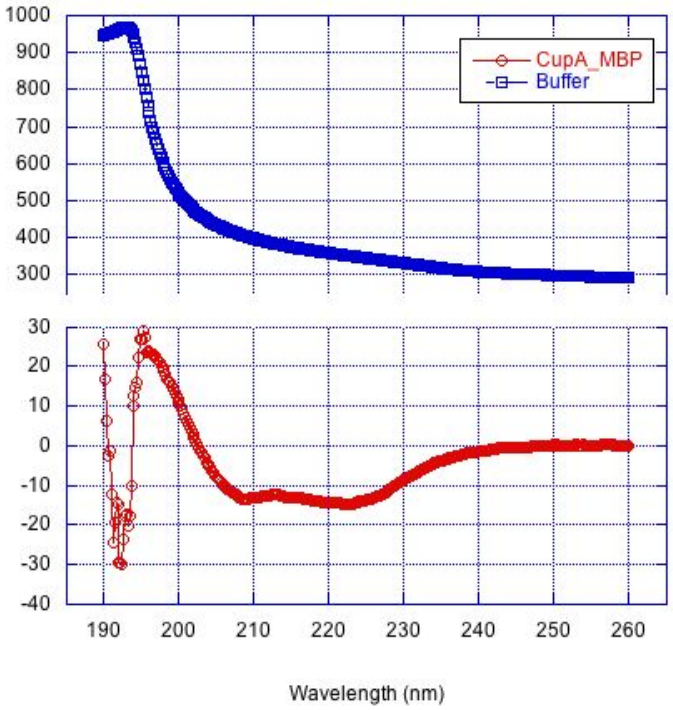

Figure 6. CD spectra of fusion protein MBP-CupA. Far-UV spectra analysis showing a CD spectrum related to α-helix conformation as protein secondary structure. Blue traces are buffer

signals used for baseline; Red traces represent average of three replicates of MBP-CupA fusion protein analysis.

3.4 Discussion

This study shows for the first time the expression of a cyanobacterial CO_2 hydration protein, CupA, which was difficult and succeeds after many previous failed attempts (Prof. Dear Price, Australian National University, personal communication) (Price *et al.*, 2002). The basis for the successful expression was to couple what appears to be a very unstable and, apparently, difficult to fold protein, CupA, with a highly stable and highly soluble protein, MBP. Although we were unable to make a preparation with detectable CA activity, the expression strategy allowed us to produce a highly specific antibody against CupA (see more discussion in Chapter 4, Figure 10). This was used to confirm presence/absence on CupA proteins in studies presented in this dissertation and will be of great help on future studies of NDH-1$_3$ and cyanobacterial CCM.

Interestingly, the results from MBP-CupA fusion far-UV CD spectroscopy used to investigate the secondary structure content shows that the fusion contains a significant proportion of α-helical structure. However, analysis of the secondary structure ratios showed that about 26 ±5% was unstructured. It is possible that the α-helical structure data is from the MBP structure, which has a highly α-helical structure (Pioszak and Xu, 2008). Hence, the CupA would be the unstructured portion, although bioinformatic analysis (see Chapter 5) suggests abundant α-helical structures. It is possible that CupA is only

structured and functional when attached to the NDH-1_3 complex, which would explain the lack of CA activity and metal cofactor detection. From a physiological point of view, this may reflect the evolution of a system that only exhibits CA activity once it is coupled to the NDH-1 complex, thereby preventing the lethal expression of free, uncoupled CA activity in the cytoplasm, which has been shown to destroy the accumulation of HCO_3^- in the cytoplasm by the CCM (Price and Badger, 1989c).

The possibility of the whole *cupA* operon expression being functional in *E. coli* needs to be further explored. Development of cells lines that allow modulated expression of membrane proteins are promising (Schlegel *et al.*, 2012; Wagner *et al.*, 2008). The molecular constructs presented in this Chapter 3 may be used for this analysis. The heterologous expression of a functional CO_2 hydration system is of great interest, with potential for insertion into chloroplasts, which would help raise internal C_i concentration by reducing CO_2 leakage, increasing CO_2 availability as substrate for Rubisco (Long *et al.*, 2016; Price *et al.*, 2013).

4 CHAPTER IV

SYNTHETIC DNA SYSTEM FOR STRUCTURE-FUNCTION STUDIES OF THE HIGH AFFINITY CO_2 UPTAKE NDH-1_3 PROTEIN COMPLEX IN CYANOBACTERIA [ǂ]

[ǂ]This chapter is reproduced with slight modification from the following publication:

Artier, J., Holland, S. C., Miller, N. T., Zhang, M., & Burnap, R. L. (2018). Synthetic DNA system for structure-function studies of the high affinity CO_2 uptake NDH-1_3 protein complex in cyanobacteria. *Biochimica et Biophysica Acta (BBA)-Bioenergetics*.

4.1 Introduction

Cyanobacteria evolved multiple mechanisms to adapt and survive adverse conditions, including changes in the concentration of CO_2 in the atmosphere. The CO_2-concentrating mechanism (CCM, Figure 7) is a complex network of inorganic carbon (C_i: HCO_3^-, CO_2) transporters and the carboxysome (Burnap *et al.*, 2015; Price, 2011).

The carboxysome is a bacterial microcompartment that contains Rubisco, which is the major carbon-fixing enzyme of the photosynthetic Calvin-Benson-Bassham (CBB) cycle, the main pathway for the assimilation of C_i into sugars. The overall function of the CCM is to provide Rubisco with sufficient concentrations of CO_2 to catalyze the carboxylation of the CBB intermediate ribulose 1,5-bisphosphate (RuBP) and to avoid the wasteful competing oxygenation reaction which occurs when O_2 outcompetes CO_2 at the Rubisco active site. This wasteful dissipation of RuBP through the competing oxygenation reaction is referred to as photorespiration and requires an energy consuming scavenging pathway to recover the lost CBB cycle intermediate. The basic biochemical problem is catalytic performance of Rubisco (reviewed in (Hanson, 2016)). Like other forms of the enzyme, the cyanobacterial Rubisco exhibits a low affinity for CO_2 (typically around 150 μM) and a slow intrinsic catalytic turnover time (~100 milliseconds). These characteristics necessitate high cellular concentrations of Rubisco and/or CO_2 to meet the demands for RuBP of the CBB cycle. However, this is confounded by the fact that ambient inorganic carbon concentrations are often limiting (<20 μM). Moreover, the ambient concentration of O_2 is comparatively high and exacerbated by photosynthetic O_2 production on photosystem II (PSII), known as O_2 evolution. This combination of low C_i availability, slow intrinsic catalytic turnover of the carboxylation reaction, and high O_2 concentration ostensibly favors the wasteful photorespiratory pathway and, yet, the actual measured rates of photorespiration are paradoxically low in cyanobacteria (Eisenhut *et al.*, 2008). The cyanobacterial CCM overcomes the potential problem of photorespiration by concentrating

bicarbonate (HCO_3^-) in the cytoplasm to high levels (20-40 mM), where it can diffuse into the carboxysome, which besides Rubisco, contains a specialized carboxysomal carbonic anhydrase (CA). The ensuing HCO_3^- dehydration reaction catalyzed by CA thereby saturates Rubisco active sites and thus enables efficient photosynthetic carboxylation and a minimal level of photorespiratory oxygenation (Price *et al.*, 2008).

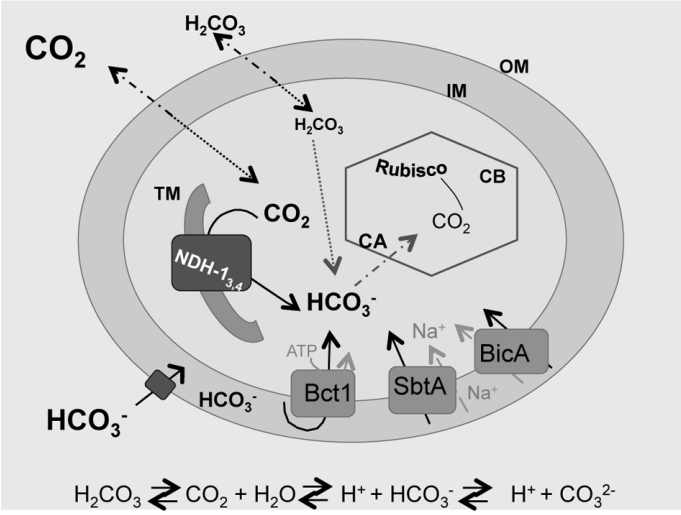

Figure 7. Schematic drawing of cyanobacterial CCM (β-type) showing the five known C_i transporters and the carboxysome (CB), which houses the carbonic anhydrase (CA) on the shell and Rubisco inside as is found in *Synechocystis* sp. PCC6803. Two Type-1 NADH dehydrogenase complexes (NDH-1) are known CO_2 uptake (CUP) systems present on the thylakoid membrane (TM). NDH-1_4 is the constitutive system, and NDH-1_3 is the low C_i (LC) inducible one. Among the three bicarbonate transporters present on the inner membrane (IM), two (SbtA and BicA) are sodium symporters and one (BCT1) is an ABC-type transporter. Inorganic carbon (C_i) is present in water as the dehydrated (CO_2) or hydrated (HCO_3^-) form and equilibrates quickly, as shown by the equation. Bicarbonate is transported through the outer membrane (OM) into the periplasmic space. For more information, see reviews (Burnap *et al.*, 2015; Price, 2011).

The accumulation of high concentrations of cytoplasmic HCO_3^- is achieved by the combination of five transport/uptake components of the CCM, including active uptake bicarbonate transporters located in the cytoplasmic membrane and CO_2 uptake enzymes situated in the thylakoid membrane, which function to convert dissolved CO_2 into HCO_3^-. There are three known bicarbonate transporters systems in the inner membrane, BCT1, SbtA and BicA, powered either by ATP (BCT1) or a Na^+ gradient (SbtA and BicA). Dissolved CO_2 and H_2CO_3 can passively enter the cell wall, possibly via aquaporins (Ding *et al.*, 2013; Tchernov *et al.*, 2001). Yet, as internal C_i is present as HCO_3^-, it can naturally be converted to CO_2 or leak from the CB. In addition, there are two types of CO_2 uptake proteins, each functioning only when complexed with Type-1 NAD(P)H dehydrogenase complexes (NDH-1) (Figure 2 and 3). These are forms of the NDH-1 complexes known to function in respiratory metabolism in bacteria and mitochondria, and in photosynthetic cyclic electron flow (CEF) in plant and algal chloroplasts.

In cyanobacteria, NDH-1 complexes are expressed in several forms (reviewed in (Battchikova *et al.*, 2011a; Ma and Ogawa, 2015; Price *et al.*, 2008). *Synechocystis* sp. PCC 6803 has four types of NDH-1 complexes (1 NDH-1_1- NDH-1_4) where two are involved in the CO_2 uptake system (Maeda *et al.*, 2002; Shibata *et al.*, 2001). All four have a multi protein core, with about 11 proteins homologous to Complex 1 in *Escherichia coli* (Battchikova *et al.*, 2011a). The function of the complexes is dependent on the proteins that are attached to the core, with multiple NdhD and NdhF paralogs defining the variants (Battchikova *et al.*, 2011a). Two forms, NDH-1_1 and NDH-1_2, function in both respiration

and photosynthetic CEF. The other two forms, NDH-1_3 and NDH-1_4 contain CO_2-uptake proteins (Cup, or alternatively, CO_2-hydration protein, Chp) and may couple energy of electron flow to energetically driving the hydration of CO_2. This capacity to couple CO_2-hydration to electron flow contributes to the high and far-from equilibrium concentrations of cytoplasmic HCO_3^- (Arteni *et al.*, 2006; Battchikova *et al.*, 2011a; Folea *et al.*, 2008; Ohkawa *et al.*, 2000a; Zhang *et al.*, 2004). The ability to enzymatically couple CO_2-hydration to metabolic energy also distinguishes the Cup proteins from typical carbonic anhydrases, which operate to accelerate an equilibrium between CO_2 and bicarbonate, rather than drive the reaction far-from-equilibrium as with the Cup proteins.

NDH-1_4 (also known as NDH-1MS') is a constitutive CO_2 uptake system that is composed of three proteins, NdhF4, NdhD4 and CupB (or ChpX in *Synechococcus* sp. PCC 7942). NDH-1_3 (also known as NDH-1MS) is induced under low C_i (LC) conditions, having NdhD3, NdhF3, CupA (or ChpY in *Synechococcus* sp. PCC 7942) and CupS, all expressed part of the *cupA* operon. The CO_2 hydration mechanism, typically referred to as the CO_2-uptake or 'Cup' system, remains enigmatic and requires further study. The poorly understood mechanism may involve a possible special type of carbonic anhydrase CupA and CupB and proton transport (involving NdhD3F3 and NdhD4F4) as constituents (Han *et al.*, 2017; Price *et al.*, 2002). It is known that the carbonic anhydrase inhibitor ethoxyzolamide (EZ) decreases CO_2 uptake in cyanobacteria (Price and Badger, 1989a; Price and Badger, 1989b; Tyrrell *et al.*, 1996). However, the mechanism of their action remains obscure, though the preponderance of evidence suggests that they affect CO_2

uptake, rather than bicarbonate transport. The dependence upon the core NDH proteins (Han *et al.*, 2017) would indicate an energized system utilizing the redox power of NADPH or reduced ferredoxin (Fd) (reviewed by (Battchikova *et al.*, 2011a). However, how CO_2 uptake is associated with the photosynthetic electron transport remains unclear. To better understand the mechanism of the Cup complexes, we developed a knockout mutant lacking genes necessary for the function of NDH-$1_{3,4}$, referred to as C2. Later we reintroduced the genes for NDH-1_3 (*cupA* operon) under the regulation of a Rubisco promoter integrated on a neutral site (NS), a mutant referred here as C2A. Here we describe the physiological effects of cyanobacterial strain with a constitutive expression of the NDH-1_3 system under high C_i (HC) and after depletion of C_i.

4.2 Materials and Methods

4.2.1 Constructions of mutants

Synechocystis sp. PCC6803 (here *Synechocystis* 6803, Genbank GCA_000009725.1), a naturally transformable and glucose tolerant cyanobacteria, was used as the wild-type (WT) organism of study and the background strain for the mutants' construction. The mutants were constructed sequentially to eliminate the CO_2 hydration function based on NDH-1 complexes. First, for the C1 mutant, all genes involved on NDH-1_3 (NdhF3/D3/CupA/CupS) were deleted. These genes are clustered under an operon in *Synechocystis* 6803, containing five genes (5917 bp). The genetic construct was designed

using MacVector software and then synthesized by Blue Heron Biotechnology Inc. Using the Blue Heron pUC plasmid (3150 bp, derivative of pUC119), 501 bp upstream region and 526 bp downstream region of the native *cupA* operon were added, between HindIII and EcoRI sites forming the pCUPopsap (Blue Heron Biotechnology Inc.). Two SapI/BspQI sites were added between the upstream and downstream region. Later, these used to introduce the spectinomycin resistance marker cassette from the vector pRL277, also containing *sacB* gene, conferring sucrose sensitivity, by Golden gate assembly (Engler *et al.*, 2009), making the pCUPopSS. The plasmid pCUPopSS was used to transform *Synechocystis* 6803 via double homologous recombination, resulting in replacement of genes, and full chromosomal segregation was confirmed by PCR. Later, the vector pCUPopsap lacking the marker cassette was used for transformation following selection in 5% sucrose, where the cassette is fully removed (Cai and Wolk, 1990).

C1 strain was used as a background for the construction of the C2 mutant. The Sp^R/*sacB* cassette from pRL277 was used for the removal of the *cupB* gene, where 700 bp of *cupB* upstream region and 631 bp of downstream region were assembled flanking the Sp^R/*sacB* cassette using Gibson assembly (Gibson *et al.*, 2009). This construct was used to transform C1, segregation was confirmed with PCR, originating the C2 mutant. To complement the C2 stain by restoring the genes necessary to synthesize a NDH-1_3 system, an ectopic chromosomal integration strategy was employed. For this, the *cupA* operon region (6032 bp) was inserted into chromosomal integration vector 5 (pV5) using Gibson assembly. The vector pV5 has the *rbcL* promoter region and sequences for the integration into the neutral,

noncoding site between slr1704 and sll1575 (Gonzalez-Esquer and Vermaas, 2013). The construct was used to transform C2 and integration into genomic DNA was confirmed by PCR, and extracted genomic DNA was used for sequencing *cupA* operon integrated to evaluate proper nucleotide sequence, compared to *Synechocystis* 6803 database.

4.3 Results

4.3.1 Genetic systems for studying NDH-1 associated CO_2-uptake proteins in Synechocystis 6803

The CO_2 concentrating mechanism utilizes a set of C_i acquisition proteins that either actively transport bicarbonate from the environment into the cytoplasm or actively hydrate CO_2 to form bicarbonate within the cytoplasm. The CO_2 uptake systems, which are specialized forms of NDH-1 type redox proteins, are especially enigmatic since virtually nothing is known about their catalytic mechanism. Although NDH-1 complexes have ancient origins and have a wide phylogenetic distribution (Efremov and Sazanov, 2012), the Cup proteins are unique to and widely distributed within the cyanobacteria and appear to be a more recent evolutionary innovation. The goal of this study was to develop and characterize a genetic system that would allow detailed structure-function analysis of the NDH-1_3 complex, which is the high affinity variant of the CO_2-uptake system containing the NdhF3-NdhD3-CupA/S sub-complex. The overall strategy was to construct strains deficient in both NDH-1_3 and NDH-1_4 in a manner that would then allow facile

complementation with engineered forms of the NDH-1_3 complex. A CupA/B-deficient strain, designated C2, was constructed (Figures 8 and 9). The first step involved the removal of the native *cupA* operon (*ndhF3-ndhD3-cupA-cupS-sll1734*), a total of 5917 bp, by replacement with a cassette containing the spectinomycin resistance (Sp^R) and *sacB* genes by homologous recombination (Figures 8 and 9). This was subsequently converted into a marker-less deletion by utilizing the conditional toxicity of *sacB* in the presence of sucrose. For this, mutant cells were transformed with a plasmid containing a DNA fragment consisting of upstream and downstream regions flanking the *cupA* operon and applying counter selection in 5% sucrose. As a result, the Sp^R/*sacB* cassette was fully removed, thereby yielding a marker-less mutant, C1, lacking all the genes specific to high affinity CO_2 uptake. The removal of the remaining low affinity, high flux CO_2-uptake system was accomplished by deletion of the *cupB* gene using the Sp^R/*sacB* cassette, although elimination of the marker was not performed in this case. It is known that lack of any one *ndhD*, *ndhF*, or *cup* genes for each of the two CO_2 uptake systems leads to a disruption of CO_2 uptake for that system (Maeda *et al.*, 2002; Shibata *et al.*, 2001). The C2 strain was later used as a recipient of the synthetic construction containing the *cupA* operon to test for restoration of CO_2 uptake activity as described below.

To reintroduce the genes for the NDH-1_3 complex and to test for restoration of CO_2 uptake in the C2 deletion strain background, we reintroduced the operon for NDH-1_3 (*cupA* operon) under the regulation of a Rubisco promoter (*PrbcL*) using the integration vector pV5 (Gonzalez-Esquer and Vermaas, 2013). With this vector, the *cupA* operon was

integrated into a neutral site (NS) of *Synechocystis* 6803 located in a noncoding region between *slr1704* and *sll1575* of the C2 mutants (Figures 8 and 9) to produce strains having an ectopic and constitutive expression of *cupA* operon, named here as C2A.

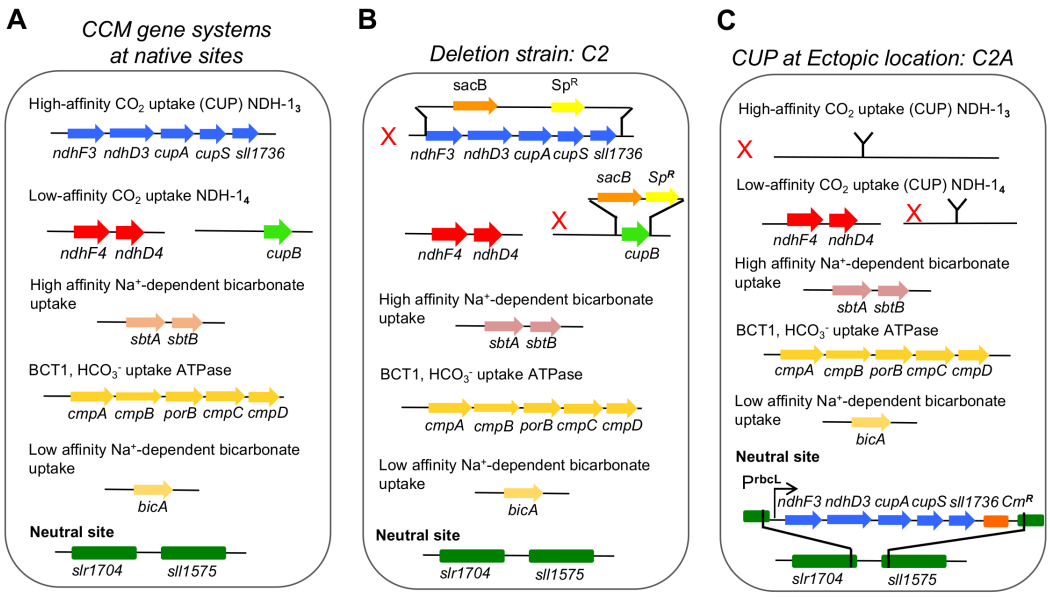

Figure 8. Construction of a genetic system to examine structure-function relationships of the CO_2 uptake dehydrogenases in cyanobacteria. A) Genomic localization of all five C_i transporters on *Synechocystis* 6803 (CCM β-type) in the wild-type strain (WT). B) Deletion by replacement of the whole NDH-1$_3$, known as the *cupA* operon (CUP); after sucrose selection for removal of *Sp*^{R}, a second deletion by replacement was performed to remove the *cupB* gene, producing the double mutant C2, with no functional CO_2 uptake systems. C) C2 was the recipient strain which received the integrational vector containing the *cupA* operon under control of a Rubisco promoter (*PrbcL*) into a neutral site.

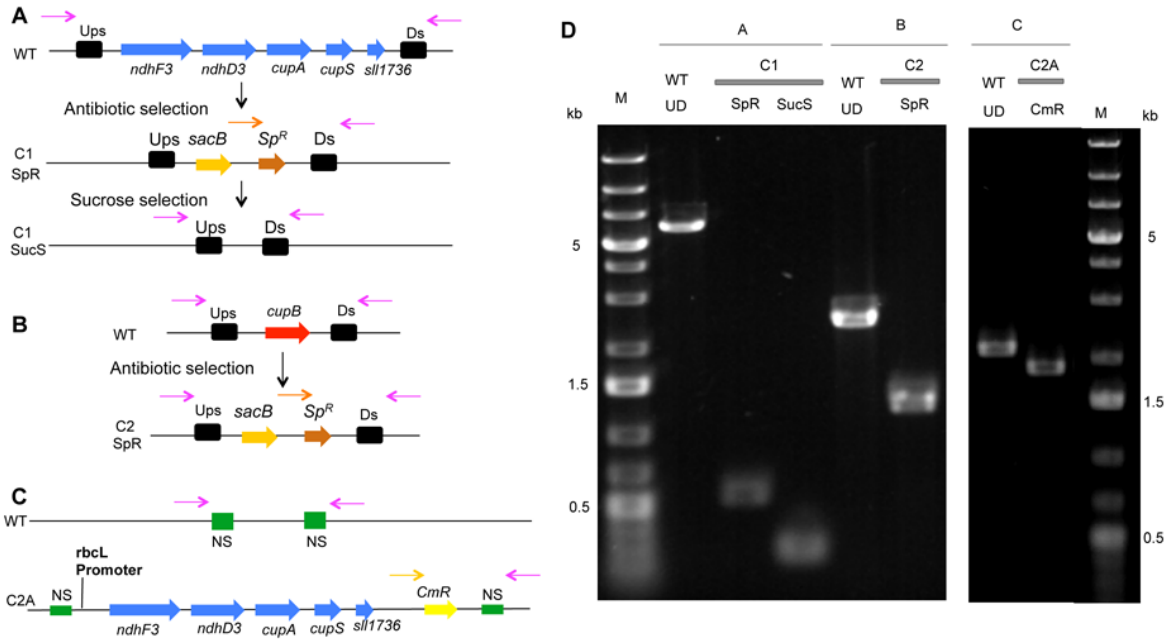

Figure 9. Schematic design of the construction of a genetic system to examine structure-function relationships of the CO_2 uptake dehydrogenases in cyanobacteria and segregation of mutants. A) genomic localization of *cupA* operon in *Synechocystis* 6803 WT containing five genes; construction of C1 mutant: *Sp*^{R}/*sacB* cassette was used for the removal of the gene with deletion by replacement of the whole NDH-1$_3$, now a spectinomycin resistant strain (Sp^R); after sucrose selection for removal of *Sp*^{R}, now a sucrose sensitive strain (SucS); B) genomic localization of *cupB* in *Synechocystis* 6803 WT; a second deletion by replacement with *Sp*^{R}/*sacB* cassette was performed to remove *cupB* gene, producing the double mutant C2 (Sp^R), with no functional CO_2 uptake systems. C) genomic localization of the neutral, noncoding site between slr1704 and sll1575 in *Synechocystis* 6803 WT (NS); C2 was the recipient strain of the integrational vector containing the *cupA* operon under control of a Rubisco promoter (*PrbcL*) into NS, acquiring chloramphenicol resistance (CmR). D) Confirmation of segregation of each mutant and integration of *cupA* operon into ectopic site as determined by PCR amplification. Primers are represented by arrows in panels A, B and C.

4.3.2 Immunodetection of CupA shows deletion and constitutive expression phenotypes of the C2 and C2A strains

To evaluate the consequences of the deletion and restoration of the *cupA* operon in the C2 and C2A strains, respectively, antibodies were raised against heterologously expressed CupA (Figure 5, see Chapter 3) and used to probe immunoblots of whole cell lysates (Figure 10). As shown in Figure 10A, a reaction is observed at the expected 47 kD mass of CupA in the wild-type grown under LC conditions (LC7), but not in cells grown under HC conditions (HC8) consistent with the inducible nature of the *cupA* operon at its native location. In the C2 strain, no reaction was observed, as expected, due to the deletion of the entire *cupA* operon. In C2A, CupA is expressed under both HC and LC growth conditions consistent with the fact that the *cupA* operon is under constitutive transcription expression of the *rbcL* promoter at the ectopic location. Moreover, the level of expression seems even higher than the native, induced level in the wild-type, although the 24-hour induction period may not allow full induction. However, improvements in the antibody will be needed for a more accurate quantitation.

To further explore the physiological state of the cells, the accumulation of the LC inducible bicarbonate transporter SbtA was also analyzed. As shown in Figure 10C, a reaction using commercial antibody is observed at the expected ~39 kD mass of SbtA in both C2 and C2A, independent of C_i availability. This indicates that even under HC conditions the mutants are starved for C_i, and therefore must try compensate for the loss of the low affinity

high flux NDH-1$_4$ complex. No accumulation of SbtA was seen in the WT under HC, and only faintly under LC, potentially indicating that the 20 h C_i limitation regime was insufficient to induce production of the protein to be visualized in whole cell extracts *vs*. thylakoid membrane samples used in previous studies (Holland *et al.*, 2016).

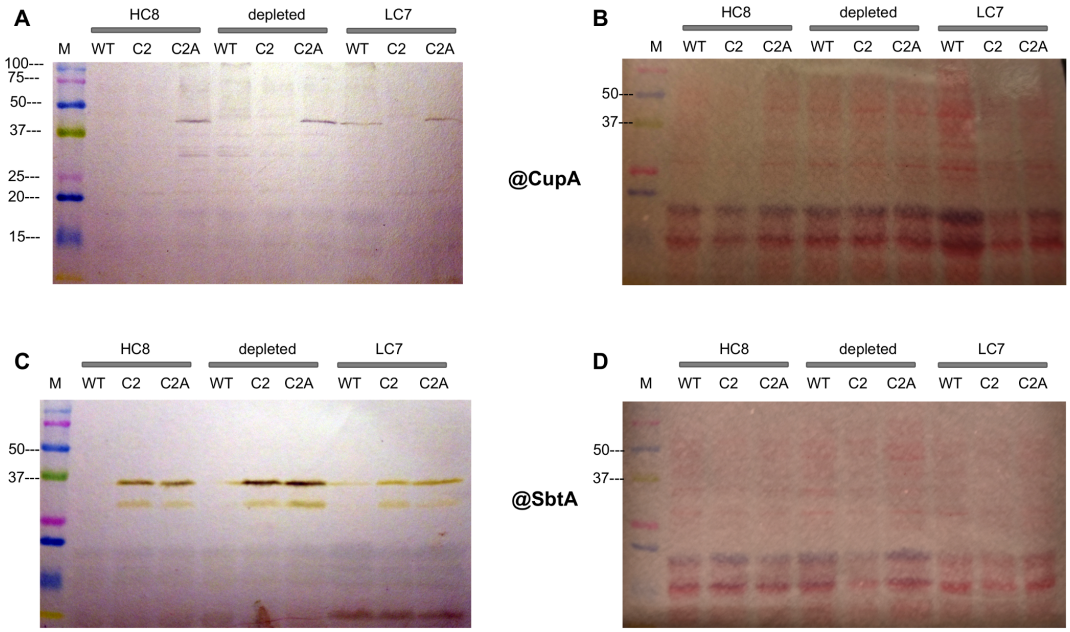

Figure 10. Immunodetection of CupA and SbtA in WT, C2 and C2A at different C_i availability. WT, C2, and C2A strains were grown in BG-11 at HC conditions with pH 8 supplemented of 3% CO_2 (HC8), later washed with modified LC7 media (BTP, no $NaNO_3$) depleted of C_i (depleted), or grown at pH 7 supplemented with 3% CO_2 and later switched to 20 h air (LC7). Whole cell extracts samples containing 1 µg Chl were loaded on a 12% SDS-PAGE gel and transferred to a PVDF membrane. Previous to detection, the membranes were stained with 0.5% Ponceau S to verify equal loading (panel B and D). CupA (panel A, ~47 kD) and SbtA (panel C, 37 kD) were detected using a produced and a commercial antibody (Agrisera), respectively. A marker was added for molecular weight comparisons (lane M) (Precision Plus Protein Kaleidascope, Bio-Rad).

4.3.3 Constitutive expression of NDH-1$_3$ restores ability of double mutant to grow under LC

Growth phenotype of WT *Synechocystis* 6803 and the mutants was evaluated using agar plate spot assays under different C_i conditions (Figure 11). All strains grow well when cells were on standard mineral medium buffered at pH 8 independently of whether they were supplemented with 5% CO_2 and 20 mM $NaHCO_3$. In contrast, the strains respond differently on a modified low C_i media buffered at pH 7 under ambient CO_2 levels, even with 20 mM $NaHCO_3$. The C2 strain failed to grow under these conditions, even with saturating C_i levels due to added $NaHCO_3$, whereas the wild-type and the C1 each grow under these low CO_2 conditions. Evidently, these conditions force reliance upon the CO_2 uptake enzymes for autotropic growth and show that NDH-1$_4$ complexes containing CupB are sufficient for this function, yet loss of both CO_2 uptake systems renders growth impossible. This is consistent with previous findings, where mutants that have a combination of deletions of single genes in both NDH-1$_3$ and NDH-1$_4$ complexes were shown to have a severe growth deficiency at ambient CO_2 levels at pH 7 (Han *et al.*, 2017; Maeda *et al.*, 2002; Ohkawa *et al.*, 2000a; Zhang *et al.*, 2004). To determine whether this phenotype could be complemented by the reintroduction of only the high affinity system, the C2 strain was the recipient where the entire operon encoding the high affinity low flux synthetic NDH-1$_3$ into an ectopic chromosomal location under the control of the Rubisco promoter was added. The transformation produced the complementation strain, C2A. The new C2A strain was able to grow in plates under the severe depletion of CO_2 (Figure 11A).

This shows that the integration of *cupA* operon on the neutral site of *Synechocystis* 6803 was efficient and removed the high-CO_2 requiring phenotype.

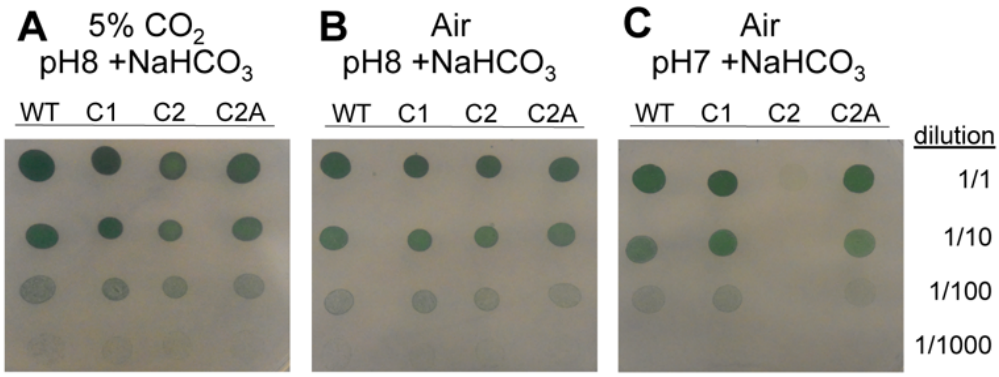

Figure 11. Spot assays for autotrophic growth under different pH and CO_2 availability conditions on agar plates. WT and mutants for the CCM were grown in liquid media modified BG-11 pH 7, pelleted by centrifugation, washed once and resuspended in BG-11 pH 8 or 7 to OD_{750} of 1, 0.1, 0.01 or 0.001 (top to bottom rows, respectively). Five µL cells at each dilution was spotted on agar plates with pH 8 or 7, supplemented with 20 mM $NaHCO_3$, and grown for five days. A) 5% CO_2-enriched air; B and C) ambient air CO_2 levels.

4.3.4 Restoration of high affinity inorganic carbon uptake in C2A

We next evaluated the inorganic carbon uptake capacity of WT *Synechocystis* 6803 and mutants by following photosynthetic oxygen evolution dependent on C_i uptake (Table 1, Figure 12). Cells that were grown under HC were then depleted of C_i in modified media lacking $NaNO_3$ and Na_2CO_3 at pH 7 (Benschop *et al.*, 2003). The depletion of Na^+ in the assay medium diminishes the contribution of the Na^+-dependent HCO_3^- transporters to support O_2 evolution and the absence of nitrate renders O_2 evolution entirely dependent on

C_i as the final electron acceptor. The buffering at pH 7 together with addition of carbonic anhydrase poises the reaction for increased CO_2 compared to the HCO_3^-, forcing cells to utilize primarily CO_2 for photosynthesis. The assays were conducted by measuring O_2 evolution, which is dependent on C_i uptake and can be used to estimate the net whole cell C_i affinity characteristics.

Table 1: Photosynthetic O_2 evolution of HC cells in response to C_i uptake. V_{max} and $K_{0.5}$ values were obtained from Figure 12. Potassium bicarbonate ($KHCO_3$) was added as source of C_i, in the presence of CA 25 μg mL^{-1}. Values are means and ± indicates standard deviations (SD) with corresponding number of experimental replicates, n.

Strain *Synechocystis* 6803		**V_{MAX} (μmol O_2 mg^{-1} Chl h^{-1})**	**$K_{0.5}$ (C_I) (μM)**	**N**
WT		232 ±17	73 ±11	7
C2		213 ±18	8700 ±418	11
C2A (biphasic)	Phase 1	93 ±15	8 ±3	10
	Phase 2	190 ±21	4600 ±970	

The WT strain grown under high C_i conditions (HC) exhibited a high V_{max} (232 μmol O_2 mg^{-1} Chl h^{-1}) and moderate $K_{0.5}$ (73μM) (Figure 12A), as would be expected for cells that are mainly dependent on the CO_2 hydration activity of NDH-1_4, which is the constitutive high flux, low affinity C_i uptake enzyme systems expressed under these HC conditions. In

contrast, the overall C_i affinity of the WT cells grown under LC conditions increases due to the additional expression of the high affinity enzyme systems, as observed before (Benschop *et al.*, 2003; Wang *et al.*, 2004). The C2 mutant exhibited O_2 evolution only under saturating concentrations of bicarbonate (>1mM) (Figure 12B) consistent with the absence of the genes necessary for the NDH-1_3 and NDH-1_4 CO_2 hydration activities. Here, the curves for C2 (Figure 4B) resemble the results previously obtained for ChpX/ChpY knock out mutant in *Synechococcus* sp. PCC 7942 (Woodger *et al.*, 2005). This was the case for both the potassium (Figure 12) and sodium (Figure 13) salts, which might seem surprising since it could be anticipated that the addition of $NaHCO_3$ would support at least some level of O_2 evolution due to the activity of the BicA and SbtA transporters, expressed in C2 (Figure 10). However, their K_m values are in the mM range with respect to Na^+. Accordingly, these assays primarily evaluate the affinity of the CO_2 uptake enzymes because of the pH favoring CO_2 over HCO_3^- and due to low sodium content (approximately 0.39 μM). From the very high added [C_i] requirement of C2 under these conditions, we conclude that the supply of C_i in this mutant primarily depends upon physical diffusion into cells, perhaps entering as CO_2 through aquaporins (Tchernov *et al.*, 2001). This high physiological requirement for C_i –dependent O_2 evolution is consistent with the fact that high CO_2 supplementation rescues growth in C2. The relatively small but measurable difference observed between Na^+ and K^+ bicarbonate sources is presumably due the Na^+-dependent activity of BicA and SbtA. Previous studies showed that WT subjected to LC has a maximal peak of *sbtA* mRNA abundance only 3 h after the HC to LC switch (Wang

et al., 2004). In the ΔccmR mutant, *sbtA* transcription was only partially de-repressed under HC growth (about 40%) and *bicA* was slightly induced (Klähn *et al.*, 2015). The Δ4 mutant, containing only *bicA* as part of the CCM, also has an increased *bicA* transcription under HC (Orf *et al.*, 2015). These results suggest that even small changes in the physiological state signal the LC condition and would be strong enough to elicit a LC phenotype, and *Synechocystis* 6803 may adapt to this by inducing SbtA and BicA expression. This would also explain the expression of SbtA in the C2 and C2A, even under HC (Figure 10). Multiple layers of regulation may exist guiding the expression of the CCM components, including sensing metabolic changes (Orf *et al.*, 2015).

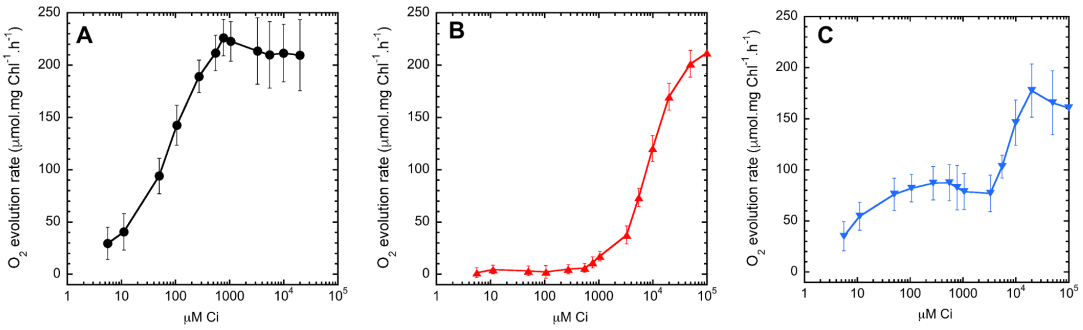

Figure 12. Assays for C_i affinity measuring photosynthetic O_2 evolution rates in *Synechocystis* 6803 strains with different CO_2 uptake system under low sodium. Cells were grown in BG-11 pH 8, supplemented with 3% CO_2 (HC8) and illumination at 70 μmol (photons) m^{-2} s^{-1}. Before assay cells were washed with modified LC7 media (BTP, no $NaNO_3$) depleted of C_i. $KHCO_3$ was added as source of C_i, in the presence of CA 25 μg mL^{-1}. Traces are representative of at least three biological replicates, and bars indicate ±SD. A) Wild-type HC cells, in black, containing the constitutive NDH-1_4. B) In red, C2 double knockout mutant, with no functional NDH-$1_{3,4}$ CO_2 uptake systems. C) C2A,

in blue, containing the ectopic constitutive expression of the high CO_2 affinity NDH-1_3 uptake system with low flux.

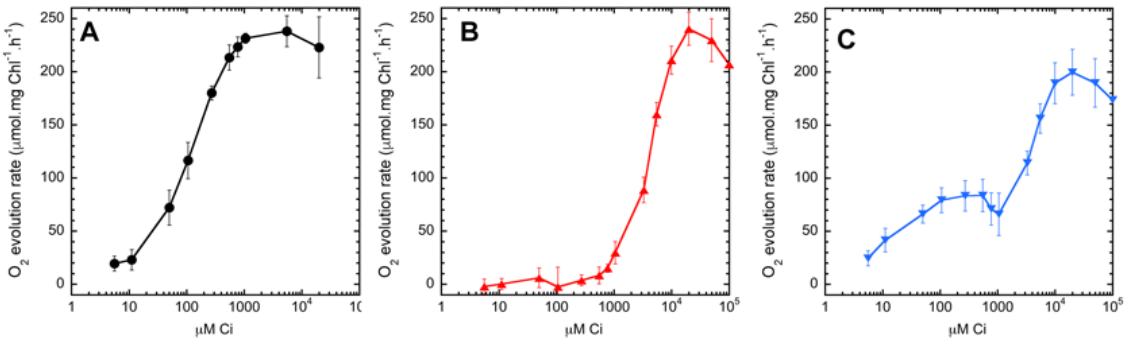

Figure 13. Assays for C_i affinity measuring photosynthetic O_2 evolution rates in *Synechocystis* 6803 strains with different CO_2 uptake systems. Cells were grown in BG-11 pH 8, supplemented with 3% CO_2 (HC8) and illumination at 70 µmol (photons) m^{-2} s^{-1}. Before assay cells were washed with modified LC7 media (BTP, no $NaNO_3$) depleted of C_i. $NaHCO_3$ was added as source of C_i. Traces are representative of at least three biological replicates, and bars indicate ±SD. A) Wild-type HC cells, in black, containing the constitutive NDH-1_4. B) In red, C2 double knockout mutant, with no functional NDH-$1_{3,4}$ CO_2 uptake systems. C) C2A, in blue, containing the ectopic constitutive expression of the high CO_2 affinity NDH-1_3 uptake system with low flux.

The complementation strain C2A presented a biphasic C_i affinity curve, with the first phase having a $K_{0.5}$ of 8 µM (Figure 12C) and saturating with C_i <1 mM, and a second component starting with C_i >1 mM similar to that present in C2 (Figure 12B), likely due to the function of the bicarbonate transporters, such as BCT1 (dependent of ATP) or diffusion of CO_2 now at levels sufficient to sustain Rubisco activity. The results show that HC C2A mutant, with the constitutive expressed NDH-1_3, has a low V_{max} (93 µmol O_2 mg^{-1} Chl h^{-1}) and $K_{0.5}$ (8 µM) for C_i as expected for when this system is active, a low flux and high affinity CO_2

uptake system. This suggests that the constitutive ectopic expression is functional and acting similar to the native *cupA* operon normally induced in WT under low C_i.

4.3.5 The carbonic anhydrase inhibitor EZ abolishes NDH-1$_3$-dependent C_i uptake

The carbonic anhydrase inhibitor ethoxyzolamide (EZ) affects the C_i accumulation of cells under HC or LC by inhibiting CO_2 uptake without disrupting internal carboxysome CA (Price and Badger, 1989a; Price and Badger, 1989b; Tyrrell *et al.*, 1996). Although it is presumed that EZ inhibits the NDH-1$_3$ and/or the NDH-1$_4$ uptake system CO_2 uptake system(s), information on the specific inhibitory target of EZ remains sparse. To test whether the NDH-1$_{3,4}$ complex is inhibited by EZ, photosynthetic O_2 rates dependent of C_i in C2A and WT HC cells were assayed after the addition of 200 μM EZ (Figure 14).

WT cells grown under HC exhibited a moderately diminished V_{max} when in the presence of EZ (176 *vs* 232 μmol.mg^{-1} Chl.h^{-1}, with or without EZ, respectively) (Figure 14A). The $K_{0.5}$ was more significantly affected by the addition of EZ (240 *vs* 73 μM) increasing more than three times, suggesting a significant decrease in the affinity for CO_2. Considering that WT at HC growth is highly dependent on NDH-1$_4$, it is expected that, even at saturating levels of bicarbonate (V_{max} at approximate 700-1000 μM), the photosynthetic rate diminished, similar to that seen previously in *Synechococcus* (Price and Badger, 1989a; Tyrrell *et al.*, 1996).

The C2A strain had the most pronounced EZ inhibition indicating that NHD-1$_3$, the sole source of CO_2 uptake, is strongly inhibited by EZ (Figure 14B, phase 1). Correspondingly,

the C2 strain, lacking NHD-1_3, was not discernibly affected by the addition of EZ (results not shown). These results show that the CO_2 activity of the NHD-1_3 is disrupted by the traditional CA inhibitor EZ, consistent with the interpretation that the active site of NHD-1_3 shares structural similarities with the known active sites of alpha and beta carbonic anhydrases (Menchise *et al.*, 2006; Modak *et al.*, 2016; Price *et al.*, 2002). As discussed below, this is interesting since there is no detectable sequence similarity between any of the NHD-1_3 polypeptides and known CAs as noted previously in this context (Maeda *et al.*, 2002; Price *et al.*, 2002). Interestingly, EZ inhibition is only partial at these concentrations in the wild-type, consistent with earlier measurements (Price and Badger, 1989b), suggesting that NHD-1_4 may not be as sensitive to EZ compared to NHD-1_3.

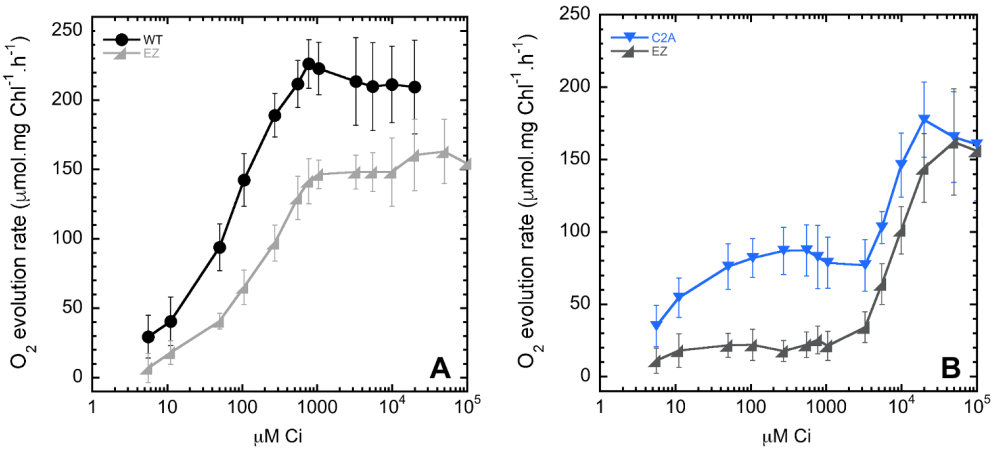

Figure 14. The carbonic anhydrase inhibitor ethoxyzolamide (EZ) inhibits CO_2 uptake by NHD-1_3 complexes. Cells were grown in BG-11 pH 8, supplemented with 3% CO_2 (HC) with illumination at 70 µmol (photons) m^{-2} s^{-1}. Cells were washed with modified LC7 media (BTP, no

$NaNO_3$) depleted of C_i. Potassium bicarbonate ($KHCO_3$) was added as source of C_i in the presence of CA 25 μg mL^{-1} or EZ 200 μM, a carbonic anhydrase inhibitor. Traces are representative of at least three biological replicates, and bars indicate ±SD. A) Wild-type HC cells, in black, and in presence of EZ, grey. C) HC C2A, in blue, and in the presence of EZ, dark grey.

4.3.6 Chlorophyll fluorescence as a function of C_i availability and ethoxyzolamide inhibition.

Analysis of Chl fluorescence transients provides a non-invasive technique to probe photosynthetic electron transport and metabolic processes in intact cells under different conditions of C_i-availability (Holland *et al.*, 2015). Cells of the WT, C2 and C2A were subjected to C_i depletion, dark adapted, and then exposed to moderate actinic illumination (nominally 53 μmol (photons) m^{-2} s^{-1}), while measuring fluorescence yield using a PAM fluorometer (Figure 15A). The most obvious difference among strains is the magnitude of the high fluorescence state associated with insufficient cellular supply of C_i (Holland *et al.*, 2015; Miller *et al.*, 1996; Miller *et al.*, 1988). As expected, all strains developed a high fluorescence state after approximately 2 minutes of actinic illumination, with the C2 strain (Figure 15A, red trace) exhibiting the most pronounced features of C_i-starvation as evidenced by its fluorescence level reaching maximal fluorescence (F_m'), indicating PSII can no longer be oxidized by a, presumably, over-reduced PQ pool. The C2A and WT strains are also exhibiting signs of C_i starvation, but with the WT (black trace) less so than C2A (blue trace). Deviations between maximal fluorescence (F_m'), obtained in the

presence of 10 µM DCMU and multiple turnover flashes were not observed for these experiments conducted at cell densities corresponding to 5 µg Chl mL^{-1}.

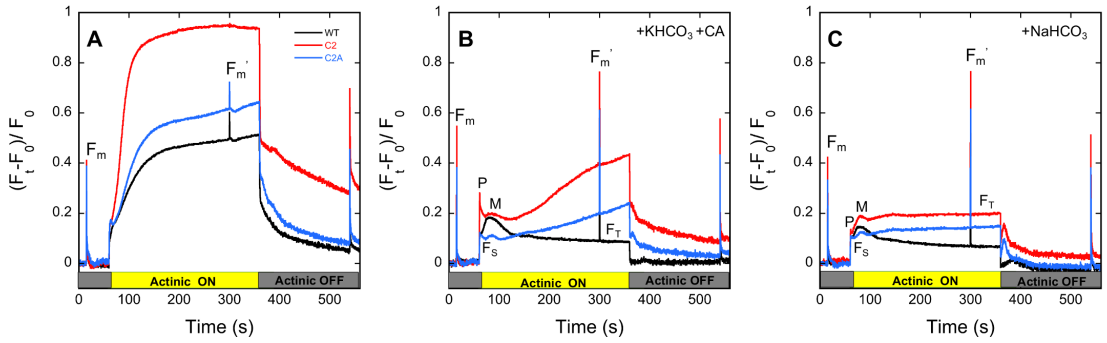

Figure 15. Chl fluorescence of cells as a function of C_i: Cells grown in HC were depleted of C_i, dark adapted, and measured for variable PAM fluorescence yield with no addition (Panel A), following addition of 5mM $KHCO_3$ (Panel B) or $NaHCO_3$ (Panel C). Dark adapted cells of the wild-type (black traces), C2 (red traces) and C2A (blue traces) were exposed to five min actinic illumination (nominally 53 µmol (photons) m^{-2} s^{-1}). Traces were acquired at a rate of one point per millisecond, but curves are presented smoothed with a running average of 300 points. Three high intensity, multiple turnover flashes (300 millisecond) were applied in the dark (F_m) and light (F_m') periods to establish maximal variable fluorescence (Campbell *et al.*, 1998). Transient traces are representative of at least three biological replicates.

As shown in Figure 15B, the over-reduced pattern due to C_i depletion can be rescued by addition of 5 mM bicarbonate (Holland *et al.*, 2015; Miller *et al.*, 1988). When $KHCO_3$ was added in the presence of CA (to ensure more CO_2 in order to evaluate activity of CO_2 uptake systems), WT responded as expected. Upon illumination, Chl fluorescence reached

the peak F_P (labeled, P) with a brief decrease to F_S. Soon after, the Chl fluorescence rises reaching a maximum (labeled, M), an indication that the cells entered the state 2 to state 1 transition, where now the light excitation is also obtained by phycobilisomes (Kana *et al.*, 2012). Later, the Chl fluorescence declines from M to a steady state level F_T, as reductant is consumed by the CBB cycle, which is active due to the availability of C_i. However, this is not entirely the case for C2A, where after a short steady state level, the Chl fluorescence rises slightly, indicating that NDH-1_3 alone is not sufficient to deliver C_i for full CBB activity. This effect is even more pronounced in C2 (Figure 15B), consistent with the absence of a CO_2 hydration system. Addition of $NaHCO_3$ as a source of C_i (Figure 15C), however, allows restoration of a low F_T possibly due to the activity of bicarbonate transporters. Yet, the PQ pool still is more reduced in C2 and C2A compared to the WT (Figure 15C), indicating the importance of NDH-1_4 on CO_2 uptake, presumably due to its role in mitigating leakage of CO_2 even in the presence of robust bicarbonate uptake (Maeda *et al.*, 2002).

Addition of EZ to C2A HC dark adapted cells induces a quick rise in the Chl fluorescence is seen, similar to the rise from C_i depleted cells (Figure 16). This is consistent with NDH-1_3 as a target of EZ inhibition (see also Figure 14) and underlines the importance of the NDH-1_3 in the C2A strain, where it is critical for CO_2 uptake and mitigation of the CO_2 leakage, even under normal HC growth conditions.

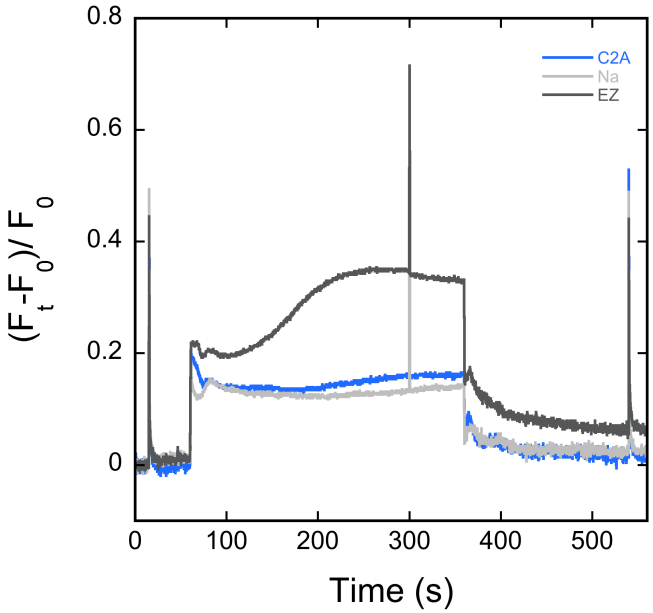

Figure 16. Chl fluorescence of HC grown cells: Cells grown in HC were washed with BG-11 pH 8 gassed with 3% CO_2, dark adapted for five minutes, and exposed to five min actinic illumination (nominally 53 µmol (photons) m^{-2} s^{-1}) were measured for variable PAM fluorescence yield. C2A HC cells (blue traces), with addition of 5mM $NaHCO_3$ (light grey traces) or 200 µM EZ (dark grey traces). Traces were acquired at a rate of one point per millisecond, but curves are presented smoothed with a running average of 300 points. Three high intensity, multiple turnover flashes (300 millisecond) were applied in the dark (F_m) and light (F_m') periods to establish maximal variable fluorescence (Campbell *et al.*, 1998).

4.3.7 Interactions between C_i metabolism and electron transport in the dark

Fluctuations in Chl fluorescence yield observed after switching off the actinic light (Figure 15 after 360 sec) are due to redox mechanisms involving the transfer of electrons from carriers in the cytoplasm (stroma in chloroplasts) to thylakoid complexes that mediate the re-reduction of the PQ pool in the dark including, but not limited to, ferredoxin-mediated

CEF (Deng *et al.*, 2003; Holland *et al.*, 2015). These transients can be observed more clearly in a slightly different experiment (Figure 17A-C). Here, a shorter actinic illumination period and lack of saturating MT pulses makes the post-illumination Chl fluorescence more pronounced primarily because CBB cycle activation is incomplete, resulting in lowered consumption of photosynthetically generated reductant and a greater flux toward the reduction of the PQ pool (Holland *et al.*, 2015). At least two Chl fluorescence rises are observed under these conditions. The first rise, F_N, occurs 2 to 6 seconds after the cessation of illumination and is assigned to the oxidation of reduced NADPH and/or ferredoxin due to CEF through NDH-1 (Battchikova *et al.*, 2011b; Holland *et al.*, 2015). The second rise, F_R, occurs 25-50 seconds post-illumination, and is assigned to the oxidation of reduced metabolite pools accumulated in the light. Figure 17A shows a noticeable difference in the levels of both F_N and F_R between C2 (red traces) and strains that contain at least one of these systems (WT and C2A, black and blues traces, respectively). Moreover, the addition of 5 mM $KHCO_3$ (Figure 17B) and especially $NaHCO_3$ (Figure 17C), enhances the respiratory peak F_R for all strains. Enhancing F_R is interpreted to reflect great fluxes of reductant into the PQ pool because of the greater accumulation of reduced carbon skeletons from the operation of the CBB cycle when a functioning CO_2-hydration system is present (WT and C2A) or when C_i is made available by the addition of bicarbonate. A similar pattern is observed for NADPH transients after the AL is switched off (Figure 17D-F), where the rise in fluorescence, N_R, is related to re-reduction of $NADP^+$ pools due to oxidation of photosynthetically derived sugars (Holland

et al., 2015). This again indicates greater accumulation of photosynthetic carbon skeletons when a functioning CO_2-hydration system is present (WT and C2A) or by the addition of exogenous C_i. In the case of C2, the observation is largely dependent upon the addition of exogenous C_i consistent with acute starvation.

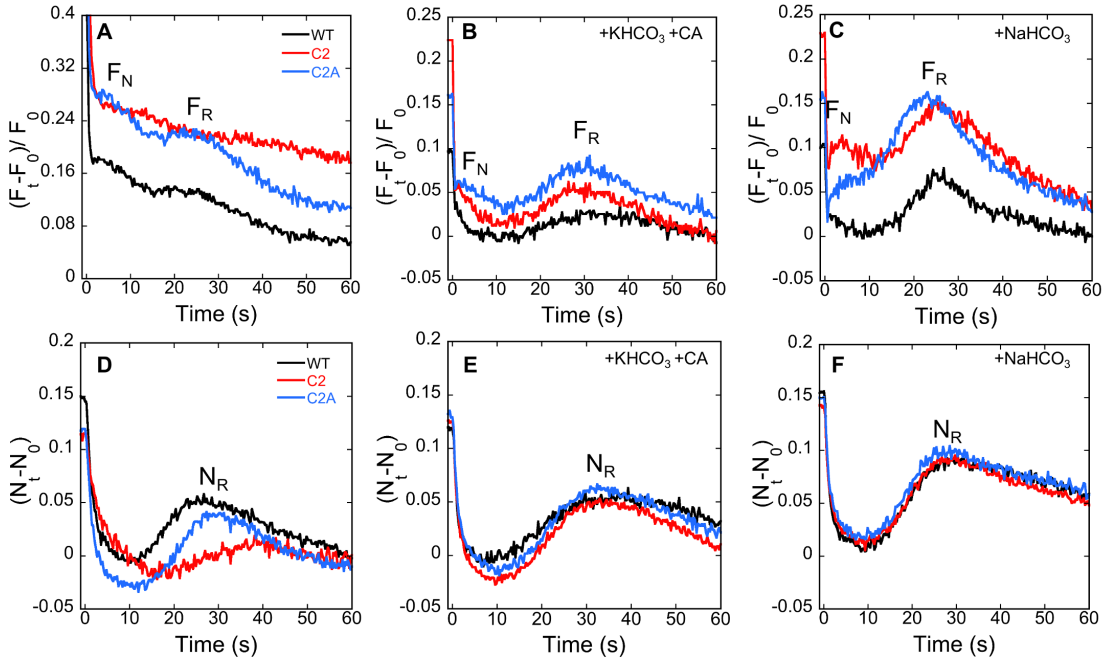

Figure 17. Effects of bicarbonate re-addition on the post-illumination Chl (Panels A-C) and NADPH (Panels D-F) fluorescence transients in C_i depleted cells. Dark adapted, C_i-depleted cells of WT, C2 and C2A strains were measured after C_i depletion (Panels A&D), with the addition of 5 mM $KHCO_3$ (Panels B&E), or $NaHCO_3$ (Panels C&F). Actinic illumination was restricted to 60 seconds (not shown) with time zero corresponding to the termination of actinic illumination. Transient traces are representative of at least three biological replicates.

Besides the partial restoration of the ability to supply C_i to the CBB cycle by re-introducing the *cupA* operon to the CO_2-hydration deficient C2 strain, another shared property of C2 and C2A is revealed in these experiments. The addition of $NaHCO_3$, dramatically enhances the respiratory F_R peak. This is not observed in the WT strain and appears to be associated with induction of a metabolic state due to chronic C_i limitation as seen previously (Holland *et al.*, 2016). This is consistent with the observation that the bicarbonate transporter SbtA is induced even under 3% CO_2 growth in both C2 and C2A (Figure 10), which is indicative of chronic C_i starvation in the absence of a full CO_2-hydration mechanism (both NDH-1_3 and NDH-1_4) in *Synechocystis* 6803.

4.3.8 LEF and CEF are affected by NDH-1_3 presence in HC grown cells

In order to understand more about the energetic status of the strains, CEF and linear electron flow (LEF) of the strains were assessed by following changes of PSI (P700) redox state (Bernat *et al.*, 2011). Samples with equal Chl concentration (5 μg mL^{-1}) were used so relative units of PSI/Chl could be compared (Holland *et al.*, 2016). Upon intense actinic illumination, the oxidation state of P700 fluctuates such that its immediate oxidation is followed by a transient re-reduction (maximal ~0.5 sec) and then a re-oxidation to an oxidation level that is steady until the actinic illumination is turned off (Figure 18A-C). This transient re-reduction was shown to be influenced by the pool of metabolic reductants present in the cell and can be enhanced by the addition, for example, of glucose, but is also dependent upon reduction of the PQ pool by PSII (Holland *et al.*, 2016). It is interesting to

note that the transient re-reduction event is slightly more pronounced in C2A than WT and C2, independent of C_i availability. This feature most likely reflects the fact that while both C2 and C2A have increased metabolic flux towards the thylakoid membranes due to C_i limitation (see discussion of Figure 17), C2A has the additional pathway involving NDH-1_3 thereby enhancing the re-reduction transient. Nevertheless, the overall characteristics of LEF appear largely unaffected over this relatively brief illumination period, consistent with little or no alterations in the functioning of the main complexes of electron transport and that the over-reduction of the PQ pool evident from the Chl fluorescence analysis occurs over the longer time periods associated with the consumption of the electron acceptors affiliated with C_i consumption.

Use of red saturating light, together with the addition of DCMU, a PSII inhibitor, was used to evaluate CEF in the strains (Figure 18D-F). Interestingly, re-reduction of $P700^+$ in the dark in C2A was faster than WT and C2 indicating a greater flux of reductant into inter-system electron transport chain by CEF and other process such as respiratory flux. The faster dark re-reduction of $P700^+$ indicates that the C2 and C2A strains are likely to have greater flux of cytosolic sources of reductant, including carriers of CEF, such as ferredoxin, to the thylakoids than in the wild-type. Our results also indicate that the addition of C_i slowed the rate of the reaction about 25% for all strains, possibly due to the partial activation of CBB and its increased consumption of NADPH. It is known that NDH-1 has a direct effect on CEF including the CO_2 uptake systems NDH-$1_{3,4}$ (Bernat *et al.*, 2011). It is also worth noting that the approximate levels of PSI, judging from the relative amplitude

of the P700 signals, indicates that the similarly loaded samples have similar concentrations of PSI relative to the wild-type.

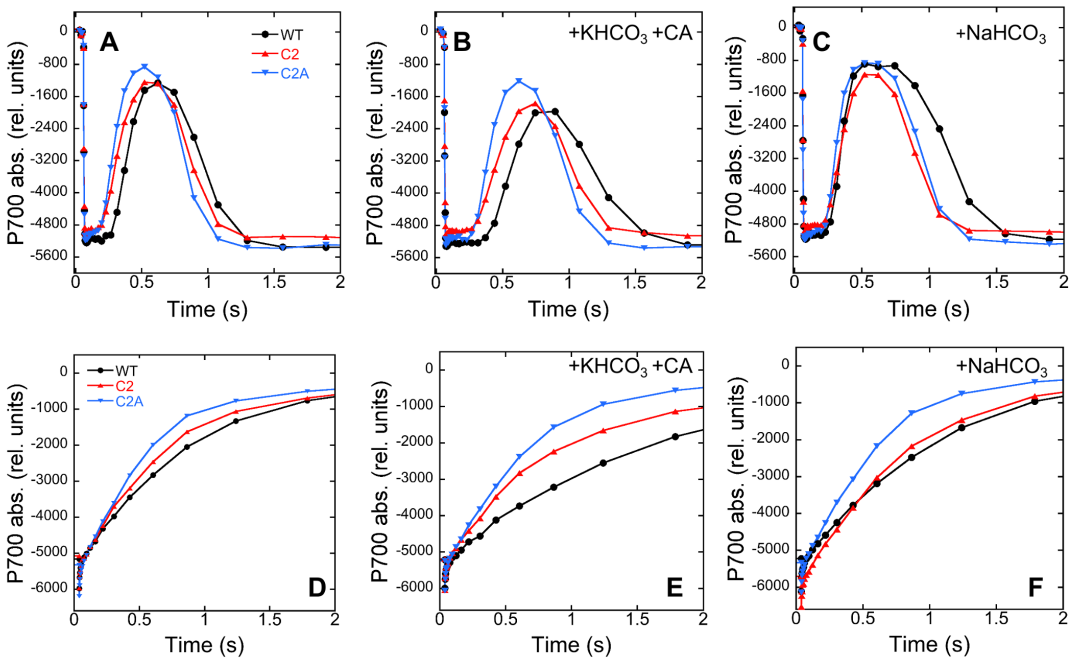

Figure 18. Photosystem I oxidation kinetics in dark-adapted cells exposed to saturating illumination. P700 absorbance was followed in strains with different forms of CO_2 uptake systems as a response to C_i absence (A) or presence (5mM $KHCO_3$, B or 5mM $NaHCO_3$, C) or additionally with the use of DCMU, a PSII inhibitor, which was added to evaluate CEF in the strains (Figure 18 D-F) After five min dark adaptation, intense actinic illumination (2050 µmol (photons) m^{-2} s^{-1}) was given for 5 s. Transient traces are representative of at least three biological replicates.

4.4 Discussion

The cyanobacterial CCM is one of several independently evolved physiological solutions to the relatively poor affinity and selectivity of the major autotrophic carbon fixing enzyme, Rubisco. Plants have evolved mechanisms, most notably C4 metabolism, that concentrate CO_2 in the proximity of Rubisco, whereas eukaryotic algae have evolved a still poorly understood CCM involving pyrenoids and a network of bicarbonate transporters and carbonic anhydrases. In contrast to these systems, cyanobacteria have evolved a CCM that involves specialized CO_2 hydration enzymes that are coupled to NDH-1 membrane complexes to drive the conversion of CO_2 into bicarbonate (CO_2 uptake, CUP). These are an integral part of the cyanobacterial CCM yet remain very poorly understood in terms of structure and function. Cyanobacterial NDH-1 membrane complexes apparently use ferredoxin to deliver electrons to plastoquinone (Ma and Ogawa, 2015), which would be consistent with chloroplast NDH-1 function as recently shown (Strand *et al.*, 2017). This exergonic electron transfer couples the pumping of protons from the N-side (cytoplasmic) to the P-side (lumenal) of the thylakoid membrane, by a still-to-be resolved mechanism that is presumably shared by all members of the NDH-1 family (Brandt, 2013). Current information suggests that the NdhD and NdhF subunits mediate at least some of the proton pumping. How this proton pumping would be adapted to the energy-requiring hydration of CO_2 in cyanobacterial thylakoids remains a mystery (Ogawa and Mi, 2007).

The project described here is a first step in an effort to probe the molecular mechanism using a combined molecular genetics and physiological approach to the problem. The overall approach involved constructing a system that will enable manipulation (e.g. amino acid site-directed mutagenesis) of each of the genes associated with CUP or explore the ability to complement these genes using homologs from other species. Although mutants lacking both functional NDH-$1_{3,4}$ were available (Maeda *et al.*, 2002; Shibata *et al.*, 2001), these involve single gene deletions and a strain lacking all the genes from the *cupA* operon, encoding the high affinity Cup functionality of NDH-1_3, had not been constructed. Here, a strain, designated C1, was developed where all the five genes of the *cupA* operon were removed using a marker-less gene excision strategy (Figure 8 and Figure 9). The subsequent removal of the *cupB* gene, part of the complementary high flux, low affinity NDH-1_4 complex, produced a strain, C2, completely devoid of CO_2 hydration systems. This is envisioned as the basal strain for the reintroduction of modified Cup genes to study structure-function relationships. The C2 strain was then transformed using a synthetic molecular construction which integrated the whole *cupA* operon into a genomic neutral site with transcriptional expression under the control of a Rubisco promoter, giving a constitutive expression. The resultant C2A construct restored the expression of the high affinity NDH-1_3 complex as evidenced by the accumulation of the CupA protein and the restoration of growth at pH 7 under ambient air. As expected, the strain shows a clear high affinity for C_i (Figure 12), yet the biphasic affinity profile of the C2A strain graphically illustrates that the NDH-1_3 complex is not able to sustain high CO_2 uptake rates, despite

(or perhaps as a consequence of) its high affinity characteristics. These findings are fully consistent with the previous assignments that NDH-1_3 and NDH-1_4 are high affinity, low flux and low affinity, high flux CO_2 uptake enzymes, respectively.

Inhibitor studies can provide insight into enzyme reaction mechanisms. It is hypothesized that a carbonic anhydrase (CA) activity is at the heart of these enzymes, yet it must be structurally organized very differently than typical CAs since the Cup proteins drive the formation of high cytoplasmic concentrations of bicarbonate rather than dissipating them, as would occur if they were not coupled to an energy source (Price and Badger, 1989c). Nevertheless, the canonical CA inhibitor, EZ, is an effective inhibitor. Price and Badger tested the effect of EZ on whole cells of *Synechococcus* 7942 and *Synechocystis* 6803 under HC and LC, with a noteworthy decrease of CO_2 uptake, yet no noticeable effect on the carboxysomal CA (Price and Badger, 1989a; Price and Badger, 1989b), possibly due to the CB select permeability (Chowdhury *et al.*, 2015; Kerfeld *et al.*, 2010). Because both complexes are potentially present in the wild-type, it is difficult to make firm conclusions about the target of inhibition. The ability to selectively express NDH-1_3 in C2A presented the opportunity to determine whether this complex is specifically inhibited by the traditional inhibitor (Figure 14 and 16). As shown, EZ completely inhibits C_i uptake in C2A. As shown previously, we observed only incomplete inhibition of C_i uptake in the wild-type. Taken together, our results lead to the tentative conclusion that the NDH-1_3 is more sensitive to EZ inhibition than the NDH-1_4 complex and, thus, may have an active site that more closely resembles the canonical CA active site. EZ is a sulfonamide molecule

that has a conserved mode of protein interaction and binds to the catalytic metal present in the CA active site. There are several known families of CA dispersed throughout multiple kingdoms, α, β, γ, δ, ζ, η, ε, θ, with numerous isoforms (DiMario *et al.*, 2017). EZ is known to be an inhibitor to a variety of CAs isoforms, in diverse families (Baranauskienė and Matulis, 2012). It possesses, however, different affinities to these and is dependent on pH and buffer conditions, which is also true for other CA inhibitors (Baranauskienė and Matulis, 2012; Price and Badger, 1989b; Supuran, 2008). In all cases studied, the inhibitor binds this metal, typically zinc, via a nitrogen atom in the sulfonamide group, thereby displacing the substrate water position otherwise located at this metal ligand position (Baranauskienė and Matulis, 2012; Lindskog, 1997; Price *et al.*, 2002). That is the water that deprotonates and attacks CO_2 during the reversible CA hydration reaction. In principal, a similar metal-binding sites may exist in NDH-1_3 (and possibly NDH-1_4) based upon the inhibitor characteristics.

Another interesting finding apparent from the analysis of the different strains under this study was the fact that even under heavy CO_2 gassing at pH 8, cells expressing the NDH-1_3 complex alone were still starved for C_i as evidenced by the induction of the high affinity bicarbonate transporter, SbtA (Figure 10), consistent with earlier results (Maeda *et al.*, 2002), as well as recent findings from the Mi group (Han *et al.*, 2017). This indicates that passive C_i uptake (by diffusion or by aquaporins) is not enough for efficient photosynthesis when CO_2 hydration systems are not present. These results point to an exceptional importance of the NDH-$1_{3,4}$ complexes in supplying C_i and/or avoiding leakage of C_i by

recycling CO_2 before it leaves the cell. Cyanobacteria internally accumulate C_i in the form of HCO_3^-, which cannot pass easily through the lipoproteic cell membranes (Price and Badger, 1989c). The CO_2 released by CA inside the carboxysome is likely only partially captured by Rubisco, thus requiring the rehydration of CO_2 to HCO_3^-, to contain the otherwise easily lost CO_2. The NDH-$1_{3,4}$ complexes are predicted to mitigate C_i leakage, which would otherwise reach 85% at pH 7 (Espie *et al.*, 1991; Kaplan and Reinhold, 1999; Mangan *et al.*, 2016; Price *et al.*, 1998). The observation of the expression of SbtA observed in both C2 and C2A, even under 3% CO_2 gassing, is consistent with this scavenging role to compensate the intense CO_2 leakage. Since SbtA is also induced in C2A, which contains NDH-1_3, suggests that a combination of both NDH-1_3 and NDH-1_4 must work in tandem for effective recapture of leaked CO_2 under our pH 8 growth conditions. Accordingly, the presence of the high CO_2 affinity system under HC is not enough to maintain internal HCO_3^- pool required for an efficient C_i fixation, indicating the importance of NDH-1_4, as previously suggested (Han *et al.*, 2017). However, improvements in the tools for quantifying the amounts of assembled and membrane integrated NDH-1_3 and NDH-1_4 complexes will be required for a quantitative analysis of the role of these crucial components of the CCM. Improvements of the present CupA antibody as well as the production of antibodies for the other components would expand this capability. This will be required for the estimation of the spatial density of NDH-1_3 that is necessary to evaluate its role in the uptake of CO_2 and control of its leakage in the cellular system. Such information will be of value for mathematical models estimating fluxes (Fridlyand *et al.*,

1996; Mangan *et al.*, 2016), where the correct parametrization of these models, including the concentrations of the NDH-1 complexes, will allow insights on how they function, including the roles of the high and low affinity systems. The development of an antibody against CupA is a first step towards this goal and improvements in its quality, along with other protein methods to evaluate the assembly state of the complexes, are currently underway.

4.5 Conclusions

The ectopic expression of a synthetic NDH-1_3 system under the control of a Rubisco promoter allows the reintroduction of the genes for NDH-1_3 involved in CO_2 hydration into a strain lacking CO_2 hydration capacity. This will enable structure-function tests using site directed mutagenesis. The synthetic system constructed here will be a powerful tool to better study each of the proteins involved in the NDH-1_3, now independent of LC acclimation requirements. At the same time, the analysis revealed that NDH-1_3 is more sensitive to EZ inhibition than NDH-1_4 indicating that the two CO_2 hydration systems likely have significant structural differences with respect to their active sites.

5 CHAPTER V

MUTATIONS ON CONSERVED HISTIDINE AND CYSTEINE OF CUP PROTEINS AFFECT CELL UPTAKE OF CO_2[‡]

[‡]Contents from this chapter will be part of a manuscript in preparation:

Artier, J., Miller, N. T., Zhang, M., Price, D. & Burnap, R. L. *Structure-function studies of CO_2 uptake proteins in cyanobacteria.*

5.1 Introduction

Aquatic environments often present growth-limiting concentrations of inorganic carbon (C_i), which is the main macronutrient for photosynthetic organisms. This critical growth substrate can be present in aqueous solution as hydrated (H_2CO_3, HCO_3^-, CO_3^{-2}) or anhydrate (CO_2) forms with relative concentrations dependent on the pH. To cope with limiting C_i cyanobacteria have evolved a CO_2 concentrating mechanism (CCM), responsible to increase internal level of C_i and organize Rubisco, the principal enzyme involved in carbon fixation of the Calvin-Benson-Bassham (CBB) cycle, near a carbonic anhydrase enclosed in a microcompartment, the carboxysome (CB) (Rae *et al.*, 2013).

The CCM efficiently increases cellular level of C_i to about 1000-fold compared to the levels of C_i in the external environment (see reviews (Badger and Price, 2003; Kaplan and Reinhold, 1999; Ogawa and Kaplan, 2003). Cyanobacteria requires this high C_i concentration in the internal pool and maintain it far-from the equilibrium as the ionic form HCO_3^-, a species that is less permeable to the membrane than CO_2. Bicarbonate can later enter the proteinaceous CB where it is quickly converted to CO_2 by a pool of CA (Yeates *et al.*, 2008), so it can supply abundantly CO_2 to Rubisco in order to decrease photorespiration (see reviews by (Burnap *et al.*, 2015; Price, 2011).

Part of the CCM involves constitutive and inducible systems that have different substrate affinities and reaction rates, and are tightly regulated (Burnap *et al.*, 2015; Price, 2011). This includes three bicarbonate transporters (SbtA, BicA and BCT1) in the inner/plasma membrane and two CO_2 uptake systems in the thylakoid membranes (Xu *et al.*, 2008; Zhang *et al.*, 2004). Bicarbonate transporters are usually coupled to sodium (Na^+) gradients in a symporter manner or with ATP hydrolysis (Price *et al.*, 2004; Shibata *et al.*, 2002; Xu *et al.*, 2008).

The CO_2 uptake systems are specialized NAD(P)H dehydrogenase type 1 (NDH-1) complexes (Battchikova and Aro, 2007; Ohkawa *et al.*, 2000a). This multiprotein complex shares many homologues with respiratory complex 1 from heterotrophic bacteria and those found in mitochondria, and has a core of proteins, either embedded in the membrane or attached and facing the cytoplasmic side, forming an L shape structure (Battchikova *et al.*,

2011a; Friedrich and Scheide, 2000). Bound to this, two membrane proteins NdhF and NdhD are required for a functional complex, with multiple cyanobacterial paralogs defining the alternative forms of the cyanobacterial NDH-1 complex (see review by (Battchikova and Aro, 2007). The four cyanobacterial variants are designated NDH-1_{1-4} and are identified as NDH-$1_{1,2}$ (or NDH-L, contains NdhF1/D1 and NdhF1/D2) with roles in respiration and NDH-$1_{3,4}$ (or NDH-1MS, contains NdhF3/D3 and NdhF4/D4) involved in CO_2 uptake (Battchikova *et al.*, 2011a). Despite these structural and functional differences among the four forms, it was shown that all cyanobacterial NDH-1 are involved in photosynthetic cyclic electron transport (Bernat *et al.*, 2011). This is in accordance with the main function of NDH-1 complexes, which is to transfer electrons from a donor (NADH/Fd_{red}/NADPH) to a plastoquinone, in a reaction coupled with proton transfer, generating *pmf* required for ATP synthesis (Friedrich and Scheide, 2000). In fact, NdhB, NdhF and NdhD are homologues of the proton transfer proteins NuoL, NuoM and NuoN from *E. coli* (Battchikova *et al.*, 2011a; Friedrich and Scheide, 2000). Also, these proteins were shown to be essential for the CO_2 uptake function of NDH-$1_{3,4}$ (Han *et al.*, 2017; Ohkawa *et al.*, 2000b), suggesting an energized process utilizing the redox power of NADPH or reduced ferredoxin (Fd_{red}).

Cyanobacterial CO_2 uptake complexes have an unique protein that sits on NdhD/F subcomplex facing the cytoplasm side giving a U shape to the complex (Folea *et al.*, 2008), and is also essential for its function (Maeda *et al.*, 2002; Shibata *et al.*, 2001). These are the "CO_2-uptake proteins" (Cup, or alternatively, "CO_2-hydration protein", Chp) present in

two forms, CupA (ChpY, in NDH-1_3) or CupB (ChpX, in NDH-1_4). Although previously many studies focused on these systems, the molecular mechanism of the reaction is not understood. Kaplan and collaborators initially proposed that presence of an "alkaline pocket" due to proton removal in the membrane portion of the complex, which would direct a possible nearby CA to hydrates CO_2 into HCO_3^- (Kaplan and Reinhold, 1999). However, it was shown that a true CA is not present in the cyanobacterial cytoplasm (Price and Badger, 1989c). Price and Badger later proposed that Chp (Cup) proteins may have a CA-like function with a potential active site of conserved Histidine (His) and Cysteine (Cys) possibly linked to a metal cofactor (Price *et al.*, 2002). This idea also included the NdhF/D proteins as responsible for the proton removal to direct the hydration of CO_2 and suggested the coupling with electron transport from Fd_{red}/NADPH to plastoquinone (PQ). Moreover, it was shown that traditional carbonic anhydrase inhibitors, particularly ethoxyzolamide (EZ), decreases CO_2 uptake in cyanobacteria with no interference on HCO_3^- transport (Espie *et al.*, 1991; Price and Badger, 1989a; Price and Badger, 1989b).

In this chapter, the synthetic system for NDH-1_3 constitutive expression developed in Chapter 4 was utilized for site-directed mutagenesis in an effort to evaluate the roles of highly conserved amino acids of *Synechocystis* 6803 CupA in CO_2 uptake. Additionally, a plasmid-based mutagenesis system to probe CupB (ChpY) that was developed in the laboratory of Professor Dean Price, together with specific mutants produced using the system, were analyzed. Our hypothesis, based on the previous proposed ideas, was developed that posits CupA (ChpY) and CupB (ChpX) proteins functioning as special

carbonic anhydrase (CA) proteins that couple CO_2 hydration directly with the proton pumping activity of the specialized NDH-$1_{3,4}$ complexes, possibly energized by the electron transfer from Fed_{red}/NADPH to PQ (Figure 19).

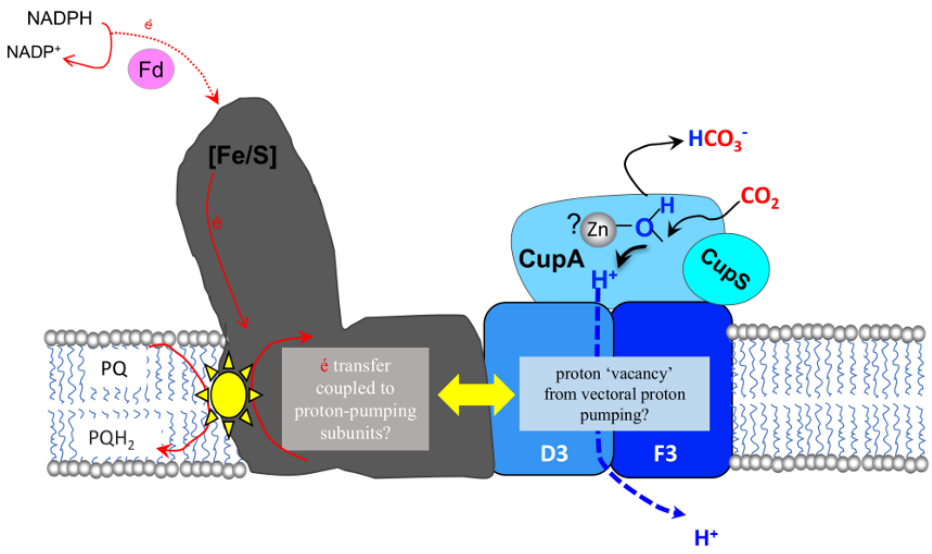

Figure 19. Hypothetical model of cyanobacterial CO_2 uptake by NDH-$1_{3,4}$. Two Type-1 NAD(P)H dehydrogenase complexes (NDH-1) are known CO_2 uptake (CUP) systems present on the thylakoid membrane.

We also hypothesize that the CupA and CupB proteins may coordinate a metal ion that, by analogy with bona fide carbonic anhydrases (CA), functions to mediate the hydration of CO_2 to bicarbonate. Our hypothesis suggests that the removal of protons from the CA-like active site by the proton pumping activity of the NDH-1 complex drives the reaction far-from equilibrium. As discussed below, multiple sequence alignment of Cup proteins from

100 cyanobacteria strains shows highly conserved amino acids in both CupA and CupB proteins. The most likely one to participate in CA activity was targeted for mutagenesis in both *Synechocystis* 6803 and *Synechococcus* 7942, and analysis of the phenotypic consequences of their mutation is presented here.

5.2 Materials and Methods

5.2.1 Multiple sequence alignments and phylogenetic analysis

Amino acid sequence for *Synechocystis* 6803 protein CupA was obtained from Cyanobase. Later it was used as the query sequence for Blastp search with E-value cutoff $1e^{-50}$ in the JGI website (Nordberg *et al.*, 2013). The resulting amino acid sequences from about 100 phylogenetically diverse cyanobacteria genomes, including both CupA and CupB proteins, were aligned with MUSCLE (Edgar, 2004) using MEGA 7 software (Kumar *et al.*, 2016). The multiple sequence alignment (MSA) was used to construct a maximum likelihood phylogenetic tree, with bootstrap analysis of 100. A second MSA was performed using MAFFT 7 (Katoh *et al.*, 2017) (run with interactive G-INS-I, for proteins with global homology), used to build a new phylogenetic tree with PhyML 3.1 (Guindon *et al.*, 2010). MSA were analyzed using Jalview 2.10 (Waterhouse *et al.*, 2009). Trees were constructed with settings considering LG substitution model, NNI tree topology and aBayes algorithm was used for branch support when in PhyML. CupA amino acid sequence and/or MSA was also analyzed by Swiss-Model workspace (secondary structure prediction) (Arnold *et al.*,

2006), PredictProtein (Yachdav *et al.*, 2014), and ConSurf (conserved and functional regions) (Ashkenazy *et al.*, 2016; Berezin *et al.*, 2004).

5.2.2 Cyanobacterial strains and constructions of mutants

Synechococcus sp. PCC 7942 wild type, a double knockout mutant Δ*chpX*/Δ*chpY* (Woodger *et al.*, 2005) and complementation mutants containing *chpX* in a shuttle vector pSE4, also with point mutations on selected amino acids were provided by our collaborator, Professor Dean Price of Australian National University. These were maintained in standard BG-11 medium (Allen, 1968), pH 8, supplemented with 10 mM HEPES-NaOH and grown in HC conditions as described (see Chapter 2), in the presence of Spec 20 μg mL^{-1} to maintain the plasmid. HC8 cells were C_i depleted and C_i affinity assays following O_2 evolution dependent on C_i uptake were measured (see details in Chapter 2). Spot assays were performed as described (see Chapter 2).

Mutants C2 and C2A used in this study are described on Chapter 3. A new plasmid pV5 containing a synthetic *cupA* operon under *rbcL* promoter was constructed, where unique RE sites were inserted between each gene by changing nucleotides sequence on the original intergenic sites. The native ribosome binding site (RBS) of each gene was estimated following previous work (Mitschke *et al.*, 2011), and were not modified. The new operon was synthesized with no codon optimization and inserted into pV5 between NdeI and NotI sites (GenScript Biotech, USA).

A second construct was developed to complement the C2 stain by restoring the *cupB* gene necessary to synthesize a functional NDH-1_4 system. For this, the *cupB* gene (1149 bp) was synthesized and inserted into chromosomal integration vector 3 (pV3) (GenScript Biotech, USA). The plasmid pV3, sibling of pV5, has the *rnpB* promoter region, Kanamycin cassette and sequences for the integration into the neutral, noncoding site between ssr2848 and sll1577. The construct was used to transform C2 and C2A, with integration into genomic DNA confirmed by PCR.

Four amino acids that were found to be highly conserved in both CupA and CupB based upon multiple sequence alignments, and estimated to participate on the hypothetical active site, were mutated by changing nucleotide of its codon, and the point mutation was synthesized into the new *cupA* operon and *cupB* constructs (GenScript Biotech, USA). Similar and additional point mutation strains were constructed by site direct mutagenesis using QuikChange Site Directed Mutagenesis kit (Agilent) accordantly to manufacturer's instructions. The original pV5 with *cupA* operon plasmid without RE was used for this.

In order to evaluate if NDH-1_3 systems are interchangeable among cyanobacteria species, the *cupA* operon from an *Arthrospira* species was homologously expressed in *Synechocystis* 6803. Similar to described on Chapter 3, the *cupA* operon region (4710 bp) from two strains of *Arthrospira* (*A. India;* Genbank KT779290.1, from Soda Lake, Lonar Crater, India; and *A. maxima CS-328*, Genbank GCA_000173555, kindly provided by Charles Dismukes, Rutgers University) were each inserted into pV5 using Gibson

assembly (Gibson *et al.*, 2009), and construct was transformed into C2, with integration into genomic DNA confirmed by PCR. The constructs were transcriptional and translational fusions, respectively, with relative to the *rbcL* promoter present in pV5.

A triple knockout mutant, C3, was developed using a similar construct as for C1 (Chapter 3), by removing genes for NDH-1_4 and BCT1 in the C1 background. In *Synechocystis* 6803 *ndhD4*/*ndhF4* genes are in the genomic region following the genes for BCT1, which are clustered on an operon, *Cmp* operon (*cmpA*, *cmpB*, *porB*, *cmpC*, *cmpD*). The upstream region of *cmpA,* 500bp, and the downstream region of *ndhF4* were inserted in the Blue Heron pUC plasmid similar to described before (pCmpopsap) (Blue Heron Biotechnology Inc.), with Spec/*sacB* cassette later added in between by Golden gate assembly (Engler *et al.*, 2009), forming the pCmpopSS. After segregation, the vector pCmpopsap without Spec/SacB cassette was used to remove the Spec/*sacB* cassette in the presence of 5% sucrose. C3 was also a recipient strain of *Synechocystis* 6803 pV5 *cupA* operon and *Arthrospira* pV5 *cupA* operon.

5.2.3 Isolation of thylakoid membranes

Four flasks containing 800 mL each of HC grown cells with OD_{750nm} of 0.4-0.6 were used for TM extraction, as previous published protocol with small modifications (Burnap *et al.*, 1989; Dilbeck *et al.*, 2012). *Synechocystis* 6803 cells were harvested by centrifugation for 10 min at 10000 *x g,* 4 °C and washed in 120 mL of HN buffer (10 mM HEPES, 30 mM NaCl, pH 7.3). Solution was kept on ice, at low light (from now on), and centrifuged at

10000 *x g*, 13 min, 4°C, then resuspended in 120 mL of thylakoid membrane breaking buffer (TBB, 50 mM MES-NaOH, 10% glycerol v/v, 1.2 M betaine, 5 mM $MgCl_2$ and 5 mM $CaCl_2$, pH 6.0). This was centrifuged at 10000 *x g*, 10 min, 4°C, and pellet was resuspended to ~14 ml with TBB up to a concentration of 0.4-1 mg of Chl mL^{-1}. The solution was incubated in darkness and on ice for at least one hour. The cell breakage was performed in a 4° C room under a dim green light. The cell suspension was transferred to a homogenizer 20 mL BeadBeater chamber and added 25 grams of pre-cooled 0.1 mm diameter zirconium/silica beads. Prior to cell breakage, benzamidine, ε-amino-η-caproic acid, and phenylmethanesufonyl fluoride (PMSF) were added to the cell suspension to a concentration of 1 mM each, together with 1.5 mg of DNase I (powder, Sigma). The small homogenizer chamber was set inside a polycarbonate chamber filled with crushed ice/water mix to keep sample cold. Cells were broken by 4 cycles (5 s on, 5 min off in ice/water) in a BeadBeater (BioSpec Products) inside a water-ice jacket. After breakage and settling of beads, the supernatant was obtained and the beads were washed 3 to 5 times with TBB up to 60 mL, final volume. Unbroken cells and remaining zirconium/silica beads were further separated from the supernatant by centrifugation at 3600 *x g* for 10 min at 4°C. The supernatant was obtained and centrifuged at 22000 rpm (approximately 60000 *x g*) for 40 min at 4°C. The pelleted thylakoid membranes were resuspended with approximately 400 μL of TSB (50 mM MES-NaOH, 10% glycerol v/v, 1.2 M betaine, 20 mM $CaCl_2$ and 5 mM $MgCl_2$, pH 6.0) to 0.9-1.5 mg mL^{-1} Chl, aliquoted, flash-frozen in liquid nitrogen, kept

in dark stored at -80°C. O_2 evolution activity of TM was verified after frozen following previous protocols of polarographic O_2 measurements (Dilbeck *et al.*, 2012).

5.2.4 Analysis of proteins from thylakoid membrane using PAGE

Proteins from TM preparation were treated before separation in a (BN) PAGE (Schägger and von Jagow, 1991). Samples with 1mg mL^{-1} Chl were solubilized in TSB with 1% n-dodecyl β-D-maltoside with stir at 4°C for 30 min, at darkness or low green light, and centrifuged 10000 *x g* for 10 min, 4°C, aliquoted and snap frozen, stored at -80°C. Treated samples containing 3μg mL^{-1} Chl, supplemented with BN sample buffer (5% Serva Blue G, 200 mM BisTris-HCl, pH 7.0, 500 mM ε-amino-n-caproic acid) were separated in a 1 mm, 4–12.5% acrylamide gradient blue native (BN) PAGE (Schägger and von Jagow, 1991). Electrophoresis was performed at 4 °C with increasing voltage (gradually from 50 to 200 V) for 6 h. BN-PAGE containing separated proteins were used for western blot and evaluation of carbonic anhydrase activity assay following previous described protocol (De Luca *et al.*, 2015).

5.3 Results

5.3.1 Multiple sequence alignments show conserved amino acids that are Cup potential active site residues

CO_2 uptake proteins (Cup/Chp) have been the focus of diverse studies, including some small multiple sequence analysis with the available cyanobacteria genomic data of the time

(Price *et al.*, 2002). Here we performed a Blast search using *Synechocystis* 6803 amino acid sequence as probe and obtained 168 amino acid sequences of both CupA and CupB from 100 phylogenetically diverse cyanobacteria strains using Joint Genome Institute (JGI) online tools. These were analyzed by performing multiple sequence alignments, to evaluate conserved sites that could be theoretically part of the Cup active site.

Our Blast search showed that Cup/Chp proteins seems to be only present in cyanobacteria, as previously mentioned in the literature (Price *et al.*, 2002). Also, although hypothesized as a possible type of CA, there were not hits with any of the numerous CA isoforms from any of the 8 CA families (α, β, γ, δ, ζ, η, ε, θ) present on NCBI, even when a distant evolutionary relationship analysis was performed using Psi-Blast (results not shown). This expands an earlier bioinformatic investigation by Price and Badger, who analyzed 10 amino acids sequences and suggested conserved Histidine and Cysteine, that may be the ligands for a putative metal in the active site of Cup/Chp proteins (Price *et al.*, 2002). Our results confirmed this and showed that Cup/Chp proteins have highly conserved (>89%) amino acids previously described. A simplified amino acid alignment is represented in Figure 20, with both CupA/B proteins from five cyanobacterial strains, where Histidine (His, H) are in blue and Cysteine (Cys, C) is shown in red. Among the 100 cyanobacterial strains, these amino acids were shown to be more than 89% conserved by analysis with Jalview (Waterhouse *et al.*, 2009) and ConSurf (conserved and functional regions) (Ashkenazy *et al.*, 2016; Berezin *et al.*, 2004).

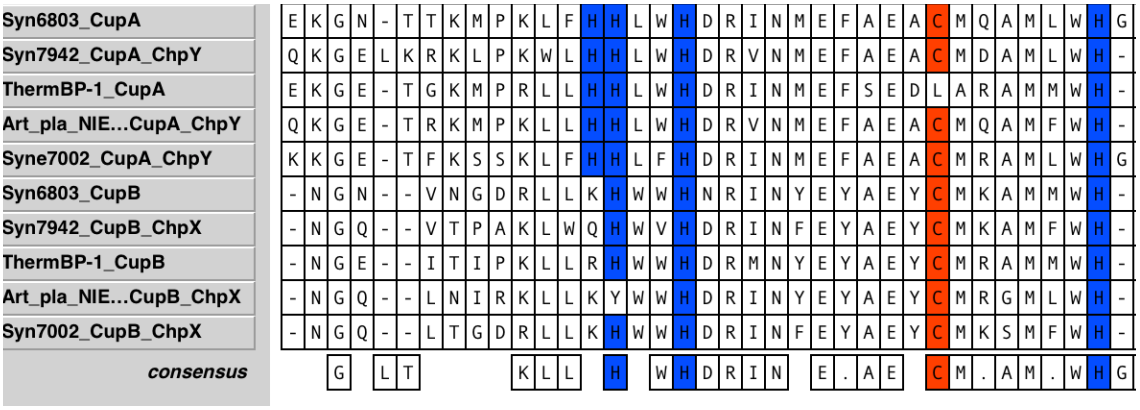

Figure 20. Cyanobacterial CO_2 uptake proteins multiple sequence alignment. Alignment of Cup/Chp amino acid sequence from 100 cyanobacteria strains shows highly conserved His (H, blue) and Cys (C, red). Only five strains of cyanobacterial Cup proteins are displayed, for easier visualization using MacVector software protein alignment tool.

5.3.2 Phylogenetic studies suggest separation of Cup proteins in two clades

Synechocystis 6803 CupA and CupB are only 46% identical in their amino acid sequence, with CupA having an extra amino acid, presumably an additional domain that may bind CupS, only present on NDH-1_3 (Korste *et al.*, 2015). Amino acid sequence of CupA/B from 100 cyanobacterial strains was analyzed by MSA using both MUSCLE (Edgar, 2004) in MEGA 7 software (Kumar *et al.*, 2016) and MAFFT 7 (Katoh *et al.*, 2017). These were each used to construct a maximum likelihood phylogenetic tree, either in MEGA 7 or PhyML 3.1 (Guindon *et al.*, 2010). Although the trees have some differences, the general unrooted pattern shows that CupA/ChpY and CupB/ChpX are clearly separated in two subgroups ("clades"). An unrooted representative tree is present on Figure 21, with CupB/ChpX in the left and CupA/ChpY on the right.

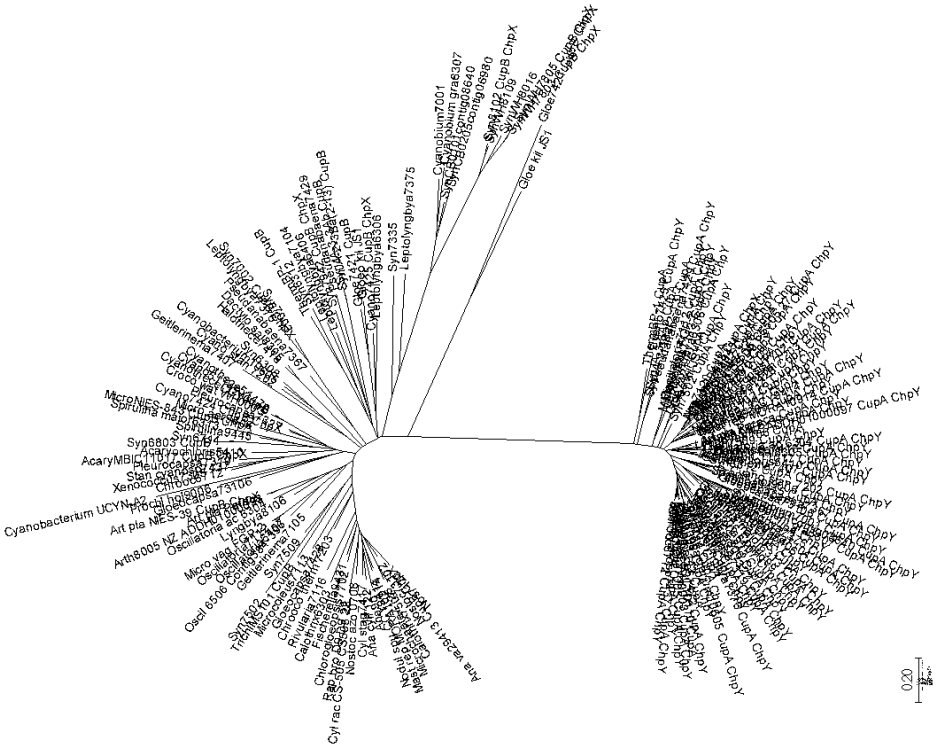

Figure 21. Unrooted maximum likelihood phylogenetic tree. Two clades are clearly distinct, CupB/ChpX in the left, CupA/ChpY in the right. The tree with the highest log likelihood is shown. Initial tree(s) for the heuristic search were obtained automatically by applying Neighbour-Join and BioNJ algorithms to a matrix of pairwise distances estimated using a JTT model, and then selecting the topology with superior log likelihood value using MEGA7. The analysis involved 168 amino acid sequences from 100 cyanobacteria strains, obtained from JGI using protein Blast against *Synechocystis* 6803 CupA.

5.3.3 Point mutations on Chp/Cup proteins affect cell CO_2 uptake

In order to investigate the possible role of highly conserved His and Cys in the CO_2 hydration function of Cup/Chp proteins, we introduced point mutations on *cupA* using the neutral site integration genetic system developed described in Chapter 4. Also,

Synechococcus 7942 strains containing only the ChpX (CupB) protein being expressed (*chpX* in a shuttle vector, background is double knockout mutant Δ*chpX*/Δ*chpY*), with amino acids substitution were obtained from Dean Price. The amino acid substitutions studied here are represented on Table 2. The Histidine (H) was replaced by a Glutamine (Q), an uncharged amino acid of similar size. Cysteine (C) was substituted with a Serine (S) that has similar size but lacks the thiol group, or with an Alanine (A), a small hydrophobic amino acid.

Table 2. Mutations of conserved sites in CupA (ChpY) and ChpX (CupB) used in this work, identified by multiple sequence alignment. Correspondence between rows in the CupA and ChpX indicate homology based upon the multiple sequence alignments.

	Mutants	
Site conservation	Syn6803 CupA	Syn7942 ChpX
79%	H15Q	
48%	H126Q	
89%	H127Q	H86Q
95%	H130Q	H89Q
96%	C141A/C141S	C100S
100%	H148Q	H107Q
39%	C263A/C263S	
50%	C356S	

Growth phenotype of *Synechococcus* 7942 and mutants was evaluated using spot assays with growth in agar under different C_i availability (Figure 22). All strains grew well at pH 8 or supplemented with 20 mM $NaHCO_3$, independent of CO_2 supplementation (results not shown). The strains responded differently when grown on modified pH 7 BG-11 media under air conditions. The strains containing ChpX, such as wild type (WT) and complementation strain with only ChpX both grew well, while the double knockout strain Δ*chpX*/Δ*chpY* failed to grow. This is consistent with previous findings for *Synechocystis* 6803 shown in Chapter 4. Most mutants with single or double mutation on highly conserved amino acids highlighted in Figure 20 have an intermediate growth, with some very similar to the complementation strain with ChpX. Yet, the His 86 failed to grow, similar to Δ*chpX*/Δ*chpY* mutant. This suggests an essential role for this His 86 in CO_2 hydration activity of *Synechococcus* 7942 ChpX (CupB).

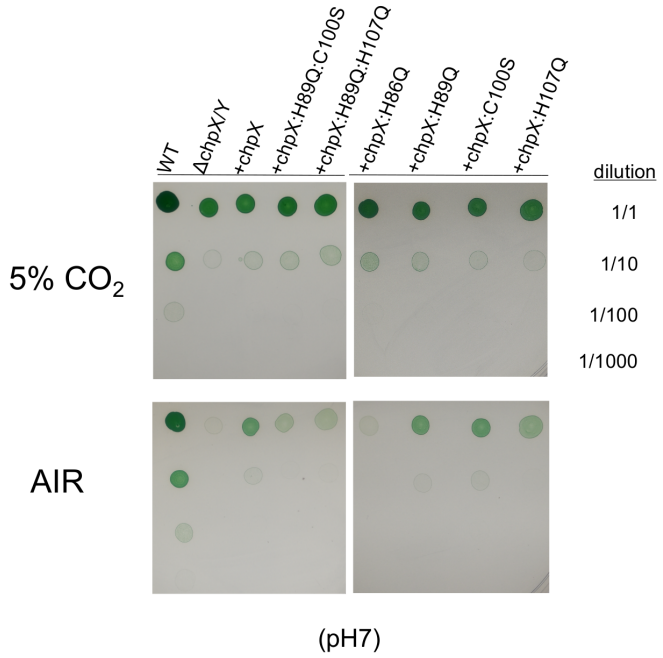

Figure 22. Spot assays for autotrophic growth under pH7 with different CO_2 availability conditions on agar plates. WT and ChpX point mutants were grown in liquid media modified BG-11 pH 7, pelleted by centrifugation, washed once and resuspended in BG-11 7 to OD_{750} of 1, 0.1, 0.01 or 0.001 (top to bottom rows, respectively). Five µL cells at each dilution was spotted on agar plates with pH 7 and grown for five days. Upper panel: 5% CO_2-enriched air; Lower panel: ambient air CO_2 level.

We also evaluated the C_i uptake capacity of *Synechococcus* 7942 ChpX mutants by following photosynthetic oxygen evolution dependent on C_i uptake (Table 3, Figure 23).

In this assay O_2 evolution is entirely dependent on C_i as the electron acceptor, under conditions that poises the reaction for increased CO_2 compared to the HCO_3^-, forcing cells to utilize primarily CO_2 for photosynthesis (modified media lacking nitrate, with pH 7, and

presence of carbonic anhydrase) and can be used to estimate the net whole cell C_i affinity characteristics.

The mutation H86Q again showed the most extreme response, with similar V_{max} of the ChpX complement, but with $K_{0.5}$ in the mM range, comparable to the double mutant knockout Δ*chpX*/Δ*chpY*. This reinforces the importance of H86 in the CO_2 hydration, which absence completely obliterates ChpX function. Mutation on the other two highly conserved His (H89Q and H1007Q) and Cys (C100S) slightly affected the C_i affinity of the ChpX.

Table 3. Photosynthetic O_2 evolution of HC cells of *Synechococcus* 7942 ChpX mutants in response to C_i uptake. V_{max} and $K_{0.5}$ values were obtained from data shown in Figures 23. Potassium bicarbonate ($KHCO_3$) was added as source of C_i, in the presence of CA 25 μg mL^{-1}. Values are means and ± indicates standard deviations (SD) with experimental replicates, n=4.

Strain	**V_{MAX}**	**$K_{0.5}$ (C_I)**
***Synechococcus* 7942**	**(μmol O_2 mg^{-1} Chl h^{-1})**	**(μm)**
Δ*chpX*Δ*chpY*	130 ±3	7600 ±1200
ChpX	142 ±29	27 ±8
H86Q	166 ±9	4600 ±300
H89Q	126 ±22	89 ±15
C100S	150 ±16	68 ±12
H107Q	131 ±9	80 ±15

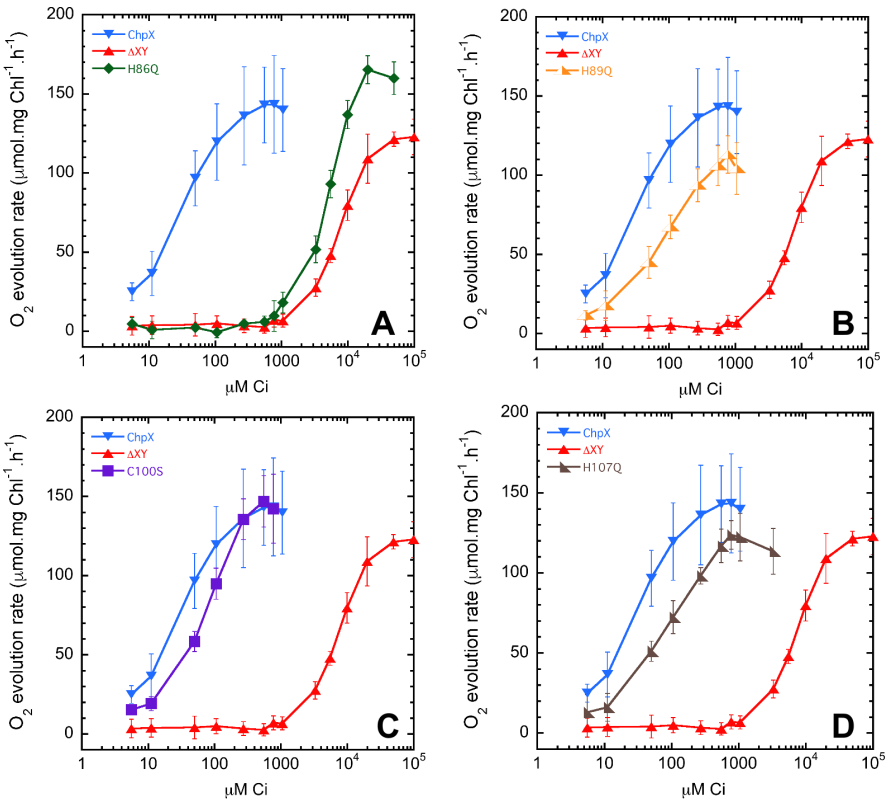

Figure 23. Assays for C_i affinity measuring photosynthetic O_2 evolution rates in *Synechococcus* 7942 strains with different CO_2 uptake system under low sodium. Cells were grown in BG-11 pH 8, supplemented with 3% CO_2 (HC8) and illumination at 70 µmol (photons) m^{-2} s^{-1}. Before assay cells were washed with modified LC7 media (BTP, no $NaNO_3$) depleted of C_i. $KHCO_3$ was added as source of C_i, in the presence of CA 25 µg mL^{-1}. Traces are representative of at least two biological replicates (n=4), and bars indicate ±SD. The double knockout strain Δ*chpX*Δ*chpY* (ΔXY, red) and complementation with ChpX (blue) strains are shown as references. A) H86Q (dark green); B) H89Q (orange); C) C100S (purple); D) H107Q (brown).

Similar mutations were constructed in *Synechocystis* 6803 CupA using the constitutive expression system described in Chapter 4. Additional amino acids with lower conservation

scores were also substituted as represented in Table 2. Here we present the result for two Cys mutations, the highly conserved C141A, and a less conserved (39%) C263S. O_2 evolution assays were used similar to described in the above section, which can be used to estimate the net whole cell C_i affinity characteristics and results are presented in Table 4 and Figure 24. The mutation on CupA:C141A, had no significant effect on the CO_2 hydration, even less than seen in ChpX (Table 3, Figure 23). Yet, the strain with CupA:C263S, a less conserved amino acid, decreased the reaction flux (58±4 μmol O_2 mg^{-1} Chl h^{-1}) compared to C2A (93 ±15 μmol O_2 mg^{-1} Chl h^{-1}).

Table 4: Photosynthetic O_2 evolution of HC cells with point mutation in Cysteine of NDH-1$_3$/CupA in response to C_i uptake. V_{max} and $K_{0.5}$ values were obtained from data shown in Figure 24. Potassium bicarbonate ($KHCO_3$) was added as source of C_i, in the presence of CA 25 μg mL^{-1}. Values are means and ± indicates standard deviations (SD) with corresponding number of experimental replicates, n.

Strain *Synechocystis* **6803**	**V_{MAX} (μmol O_2 mg^{-1} Chl h^{-1})**	**$K_{0.5}$ (C_I) (μm)**	**N**
C2A	93 ±15	8 ±3	10
C141A	93 ±3	8 ±4	4
C263S	**58 ±4**	5 ±1	4

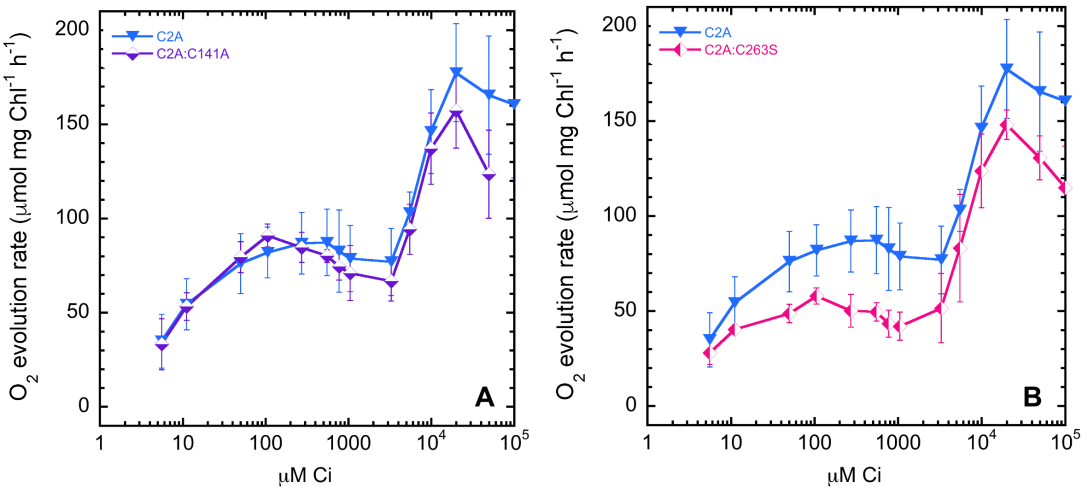

Figure 24. Assays for C_i affinity measuring photosynthetic O_2 evolution rates in *Synechocystis* 6803 strains with point mutation in CupA CO_2 uptake protein under low sodium. Cells were grown in BG-11 pH 8, supplemented with 3% CO_2 (HC8) and illumination at 70 µmol (photons) m^{-2} s^{-1}. Before assay cells were washed with modified LC7 media (BTP, no $NaNO_3$) depleted of C_i. $KHCO_3$ was added as source of C_i, in the presence of CA 25 µg mL^{-1}. Traces are representative of at least two biological replicates (total: n=4), and bars indicate ±SD. C2A, in blue, containing the ectopic constitutive expression of the high CO_2 affinity NDH-1_3 uptake system with low flux was used as reference. A) In purple, C2A:C141A point mutation strain. B) In strawberry, C263S point mutation strain.

The effect of the liposoluble traditional CA inhibitor EZ was evaluated under similar conditions described in the above section. This was used to test whether the point mutations altered the structure/function of the CupA active site, disrupting the CupA inhibition by EZ, described in Chapter 4. Photosynthetic O_2 rates dependent of C_i in C2A:C141A and C2A:C141A, HC cells, were assayed after the addition of 200 µM EZ. The mutation of

CupA:C141A, had decreased inhibition by EZ (49±4 μmol O_2 mg^{-1} Chl h^{-1}) compared to C2A (32 ±6 μmol O_2 mg^{-1} Chl h^{-1}). It is possible that this mutation caused a change of the structure of the active site, due to its proximity, and binding of EZ is slightly weakened.

Table 5: Photosynthetic O_2 evolution of HC cells with point mutation in Cysteine of NDH-1$_3$/CupA in response to C_i uptake. V_{max} and $K_{0.5}$ values were obtained from data shown in Figure 25. Potassium bicarbonate ($KHCO_3$) was added as source of C_i, in the presence of EZ 200 μM. Values are means and ± indicates standard deviations (SD) with corresponding number of experimental replicates, n.

Strain *Synechocystis* **6803**	**V_{MAX} (μmol O_2 mg^{-1} Chl h^{-1})**	**$K_{0.5}$ (C_I) (μM)**	**N**
C2A	32 ±6	6 ±3	10
C141A	**49 ±5**	6 ±2	4
C263S	17 ±7	7 ±3	4

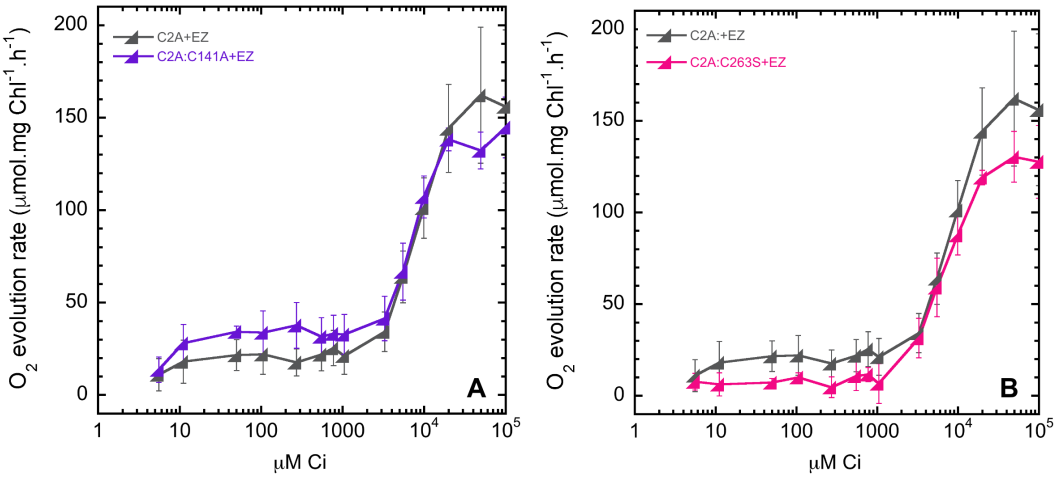

Figure 25. Assays for C_i affinity measuring photosynthetic O_2 evolution rates in *Synechocystis* 6803 strains with point mutation in CupA CO_2 uptake protein under low sodium. Cells were grown in BG-11 pH 8, supplemented with 3% CO_2 (HC8) and illumination at 70 µmol (photons) m^{-2} s^{-1}. Before assay cells were washed with modified LC7 media (BTP, no $NaNO_3$) depleted of C_i. $KHCO_3$ was added as source of C_i, in the presence of EZ 200µM. Traces are representative of at least two biological replicates (n=4), and bars indicate ±SD. C2A, in dark grey, containing the ectopic constitutive expression of the high CO_2 affinity NDH-1_3 uptake system with low flux was used as reference. A) In purple, C2A:C141A point mutation strain. B) In strawberry, C263S point mutation strain.

5.3.4 CupA constitutively expressed is bound to NDH-1_3 in C2A strains

In order to evaluate if the constitutively expressed NDH-1_3 in C2A, beside functional, has the correct colocalization in the thylakoid membrane (TM), immunoblot assays were performed. Figure 26A shows a clear reaction at the expected 47 kD mass of CupA in the extracted TM of both C2A grown in HC and the wild type (WT) grown under LC

conditions (LC7) for 36 h. The reaction is stronger than in the total cell extracts proteins (T) samples, probably since it is in higher concentration in the TM extracts. However, the reason for the higher concentration in the membrane sample is not clear since equal amounts of Chl (μg) were loaded and the amount of CupA protein should be directly proportional to the amount of Chl. One possibility is that the total cell extracts have a residual protease activity that was not inhibited by the added protease inhibitor cocktail. The result shows that in both C2A and WT under HC conditions, CupA is attached to NDH-1_3 complex, present in the TM, although a small amount is also detectable in the supernatant (Sup) fraction. Sup was obtained after pelleting the TM and contains cytoplasmic proteins. These results combined with the finding that all of the SbtA reaction is confined to the membrane fraction indicate that a fraction of CupA was either never bound to the membrane, or more likely, lost during the membrane purification process, even in the wild type. SbtA presence was also evaluated using commercial antibody, and a reaction is seen at the expected ~39 kD mass (Figure 26C). This protein is a LC inducible bicarbonate transporter, and as shown in Chapter 4, is detectable in both C2 and C2A, independent of C_i availability. A reaction is visible in the total protein as well as in thylakoid membrane extract, even stronger in WT LC7, suggesting contamination of TM with inner/plasma membrane. Further purification of TM proteins using a sucrose gradient fractioning would be necessary to remove inner/plasma membrane, as described formerly (Zhang *et al.*, 2004). Yet, this assay will be useful to evaluate if the CupA mutants with

amino acids substitution cause a severe damage in the structure of CupA that would displace it from the NDH-1_3 complex.

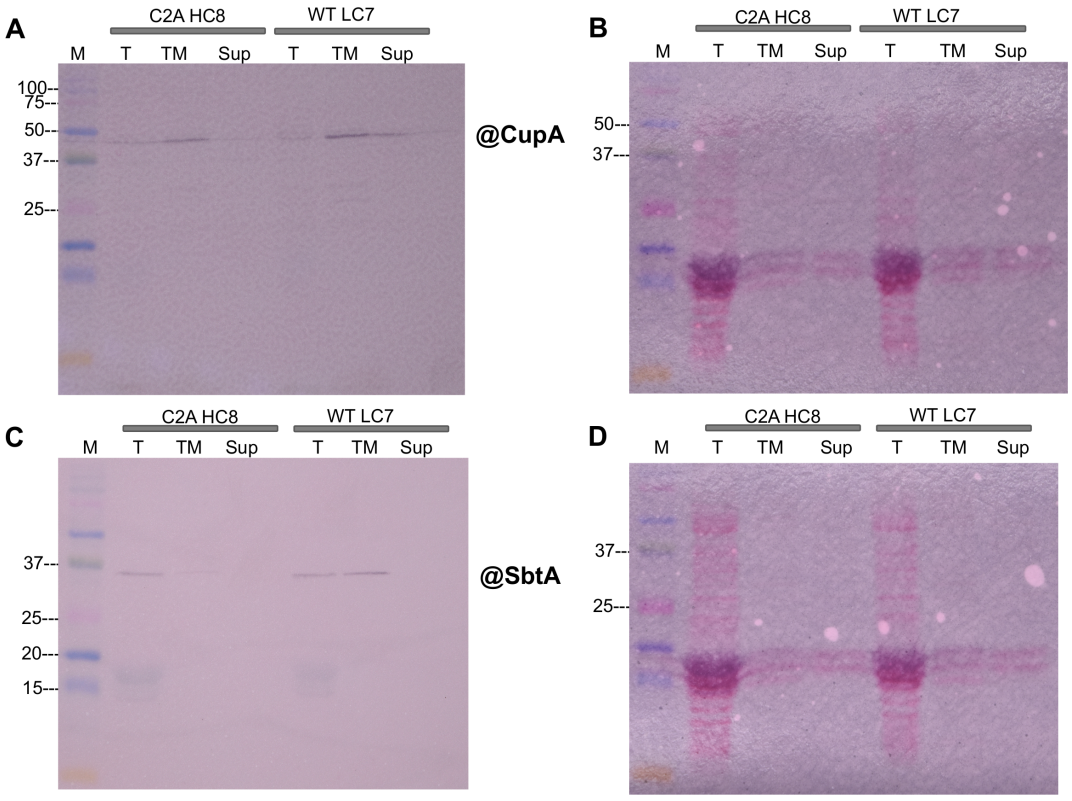

Figure 26. Immunodetection of CupA and SbtA in WT and C2A at different C_i availability. C2A was grown in BG-11 at HC conditions with pH 8 supplemented of 3% CO_2 (HC8). WT was grown at modified BG-11 pH 7 supplemented with 3% CO_2 and later switched to 36 h air (LC7). Total cell extracts (T) and thylakoid (TM) samples containing 3 µg Chl were loaded on a 12% SDS-PAGE gel and transferred to a PVDF membrane. Previous to detection, the PVDF membranes were stained with 0.5% Ponceau S to verify equal loading (panel B and D). CupA (panel A, ~47 kD) and SbtA (panel C, 37 kD) were detected using a produced and a commercial antibody (Agrisera), respectively. A marker was added for molecular weight comparisons (lane M) (Precision Plus Protein Kaleidoscope, Bio-Rad). T, total cell protein; TM, proteins from thylakoid membrane extraction; Sup, supernatant obtained after TM precipitation, containing cytoplasmic proteins.

5.3.5 *Functional heterologous expression of an Arthrospira* sp. NDH-1$_3$ in *Synechocystis* 6803.

Studies of cyanobacterial NDH-1$_{3,4}$ complexes are restricted to model organisms such as *Synechocystis* 6803 and *Synechococcus* 7942, among a few others. In order to test if the system developed on Chapter 4 could be used for heterologous expression of diverse cyanobacterial *cupA* operons, we constructed a similar plasmid to the one described in Chapter 4, using pV5, yet containing the *cupA* operon from two strains of *Arthrospira* (*A. India* and *A. maxima CS-328*). This project was performed in collaboration with a group from India who characterized a new *Arthrospira* strain (Zawar *et al.*, 2016), so we named the construct C2AInd (India). O_2 evolution dependent on Ci uptake were used to evaluate complex function and results are presented in Figure 27. The C2AInd strain grown under high C_i conditions (HC8) exhibited a medium V_{max} (144 μmol O_2 mg^{-1} Chl h^{-1}) and moderate $K_{0.5}$ (73 μM). Comparatively to C2A, C2AInd presented a higher reaction flux, and lower substrate affinity. Besides, 200 μM EZ completely inhibited Ci uptake (Figure 27B), suggesting a similar active site as for *Synechocystis* 6803 and *Synechococcus* 7942.

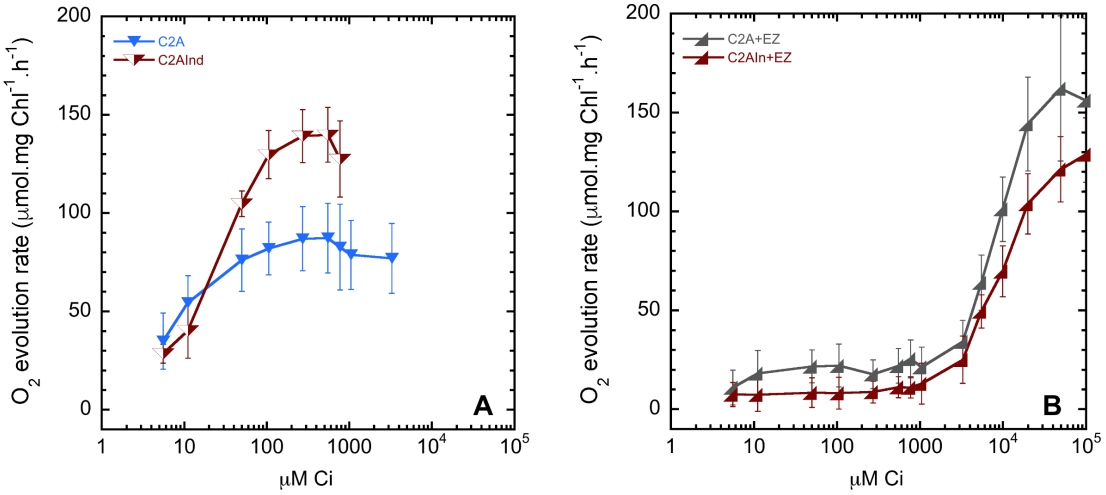

Figure 27. Assays for C_i affinity measuring photosynthetic O_2 evolution rates in *Synechocystis* 6803 strains with an *Arthrospira* sp. (India) *cupA* operon. Cells were grown in BG-11 pH 8, supplemented with 3% CO_2 (HC8) and illumination at 70 µmol (photons) m^{-2} s^{-1}. Before assay cells were washed with modified LC7 media (BTP, no $NaNO_3$) depleted of C_i. $KHCO_3$ was added as source of C_i, in the presence of CA 25 µg mL^{-1} (only Panel A). Traces are representative of at least three biological replicates (n=6), and bars indicate ±SD. A) C2A, in blue, containing the ectopic constitutive expression of the high CO_2 affinity NDH-1_3 uptake system with low flux. In dark brown, C2AInd strain expressing *Arthrospira* sp. *cupA* operon. Note: Only the first phase in shown in the no inhibitor test (A). In B) EZ, a carbonic anhydrase inhibitor, was added at 200 µM.

5.4 Discussion

CO_2 uptake is an essential process for cyanobacteria living under ambient air level. In previous studies, researchers suggested that Cup/Chp are the proteins involved in the CO_2 hydration reactions (Price *et al.*, 2002). Results shown in here and Chapter 4 together with previous data described in the literature, demonstrate that in absence of both CupA and

CupB, cyanobacteria cells acquire a high-CO_2 requiring phenotype, losing its ability to grown under pH 7 and air level of CO_2 (Ohkawa *et al.*, 2000a). Besides, data suggests that each CO_2 complex containing either CupA or CupB have different affinity for the C_i substrate and reaction flux rate (Maeda *et al.*, 2002; Shibata *et al.*, 2001). Here, we investigated the structure-function of Cup/Chp proteins as a potential CA-like enzyme, by mutating highly conserved amino acids, as found in the bioinformatic analysis (Figure 22), as a potential metal coordinating ligands of the active site. The mutation C141A, with substitution of Cys for alanine (A), presented no apparent effect on CO_2 hydration activity, yet the inhibition by EZ was reduced. It is possible that C141 is important for maintenance of the active site structure in a manner affecting the coordination of the inhibitor, but is not an amino acid directly required for the putative metal coordination. This would also explain the decrease in the efficiency of inhibition by EZ, possibly due to a problematic active site environment. We also tested a second Cys, with low to average conservation among Cup variants was also mutated. The strain containing C263S, with substitution of Cys for serine (S), showed decreased flux rate (V_{max}, first phase), with no effect on affinity or EZ inhibition. It is known that some CA have Cys forming disulfide bonds, necessary for the whole protein structure conservation (Waheed *et al.*, 1996), a possible role for C263.

Analysis of highly conserved (>89%) His through point mutations in *Synechococcus* 7942 ChpX (CupB) suggests that His86 is essential for CO_2 hydration activity (Figures 22 and 23). It is possible that this mutation disrupts the binding of a potential metal cofactor. The human α CA II has three His (H94, H96, H119) forming the catalytic metal binding site

with these His residues serving as Zn ligands. This may resemble highly conserved amino acid region of Cup/Chp shown in Figure 20 (H86, H89, H107). Studies using X-ray crystal structure determination of human CA II with mutations on H94 and H119 (including H to Q replacements) showed that substitution of H94 led to displacement of zinc (Zn), and both change of H94 and H119 coordination geometry and a highly impaired Zn affinity and CO_2 hydration function of the enzyme (Alexander *et al.*, 1993; Lesburg *et al.*, 1997). The authors suggested that this was possibly due to disturbing the metal from its native position or even producing minor conformational changes of metal ligands and neighboring residues since H-bonding and proton transfer is strongly sensitive to distance and angle variations between donor-acceptor. It is plausible that ChpX/CupB H86 is a metal ligand analogous to CAII H94, and its substitutions displaces the metal cofactor. Also, decreased CO_2 hydration activity was seen on mutants with substitution of H89 and H107, suggesting these may be the other His required for binding the metal cofactor. However, since the replacement of ChpX (CupB) H87 completely impaired CO_2 hydration, we cannot discard the alternative possibility of this His being involved with proton transfer, such as the essential H64 from CAII. If so, H87 would be part of the proton "wire", with this subsequently transported to the NdhF/D proteins. In this case, it would also be possible that a third amino acid Histidine (or Cys or Gln) required for proper metal cofactor arrangement be located in one of the NdhF/D proteins, similar to the active site of γCas, where the metal cofactor is coordinated by His between two subunits (see reviews by (Lindskog, 1997; Supuran, 2016). We separated thylakoid membranes from WT LC7, C2 and C2A HC8

using blue-native gradient gel and attempted to tested carbonic anhydrase activity using a "in-gel" assay following previous described protocol (De Luca *et al.*, 2015). Although we got successful repetition of αCA activity as a control, no activity was observed in the *Synechocystis* 6803 thylakoid membrane extracts (results not shown). Additionally, CupA by itself does not seem to have a carbonic anhydrase activity, as indicated by studies with the heterologous expressed protein (Chapter 3). This suggests the possibility that Cup needs to be attached to its NDH-$1_{3,4}$, and possibly requires to be energized by the electron-proton transfer coupled reactions, the main function of NDH-1 complexes and related forms such as respiratory complex I in *E. coli* (Friedrich and Scheide, 2000). This would support the idea of formation of an "alkaline pocket" (Kaplan and Reinhold, 1999), necessary to drive the reaction, together with Cup being a special type of CA (Price *et al.*, 2002).

Interestingly, the phylogenetic analysis shows that CupA (ChpY) and CupB (ChpX) had apparently evolved into two separated subgroups (Figure 21), in spite of both functioning in cyanobacterial CO_2 hydration activity, and be inhibited by carbonic anhydrase EZ, which suggest a similar CA site. Together, the data indicates that CupA (ChpY) and CupB (ChpX) may had convergent evolution of CA like active site, yet may have diverged later. It would explain the presence of only one version in some cyanobacteria, while *Prochlorococcus marinus* has none (Badger and Price, 2003). In addition, we expressed only CupA using a similar constitutive expression system described in Chapter 4 in the C2 background strain, where *cupB* is deleted, while *ndhD4/F4* are still part of the genome. Yet, no CO_2 hydration activity measured by O_2 evolution dependent on C_i was seen (results

not shown), indicating that CupA and CupB are not interchangeable, but can only be active within their own NDH-1 compartment. This is another piece of evidence that CupA (ChpY) and CupB (ChpX) have similar yet unique function, and helps explain their contrasting substrate affinity and reaction flow rates.

Overall, we also show here that the NDH-1_3 proteins are extremely conserved in cyanobacteria based on the phylogenetic analysis. Hence, the successful heterologous expression of the *Arthrospira cupA* operon functional in the model organism *Synechocystis* 6803 opens wide perspectives for studying CO_2 hydration systems from many cyanobacteria strains, well beyond the model organisms.

Interesting, no affinity for CO_2 was observed when NDH-1_3 was expressed in a strain lacking the ATP dependent HCO_3^- transporter BCT1 (C3, results not shown). This is puzzling and requires furthers studies. It raises the question of dependency between these C_i systems.

5.5 Conclusion

The analysis of mutations on conserved amino acids has long been used in diverse proteins structure-function studies. The results presented on this Chapter 5 shows that this is also a prospective way to investigate the still puzzling Cup proteins and NDH-$1_{3,4}$ CO_2 hydration activity.

6 CHAPTER VI

CONCLUSION

Photosynthesis is an essential process, essentially divided in two main stages, formerly known as the light and dark reactions. In the first step, energy of light is captured and transformed into chemical energy, stored as ATP and NADPH. These will be used in the second step for fixation of CO_2 and biomass production. This is an essential and basic biological reaction, that most of us learn in the young phases of education. Yet, this process is so much detailed and complex, where many questions are still open. One of them is how cyanobacterial CO_2 "pumps" work.

Cyanobacterial CCM, used by the organism to increase the internal level of inorganic carbon, has been the focus of intense research (see reviews by (Kaplan, 2017; Price *et al.*, 2008). As these organisms have an important role in the global Net Primary Productivity, it is vital to well understand the CCM and its components. Yet, two out the five CCM systems are not well understood and their proper mechanism remains obscure.

This dissertation focus was to investigate the molecular mechanism of the CO_2 uptake activity found in cyanobacteria, involving specialized NDH-1 complexes. It was previously shown that two out of the four cyanobacterial NDH-1 are CO_2 uptake systems. NDH-$1_{3,4}$ are comprised by the complex core proteins together with three essential proteins for proper activity, NdhF3/4, NdhD3/4 and CupA/CupB (CupS is part of the NDH-1_3, but not essential for the CO_2 activity) (Ohkawa *et al.*, 2000a; Ohkawa *et al.*, 2000b). The two have some differences, where NDH-1_4 is constitutive, and its kinetic characteristics exhibit a comparatively low affinity for CO_2, but a higher flux (V_{max}) as evaluated via whole cell studies. On the other hand, NDH-1_3 is inducible under low C_i conditions, has a high affinity but low flux kinetic profile (Maeda *et al.*, 2002; Shibata *et al.*, 2001). Two hypotheses were previously suggested regarding the system mechanism: 1) an "alkaline pocket" formed due to proton pumping across the membrane directs a carbonic anhydrase to hydrate CO_2 (Kaplan and Reinhold, 1999), 2) Cup/Chp proteins are CA-like enzymes that sits on NdhF/NdhD, where hydration of CO_2 is dependent on the NDH-1 electron transfer coupled with proton transport (Price *et al.*, 2002).

Here, we started our research by investigating CupA protein using a heterologous expression in *Escherichia coli*. In Chapter 3 I present the results obtained after intense efforts with one final important achievement, in the effort of characterizing CupA structure-function. Chapter 3 present the results of several attempts on heterologous expressing *Synechocystis* 6803 CO_2 uptake protein CupA in *E. coli*. The protein was only soluble when stabilized by fusion to a second protein, here maltose binding protein. Yet,

studies with the purified CupA fusion were not sufficient to show CO_2 hydration activity or metal detection, besides the CD data was also not conclusive. This suggests that the protein may only be functional and/or structured when attached to the NDH-1_3. Yet, this work allowed the production of a highly specific antibody against a cyanobacterial Cup protein (CupA). Due to challenges faced after several attempts to further characterize the expressed CupA, the focus was turned to *in vivo* studies.

In this project I developed a strategy to carefully pursue some of the open questions mentioned in Chapter 1, considering difficulties found by other groups (Price *et al.*, 2002; Zhang *et al.*, 2005). On chapter 4, we detail the design, construction and characterization of a new DNA exchange system that allows the ectopic and constitutive expression of the high affinity NDH-1_3 system. Mutants lacking two out of the five CCM systems, the CO_2 uptake systems, were developed after serial deletion of the *cupA* operon and *cupB* gene, in a mutant named C2. Later, only one complex, the high affinity low flux NDH-1_3 system was reintroduced under the translational regulation of a rubisco promoter. The effect on physiological characteristics, related to oxygenic photosynthesis and CO_2 uptake, was analyzed. The resultant construct, named C2A, restored the expression of the high affinity NDH-1_3 complex as evidenced by the accumulation of the CupA protein, restoration of growth at pH 7 under ambient air, and high affinity for CO_2 seeing on the O_2 evolution curves dependent on C_i uptake. Yet, the strain still seems to be starved of C_i, since other CCM components were expressed even under HC growth. This suggests the importance of having both NDH-$1_{3,4}$ under LC and also their role in mitigating CO_2 leakage.

I also examined the previous described effect of the traditional carbonic anhydrase inhibitor EZ (Espie *et al.*, 1991; Price and Badger, 1989b), and results showed that it strongly inhibits C_i uptake in C2A, yet it only displayed incomplete inhibition of C_i uptake in the *Synechocystis* 6803 wild type, containing only NDH-1_4. The results found in chapter 4 suggests that NDH-1_3 is even more sensitive to EZ inhibition than the NDH-1_4 complex. In conclusion, we developed a new and robust tool to study the high affinity cyanobacterial CO_2 uptake system. Besides, our results show that tandem operation of both NDH-1_3 and NDH-1_4 are required for efficient cyanobacterial photosynthesis. Also, we were able to confirm previous studies, and give further evidence that NDH-1_3 has a light-dependent carbonic anhydrase-like activity highly sensitive to ethoxyzolamide.

The inhibition of CO_2 hydration activity by the traditional carbonic anhydrase ethoxyzolamide suggests an active site similar to present in CA, and also raises the possibility that a metal-binding site may exist in NDH-1_3 (and possibly NDH-1_4). Yet, there are no clear similarity between Cup (Chp) and any of the carbonic anhydrase known families, and these proteins seems to be confined (and well conserved) in the cyanobacteria group. Multiple sequence alignment with both CupA and CupB amino acids sequences from 100 cyanobacteria show a highly conserved region that resembles the Histidine and Cysteine amino acids usually found in CA active site. In chapter 5, the role of Cup (Chp) proteins is further explored using the molecular construct system developed on chapter 4, where the whole *cupA* operon under the control of a strong promoter was the recipient of site direct mutagenesis on conserved amino acids. The effect of mutations replacing these

Histidine and Cysteine in ChpX (CupB) in *Synechococcus* 7942 was also explored. The results show a decrease in the CO_2 hydration by H89 and H107, completely impairment in H86, and only a small effect on C100 mutant. The data supports the hypothesis of Chp (Cup) having a CA-like active site, possibly due to convergent evolution. The fact that ethoxyzolamide inhibits the reaction is consistent with this. In principal, a similar metal-binding site may exist in NDH-1_3 (and possibly NDH-1_4) based upon the inhibitor characteristics, as suggested by Price and colleagues (Baranauskienė and Matulis, 2012; Lindskog, 1997; Price *et al.*, 2002). In the earlier models, plastoquinone was suggested as a sink for protons arising from the hydrolysis of water on the hypothesized metal site, whereas recent information regarding the localization of CupA (Birungi *et al.*, 2010) suggest the possibility of a less direct involvement of plastoquinone according current models of proton pumping by NDH-1 complexes (Kaila *et al.*, 2014; Zickermann *et al.*, 2015). Nevertheless, the principal remains the same and also fits the 'alkaline pocket' model suggested by Kaplan and collaborators (Kaplan and Reinhold, 1999).

REFERENCES

Adam PR, Patil MK, Dickenson NE, Choudhari S, Barta M, Geisbrecht BV, Picking WL, Picking WD (2012) Binding affects the tertiary and quaternary structures of the *Shigella* translocator protein IpaB and its chaperone IpgC. Biochemistry 51 (19):4062-4071

Aggarwal M, Chua TK, Pinard MA, Szebenyi DM, McKenna R (2015) Carbon dioxide "trapped" in a β-carbonic anhydrase. Biochemistry 54 (43):6631-6638

Alexander RS, Kiefer LL, Fierke CA, Christianson DW (1993) Engineering the zinc binding site of human carbonic anhydrase II: Structure of the His-94. Cys apoenzyme in a new crystalline form. Biochemistry 32 (6):1510-1518

Allen MM (1968) Simple conditions for growth of unicellular blue-green algae on plates. Journal of Phycology 4 (1):1-&

Alric J, Lavergne J, Rappaport F (2010) Redox and ATP control of photosynthetic cyclic electron flow in *Chlamydomonas reinhardtii* (I) aerobic conditions. Biochimica Et Biophysica Acta-Bioenergetics 1797 (1):44-51. doi:Doi 10.1016/J.Bbabio.2009.07.009

Alterio V, Langella E, Viparelli F, Vullo D, Ascione G, Dathan NA, Morel FMM, Supuran CT, De Simone G, Monti SM (2012) Structural and inhibition insights into carbonic anhydrase CDCA1 from the marine diatom *Thalassiosira weissflogii*. Biochimie 94 (5):1232-1241

Aoki M, Katoh S (1982) Oxidation and reduction of plastoquinone by photosynthetic and respiratory electron transport in a cyanobacterium *Synechococcus* sp. Biochimica et Biophysica Acta (BBA)-Bioenergetics 682 (3):307-314

Arnold K, Bordoli L, Kopp J, Schwede T (2006) The SWISS-MODEL workspace: a web-based environment for protein structure homology modelling. Bioinformatics 22 (2):195-201

Arteni AA, Zhang P, Battchikova N, Ogawa T, Aro EM, Boekema EJ (2006) Structural characterization of NDH-1 complexes of *Thermosynechococcus elongatus* by single particle electron microscopy. Biochimica et Biophysica Acta (BBA) -

Bioenergetics 1757 (11):1469-1475. doi:https://doi.org/10.1016/j.bbabio.2006.05.042

Ashkenazy H, Abadi S, Martz E, Chay O, Mayrose I, Pupko T, Ben-Tal N (2016) ConSurf 2016: an improved methodology to estimate and visualize evolutionary conservation in macromolecules. Nucleic acids research 44 (W1):W344-W350

Badger MR (1980) Kinetic properties of ribulose 1, 5-bisphosphate carboxylase/oxygenase from *Anabaena variabilis*. Archives of Biochemistry and Biophysics 201 (1):247-254

Badger MR, Price GD (2003) CO2 concentrating mechanisms in cyanobacteria: molecular components, their diversity and evolution. Journal of experimental botany 54 (383):609-622

Badger MR, Price GD, Long BM, Woodger FJ (2006) The environmental plasticity and ecological genomics of the cyanobacterial CO_2 concentrating mechanism. J Exp Bot 57 (2):249-265. doi:10.1093/jxb/eri286

Baniulis D, Yamashita E, Zhang H, Hasan SS, Cramer WA (2008) Structure-function of the cytochrome b6f complex. Photochemistry and photobiology 84 (6):1349-1358. doi:10.1111/j.1751-1097.2008.00444.x

Bao H, Dilbeck PL, Burnap RL (2013) Proton transport facilitating water-oxidation: the role of second sphere ligands surrounding the catalytic metal cluster. Photosynthesis research 116 (2-3):215-229

Baranauskienė L, Matulis D (2012) Intrinsic thermodynamics of ethoxzolamide inhibitor binding to human carbonic anhydrase XIII. BMC biophysics 5 (1):12

Battchikova N, Aro EM (2007) Cyanobacterial NDH-1 complexes: multiplicity in function and subunit composition. Physiologia Plantarum 131:22-32. doi:10.1111/j.1399-3054.2007.00929.x

Battchikova N, Eisenhut M, Aro EM (2011a) Cyanobacterial NDH-1 complexes: Novel insights and remaining puzzles. Biochimica et Biophysica Acta 1807:935-944. doi:10.1016/j.bbabio.2010.10.017

Battchikova N, Wei L, Du L, Bersanini L, Aro E-M, Ma W (2011b) Identification of Novel Ssl0352 Protein (NdhS), Essential for Efficient Operation of Cyclic Electron Transport around Photosystem I, in NADPH:plastoquinone Oxidoreductase (NDH-1) Complexes of *Synechocystis* sp. PCC 6803. The Journal Of Biological Chemistry 286 (42):36992–37001. doi: 10.1074/jbc.M111.263780

Benschop J, Badger M, Dean Price G (2003) Characterisation of CO_2 and HCO_3 uptake in the cyanobacterium *Synechocystis* sp. PCC6803. Photosynthesis Research 77 (2 - 3):117

Berezin C, Glaser F, Rosenberg J, Paz I, Pupko T, Fariselli P, Casadio R, Ben-Tal N (2004) ConSeq: the identification of functionally and structurally important residues in protein sequences. Bioinformatics 20 (8):1322-1324

Bernat G, Appel J, Ogawa T, Rogner M (2011) Distinct Roles of Multiple NDH-1 Complexes in the Cyanobacterial Electron Transport Network as Revealed by Kinetic Analysis of $P700^{(+)}$ Reduction in Various ndh-Deficient Mutants of *Synechocystis* sp. Strain PCC6803. Journal of Bacteriology 193 (1):292-295. doi:Doi 10.1128/Jb.00984-10

Birungi M, Folea M, Battchikova N, Xu M, Mi H, Ogawa T, Aro EM, Boekema EJ (2010) Possibilities of subunit localization with fluorescent protein tags and electron microscopy examplified by a cyanobacterial NDH-1 study. Biochimica et Biophysica Acta (BBA)-Bioenergetics 1797 (9):1681-1686

Blankenship RE (2010) Early Evolution of Photosynthesis. Plant Physiology 154 (2):434-438. doi:10.1104/pp.110.161687

Bonacci W, Teng PK, Afonso B, Niederholtmeyer H, Grob P, Silver PA, Savage DF (2012) Modularity of a carbon-fixing protein organelle. Proceedings of the National Academy of Sciences 109 (2):478-483

Bose N, Greenspan P, Momany C (2002) Expression of recombinant human betaine: homocysteine S-methyltransferase for x-ray crystallographic studies and further characterization of interaction with S-adenosylmethionine. Protein expression and purification 25 (1):73-80

Bracey MH, Christiansen J, Tovar P, Cramer SP, Bartlett SG (1994) Spinach carbonic anhydrase: investigation of the zinc-binding ligands by site-directed mutagenesis, elemental analysis, and EXAFS. Biochemistry 33 (44):13126-13131

Brandt U (2013) Inside View of a Giant Proton Pump. Angewandte Chemie International Edition 52 (29):7358-7360. doi:10.1002/anie.201303403

Bryant DA (1994) The Molecular Biology of Cyanobacteria. Kluwer Academic Publishers, The Netherlands

Buick R (2008) When did oxygenic photosynthesis evolve? Philosophical Transactions of the Royal Society B: Biological Sciences 363 (1504):2731-2743. doi:10.1098/rstb.2008.0041

Burnap R, Koike H, Sotiropoulou G, Sherman LA, Inoue Y (1989) Oxygen evolving membranes and particles from the transformable cyanobacterium *Synechocystis* sp. PCC6803. Photosynth Res 22:123-130

Burnap RL, Hagemann M, Kaplan A (2015) Regulation of CO_2 concentrating mechanism in cyanobacteria. Life 5 (1):348-371

Burnap RL, Nambudiri R, Holland S (2013) Regulation of the carbon-concentrating mechanism in the cyanobacterium *Synechocystis* sp. PCC6803 in response to changing light intensity and inorganic carbon availability. Photosynthesis Research 118 (1):115-124. doi:10.1007/s11120-013-9912-4

Cai F, Menon BB, Cannon GC, Curry KJ, Shively JM, Heinhorst S (2009) The Pentameric Vertex Proteins Are Necessary for the Icosahedral Carboxysome Shell to Function as a CO_2 Leakage Barrier. Plos one. doi:10.1371/journal.pone.0007521

Cai YP, Wolk CP (1990) Use of a conditionally lethal gene in *Anabaena* sp. strain PCC 7120 to select for double recombinants and to entrap insertion sequences. J Bacteriol 172 (6):3138-3145

Campbell D, Hurry V, Clarke AK, Gustafsson P, Öquist G (1998) Chlorophyll fluorescence analysis of cyanobacterial photosynthesis and acclimation. Microbiology and molecular biology reviews 62 (3):667-683

Cannon GC, Bradburne CE, Aldrich HC, Baker SH, Heinhorst S, Shively JM (2001) Microcompartments in prokaryotes: carboxysomes and related polyhedra. Applied and environmental microbiology 67 (12):5351-5361. doi:10.1128/aem.67.12.5351-5361.2001

Cannon GC, English RS, Shively JM (1991) In situ assay of ribulose-1,5-bisphosphate carboxylase/oxygenase in *Thiobacillus neapolitanus*. Journal of bacteriology 173 (4):1565-1568

Cano M, Holland SC, Artier J, Burnap RL, Ghirardi M, Morgan JA, Yu J (2018) Glycogen Synthesis and Metabolite Overflow Contribute to Energy Balancing in Cyanobacteria. Cell reports 23 (3):667-672

Cassier-Chauvat C, Chauvat F (2014) Function and regulation of ferredoxins in the cyanobacterium, *Synechocystis* PCC6803: Recent advances. Life 4 (4):666-680

Catling D, Zahnle K (2002) Evolution of atmospheric oxygen.754-761

Cheng S, Liu Y, Crowley CS, Yeates TO, Bobik TA (2008) Bacterial microcompartments: their properties and paradoxes. Bioessays. doi:10.1002/bies.20830

Chowdhury C, Chun S, Pang A, Sawaya MR, Sinha S, Yeates TO, Bobik TA (2015) Selective molecular transport through the protein shell of a bacterial microcompartment organelle. Proceedings of the National Academy of Sciences 112 (10):2990-2995

Cox EH, McLendon GL, Morel FMM, Lane TW, Prince RC, Pickering IJ, George GN (2000) The active site structure of *Thalassiosira weissflogii* carbonic anhydrase 1. Biochemistry 39 (40):12128-12130

Cox J, Hein MY, Luber CA, Paron I, Nagaraj N, Mann M (2014) Accurate proteome-wide label-free quantification by delayed normalization and maximal peptide ratio extraction, termed MaxLFQ. Molecular & cellular proteomics 13 (9):2513-2526

Cox J, Mann M (2008) MaxQuant enables high peptide identification rates, individualized ppb-range mass accuracies and proteome-wide protein quantification. Nature biotechnology 26 (12):1367

Cox J, Mann M (2012) 1D and 2D annotation enrichment: a statistical method integrating quantitative proteomics with complementary high-throughput data. BMC Bioinformatics 13 (Suppl 16):S12-S12. doi:10.1186/1471-2105-13-S16-S12

Cramer WA, Hasan SS, Yamashita E (2011) The Q cycle of cytochrome bc complexes: a structure perspective. Biochimica et biophysica acta 1807 (7):788-802. doi:10.1016/j.bbabio.2011.02.006

Dai S, Johansson K, Miginiac-Maslow M, Schürmann P, Eklund H (2004) Structural basis of redox signaling in photosynthesis: structure and function of ferredoxin: thioredoxin reductase and target enzymes. Photosynthesis research 79 (3):233-248

Daley SME, Kappell AD, Carrick MJ, Burnap RL (2012) Regulation of the Cyanobacterial CO2-Concentrating Mechanism Involves Internal Sensing of $NADP^{(+)}$ and alpha-Ketogutarate Levels by Transcription Factor CcmR. Plos One 7 (7). doi:ARTN e41286_DOI 10.1371/journal.pone.0041286

De Luca V, Del Prete S, Supuran CT, Capasso C (2015) Protonography, a new technique for the analysis of carbonic anhydrase activity. Journal of enzyme inhibition and medicinal chemistry 30 (2):277-282

De Simone G, Di Fiore A, Capasso C, Supuran CT (2015) The zinc coordination pattern in the η-carbonic anhydrase from *Plasmodium falciparum* is different from all other carbonic anhydrase genetic families. Bioorganic & medicinal chemistry letters 25 (7):1385-1389

Deng Y, Ye J, Mi H (2003) Effects of Low CO2 on NAD(P)H Dehydrogenase, a Mediator of Cyclic Electron Transport Around Photosystem I in the Cyanobacterium *Synechocystis* PCC6803. Plant and Cell Physiology 44 (5):534-540

Dilbeck PL, Hwang HJ, Zaharieva I, Gerencser L, Dau H, Burnap RL (2012) The D1-D61N mutation in *Synechocystis* sp. PCC 6803 allows the observation of pH-sensitive intermediates in the formation and release of O_2 from photosystem II. Biochemistry 51 (6):1079-1091

DiMario RJ, Machingura MC, Waldrop GL, Moroney JV (2017) The many types of carbonic anhydrases in photosynthetic organisms. Plant Science

Ding X, Matsumoto T, Gena P, Liu C, Pellegrini‐Calace M, Zhong S, Sun X, Zhu Y, Katsuhara M, Iwasaki I (2013) Water and CO_2 permeability of SsAqpZ, the cyanobacterium *Synechococcus* sp. PCC7942 aquaporin. Biology of the Cell 105 (3):118-128

Dorrell RG, Smith AG (2011) Do red and green make brown?: perspectives on plastid acquisitions within chromalveolates. Eukaryotic Cell 10 (7):856-868

Du J, Förster B, Rourke L, Howitt SM, Price GD (2014) Characterisation of cyanobacterial bicarbonate transporters in *E. coli* shows that SbtA homologs are functional in this heterologous expression system. PLoS One 9 (12):e115905

Eaton-Rye J (2004) The construction of gene knockouts in the cyanobacterium *Synechocystis* sp. PCC 6803. In: Photosynthesis Research Protocols. Springer, pp 309-324

Edgar RC (2004) MUSCLE: multiple sequence alignment with high accuracy and high throughput. Nucleic acids research 32 (5):1792-1797

Efremov RG, Sazanov LA (2012) The coupling mechanism of respiratory complex I — A structural and evolutionary perspective. Biochimica et Biophysica Acta (BBA) - Bioenergetics 1817 (10):1785-1795. doi:http://dx.doi.org/10.1016/j.bbabio.2012.02.015

Eisenhut M, Huege J, Schwarz D, Bauwe H, Kopka J, Hagemann M (2008) Metabolome Phenotyping of Inorganic Carbon Limitation in Cells of the Wild Type and Photorespiratory Mutants of the Cyanobacterium *Synechocystis* sp Strain PCC 6803. Plant Physiology 148 (4):2109-2120. doi:10.1104/pp.108.129403

Engler C, Gruetzner R, Kandzia R, Marillonnet S (2009) Golden gate shuffling: a one-pot DNA shuffling method based on type IIs restriction enzymes. PloS one 4 (5):e5553

Espie GS, Kandasamy RA (1994) Monensin inhibition of Na^+-dependent HCO_3^- transport distinguishes it from Na^+-independent HCO_3^- transport and provides evidence for Na^+/HCO_3^- symport in the cyanobacterium *Synechococcus* UTEX 625. Plant Physiology 104 (4):1419-1428

Espie GS, Miller AG, Canvin DT (1991) High affinity transport of CO_2 in the cyanobacterium *Synechococcus* UTEX 625. Plant physiology 97 (3):943-953

Farrelly DJ, Everard CD, Fagan CC, McDonnell KP (2013) Carbon sequestration and the role of biological carbon mitigation: a review. Renewable and sustainable energy reviews 21:712-727

Folea IM, Zhang P, Nowaczyk MM, Ogawa T, Aro EM, Boekema EJ (2008) Single particle analysis of thylakoid proteins from *Thermosynechococcus elongatus* and

Synechocystis 6803: Localization of the CupA subunit of NDH-1. FEBS Letters 582 (2):249-254. doi:http://dx.doi.org/10.1016/j.febslet.2007.12.012

Fridlyand L, Kaplan A, Reinhold L (1996) Quantitative evaluation of the role of a putative CO_2-scavenging entity in the cyanobacterial CO_2-concentrating mechanism. Biosystems 37 (3):229-238

Friedrich T, Scheide D (2000) The respiratory complex I of bacteria, archaea and eukarya and its module common with membrane-bound multisubunit hydrogenases. FEBS Letters 479:1-5

Gao F, Zhao J, Chen L, Battchikova N, Ran Z, Aro EM, Ogawa T, Ma W (2016) The NDH-1L-PSI supercomplex is important for efficient cyclic electron transport in cyanobacteria. Plant physiology 172 (3):1451-1464

Georg J, Hess WR (2011) cis-Antisense RNA, Another Level of Gene Regulation in Bacteria. Microbiology and Molecular Biology Reviews : MMBR 75 (2):286-300. doi:10.1128/MMBR.00032-10

Gibson DG, Smith HO, Hutchison CA, Venter JC, Merryman C (2010) Chemical synthesis of the mouse mitochondrial genome. Nat Meth 7 (11):901-903. doi:http://www.nature.com/nmeth/journal/v7/n11/abs/nmeth.1515.html#supplementary-information

Gibson DG, Young L, Chuang R-Y, Venter JC, Hutchison CA, Smith HO (2009) Enzymatic assembly of DNA molecules up to several hundred kilobases. Nat Meth 6 (5):343-345. doi:http://www.nature.com/nmeth/journal/v6/n5/suppinfo/nmeth.1318_S1.html

Golbeck JH (2002) Photosynthetic Reaction Centers: So little time, so much to do. Energy Transduction in Membranes. Biophysics Textbook Online

Gonzalez-Esquer CR, Vermaas WFJ (2013) ClpB1 Overproduction in *Synechocystis* sp. Strain PCC 6803 Increases Tolerance to Rapid Heat Shock. Applied and environmental microbiology 79 (20):6220-6227. doi:10.1128/aem.01661-13

Guindon S, Dufayard JF, Lefort V, Anisimova M, Hordijk W, Gascuel O (2010) New algorithms and methods to estimate maximum-likelihood phylogenies: assessing the performance of PhyML 3.0. Systematic biology 59 (3):307-321

Han X, Sun N, Xu M, Mi H (2017) Co-ordination of NDH and Cup proteins in CO_2 uptake in cyanobacterium *Synechocystis* sp. PCC 6803. Journal of Experimental Botany 68 (14):3869-3877. doi:10.1093/jxb/erx129

Hanson DT (2016) Breaking the rules of Rubisco catalysis. Journal of experimental botany 67 (11):3180

He Z, Zheng F, Wu Y, Li Q, Lv J, Fu P, Mi H (2015) NDH-1L interacts with ferredoxin via the subunit NdhS in *Thermosynechococcus elongatus*. Photosynthesis research 126 (2-3):341-349

Hibberd JM, Sheehy JE, Langdale JA (2008) Using C4 photosynthesis to increase the yield of rice—rationale and feasibility. Current opinion in plant biology 11 (2):228-231

Hishiya S, Hatakeyama W, Mizota Y, Hosoya-Matsuda N, Motohashi KI, Masahiko, Hisabori T (2008) Binary reducing equivalent pathways using NADPH-thioredoxin reductase and ferredoxin-thioredoxin reductase in the cyanobacterium *Synechocystis* sp. strain PCC 6803. Plant and cell physiology 49 (1):11-18

Hohmann-Marriott MF, Blankenship RE (2011) Evolution of photosynthesis. Annual review of plant biology 62:515-548

Holland SC, Artier J, Miller NT, Cano M, Yu J, Ghirardi ML, Burnap RL (2016) Impacts of genetically engineered alterations in carbon sink pathways on photosynthetic performance. Algal Research 20:87-99. doi:http://dx.doi.org/10.1016/j.algal.2016.09.021

Holland SC, Kappell AD, Burnap RL (2015) Redox changes accompanying inorganic carbon limitation in *Synechocystis* sp. PCC 6803. Biochim Biophys Acta 1848 (3):355-363. doi:10.1016/j.bbabio.2014.12.001

Jensen PE, Bassi R, Boekema EJ, Dekker JP, Jansson S, Leister D, Robinson C, Scheller HV (2007) Structure, function and regulation of plant photosystem I. Biochim Biophys Acta 1767 (5):335-352. doi:S0005-2728(07)00072-2 [pii] 10.1016/j.bbabio.2007.03.004

Joliot P, Joliot A (2001) Electrogenic events associated with electron and proton transfers within the cytochrome b(6)/f complex. Biochim Biophys Acta 1503 (3):369-376.

Joliot P, Joliot A (2002) Cyclic electron transfer in plant leaf. Proc Natl Acad Sci U S A 99 (15):10209–10214

Kaila VR, Wikstrom M, Hummer G (2014) Electrostatics, hydration, and proton transfer dynamics in the membrane domain of respiratory complex I. Proc Natl Acad Sci U S A 111 (19):6988-6993. doi:10.1073/pnas.1319156111

Kana R, Kotabova E, Komarek O, Sediva B, Papageorgiou GC, Govindjee, Prasil O (2012) The slow S to M fluorescence rise in cyanobacteria is due to a state 2 to state 1 transition. Biochimica Et Biophysica Acta-Bioenergetics 1817 (8):1237-1247. doi:10.1016/j.bbabio.2012.02.024

Kaplan A (2017) On the cradle of CCM research: discovery, development, and challenges ahead. Journal of Experimental Botany 68 (14):3785-3796. doi:10.1093/jxb/erx122

Kaplan A, Reinhold L (1999) CO_2 concentrating mechanisms in photosynthetic microorganisms. Annu Rev Plant Physiol Plant Mol Biol 50:539-570

Kasting JF, Pollack JB, Crisp D (1984) Effects of high CO_2 levels on surface temperature and atmospheric oxidation state of the early Earth. Journal of atmospheric chemistry 1 (4):403-428

Katoh K, Rozewicki J, Yamada KD (2017) MAFFT online service: multiple sequence alignment, interactive sequence choice and visualization. Briefings in bioinformatics

Kerfeld CA, Heinhorst S, Cannon GC (2010) Bacterial microcompartments. Annual review of microbiology 64

Kimber MS, Pai EF (2000) The active site architecture of Pisum sativum β ‐carbonic anhydrase is a mirror image of that of α ‐carbonic anhydrases. The EMBO journal 19 (7):1407-1418

Kinney JN, Axen SD, Kerfeld CA (2011) Comparative analysis of carboxysome shell proteins. Photosynthesis research. doi:10.1007/s11120-011-9624-6

Kisker C, Schindelin H, Alber BE, Ferry JG, Rees DC (1996) A left‐hand beta‐helix revealed by the crystal structure of a carbonic anhydrase from the archaeon *Methanosarcina thermophila*. The EMBO journal 15 (10):2323-2330

Klähn S, Orf I, Schwarz D, Matthiessen JK, Kopka J, Hess WR, Hagemann M (2015) Integrated transcriptomic and metabolomic characterization of the low-carbon response using an ndhR mutant of *Synechocystis* sp. PCC 6803. Plant physiology 169 (3):1540-1556

Klemba M, Regan L (1995) Characterization of metal binding by a designed protein: single ligand substitutions at a tetrahedral Cys2His2 site. Biochemistry 34 (31):10094-10100

Kohinata T, Nishino H, Fukuzawa H (2008) Significance of zinc in a regulatory protein, CCM1, which regulates the carbon-concentrating mechanism in *Chlamydomonas reinhardtii*. Plant and Cell Physiology 49 (2):273-283

Korste A, Wulfhorst H, Ikegami T, Nowaczyk MM, Stoll R (2015) Solution structure of the NDH-1 complex subunit CupS from *Thermosynechococcus elongatus*. Biochimica et Biophysica Acta (BBA)-Bioenergetics 1847 (10):1212-1219

Kumar S, Stecher G, Tamura K (2016) MEGA7: molecular evolutionary genetics analysis version 7.0 for bigger datasets. Molecular biology and evolution 33 (7):1870-1874

Kupriyanova E, Pronina N, Los D (2017) Carbonic anhydrase — a universal enzyme of the carbon-based life. Photosynthetica 55 (1):3-19. doi:10.1007/s11099-017-0685-4

Laemmli UK (1970) Cleavage of structural proteins during the assembly of the head of bacteriophage T4. nature 227 (5259):680

Laughlin TG, Savage DF, Davies KM (2018) Revealing the Subunit Architecture of NAD (P) H Dehydrogenase Type-1 from Cyanobacteria through Cryo-EM. Biophysical Journal 114 (3):424a

Lesburg CA, Huang CC, Christianson DW, Fierke CA (1997) Histidine→ carboxamide ligand substitutions in the zinc binding site of carbonic anhydrase II alter metal coordination geometry but retain catalytic activity. Biochemistry 36 (50):15780-15791

Liljas A, Kannan KK, Bergsten P-C, Waara I, Fridborg K, Strandberg B, Carlbom U, Järup L, Lövgren S, Petef M (1972) Crystal structure of human carbonic anhydrase C. Nature New Biology 235 (57):131

Lin MT, Occhialini A, Andralojc PJ, Parry MAJ, Hanson MR (2014) A faster Rubisco with potential to increase photosynthesis in crops. Nature 513 (7519):547

Lindskog S (1997) Structure and mechanism of carbonic anhydrase. Pharmacology & therapeutics 74 (1):1-20

Long BM, Rae BD, Rolland V, Förster B, Price GD (2016) Cyanobacterial CO_2-concentrating mechanism components: function and prospects for plant metabolic engineering. Current opinion in plant biology 31:1-8

Lotlikar SR, Hnatusko S, Dickenson NE, Choudhari SP, Picking WL, Patrauchan MA (2013) Three functional β-carbonic anhydrases in *Pseudomonas aeruginosa* PAO1: role in survival in ambient air. Microbiology 159 (8):1748-1759

Ma W, Ogawa T (2015) Oxygenic photosynthesis-specific subunits of cyanobacterial NADPH dehydrogenases. IUBMB Life 67 (1):3-8. doi:10.1002/iub.1341

Maeda S, Badger MR, Price GD (2002) Novel gene products associated with NdhD3/D4-containing NDH-1 complexes are involved in photosynthetic CO_2 hydration in the cyanobacterium, *Synechococcus* sp. PCC7942. Mol Microbiol 43 (2):425-435

Maeda S, Price GD, Badger MR, Enomoto C, Omata T (2000) Bicarbonate binding activity of the CmpA protein of the cyanobacterium Synechococcus sp. strain PCC 7942 involved in active transport of bicarbonate. J Biol Chem 275 (27):20551-20555

Mangan NM, Flamholz A, Hood RD, Milo R, Savage DF (2016) pH determines the energetic efficiency of the cyanobacterial CO_2 concentrating mechanism. Proceedings of the National Academy of Sciences. doi:10.1073/pnas.1525145113

Marcus Y, Berry JA, Pierce J (1992) Photosynthesis and photorespiration in a mutant of the cyanobacterium *Synechocystis* PCC 6803 lacking carboxysomes. Planta 187 (4):511-516. doi:10.1007/bf00199970

Margulis L (1981) Symbiosis in cell evolution: Life and its environment on the early earth.

McGrath JM, Long SP (2014) Can the cyanobacterial carbon-concentrating mechanism increase photosynthesis in crop species? A theoretical analysis. Plant Physiology 164 (4):2247-2261

Menchise V, De Simone G, Di Fiore A, Scozzafava A, Supuran CT (2006) Carbonic anhydrase inhibitors: X-ray crystallographic studies for the binding of 5-amino-1,3,4-thiadiazole-2-sulfonamide and 5-(4-amino-3-chloro-5-fluorophenylsulfonamido)-1,3,4-thiadiazole-2-sulfonamide to human isoform II. Bioorg Med Chem Lett 16 (24):6204-6208. doi:10.1016/j.bmcl.2006.09.022

Messinger J, Shevela D (2012) Principles of photosynthesis. In: Fundamentals of Materials for Energy and Environmental Sustainability. Cambridge University press New York, pp 302-314

Meyer M, Griffiths H (2013) Origins and diversity of eukaryotic CO_2-concentrating mechanisms: lessons for the future. Journal of Experimental Botany 64 (3):769-786. doi:10.1093/jxb/ers390

Mi H, Endo T, Schreiber U, Ogawa T, Asada K (1992) Electron donation from cyclic and respiratory flows to the photosynthetic intersystem chain is mediated by pyridine nucleotide dehydrogenase in the cyanobacterium *Synechocystis* PCC 6803. Plant and cell physiology 33 (8):1233-1237

Michelet L, Zaffagnini M, Morisse Sl, Sparla F, Pérez-Pérez ME, Francia F, Danon A, Marchand C, Fermani S, Trost P (2013) Redox regulation of the Calvin–Benson cycle: something old, something new. Frontiers in plant science 4:470

Miller AG, Espie GS, Bruce D (1996) Characterization of the non-photochemical quenching of chlorophyll fluorescence that occurs during the active accumulation of inorganic carbon in the cyanobacterium *Synechococcus* PCC 7942. Photosynthesis Research 49 (3):251-262

Miller AG, Espie GS, Canvin DT (1988) Chlorophyll a fluorescence yield as a monitor of both active CO_2 and HCO_3^- transport by the cyanobacterium *Synechococcus* UTEX 625. Plant physiology 86 (3):655-658

Miller AG, Espie GS, Canvin DT (1990) Physiological aspects of CO2 and HCO3− transport by cyanobacteria: a review. Canadian Journal of botany 68 (6):1291-1302

Mitschke J, Georg J, Scholz I, Sharma CM, Dienst D, Bantscheff J, Voß B, Steglich C, Wilde A, Vogel J (2011) An experimentally anchored map of transcriptional start sites in the model cyanobacterium *Synechocystis* sp. PCC6803. Proceedings of the National Academy of Sciences 108 (5):2124-2129

Modak JK, Liu YC, Supuran CT, Roujeinikova A (2016) Structure–Activity Relationship for Sulfonamide Inhibition of Helicobacter pylori α-Carbonic Anhydrase. Journal of Medicinal Chemistry 59 (24):11098-11109. doi:10.1021/acs.jmedchem.6b01333

Munekage Y, Hashimoto M, Miyake C, Tomizawa K-I, Endo T, Tasaka M, Shikanai T (2004) Cyclic electron flow around photosystem I is essential for photosynthesis. Nature 429 (6991):579-582. doi:http://www.nature.com/nature/journal/v429/n6991/suppinfo/nature02598_S1.html

Nishimura T, Takahashi Y, Yamaguchi O, Suzuki H, Maeda SI, Omata T (2008) Mechanism of low CO_2-induced activation of the *cmp* bicarbonate transporter operon by a LysR family protein in the cyanobacterium *Synechococcus elongatus* strain PCC 7942. Mol Microbiol

Nordberg H, Cantor M, Dusheyko S, Hua S, Poliakov A, Shabalov I, Smirnova T, Grigoriev IV, Dubchak I (2013) The genome portal of the Department of Energy Joint Genome Institute: 2014 updates. Nucleic acids research 42 (D1):D26-D31

Notz D, Stroeve J (2016) Observed Arctic sea-ice loss directly follows anthropogenic CO_2 emission. Science 354 (6313):747-750

Ogawa T, Kaplan A (2003) Inorganic carbon acquisition systems in cyanobacteria. Photosynthesis Research 77 (2-3):105-115

Ogawa T, Mi H (2007) Cyanobacterial NADPH dehydrogenase complexes. Photosynth Res 93 (1-3):69-77. doi:10.1007/s11120-006-9128-y

Ohkawa H, Pakrasi HB, Ogawa T (2000a) Two types of functionally distinct NAD(P)H dehydrogenases in *Synechocystis* sp. strain PCC6803. J Biol Chem 275 (41):31630-31634.

Ohkawa H, Price G, Badger M, Ogawa T (2000b) Mutation of ndh genes leads to inhibition of CO_2 uptake rather than HCO_3^- uptake in *Synechocystis* sp. strain PCC 6803. Journal of Bacteriology 182 (9):2591-2596. doi:10.1128/jb.182.9.2591-2596.2000

Omata T, Gohta S, Takahashi Y, Harano Y, Maeda S (2001) Involvement of a CbbR homolog in low CO_2-induced activation of the bicarbonate transporter operon in cyanobacteria. J Bacteriol 183 (6):1891-1898

Omata T, Price GD, Badger MR, Okamura M, Gohta S, Ogawa T (1999) Identification of an ATP-binding cassette transporter involved in bicarbonate uptake in the cyanobacterium *Synechococcus* sp. strain PCC 7942. Proceedings of the National Academy of Sciences 96 (23):13571-13576. doi:10.1073/pnas.96.23.13571

Omata T, Takahashi Y, Yamaguchi O, Nishimura T (2002) Structure, function and regulation of the cyanobacterial high-affinity bicarbonate transporter, BCT1. Functional Plant Biology 29 (3):151-159. doi:https://doi.org/10.1071/PP01215

Orf I, Klähn S, Schwarz D, Frank M, Hess WR, Hagemann M, Kopka J (2015) Integrated analysis of engineered carbon limitation in a quadruple CO_2/HCO_3^--uptake mutant of *Synechocystis* sp. PCC 6803. Plant physiology:pp. 01289.02015

Ort DR, Merchant SS, Alric J, Barkan A, Blankenship RE, Bock R, Croce R, Hanson MR, Hibberd JM, Long SP (2015) Redesigning photosynthesis to sustainably meet global food and bioenergy demand. Proceedings of the national academy of sciences 112 (28):8529-8536

Parisi G, Perales M, Fornasari M, Colaneri A, Schain N, Casati D, Zimmermann S, Brennicke A, Araya A, Ferry J (2004) Gamma carbonic anhydrases in plant mitochondria. Plant molecular biology 55 (2):193-207

Parry MAJ, Hawkesford MJ (2010) Food security: increasing yield and improving resource use efficiency. Proceedings of the nutrition Society 69 (4):592-600

Pioszak AA, Xu HE (2008) Molecular recognition of parathyroid hormone by its G protein-coupled receptor. Proceedings of the National Academy of Sciences 105 (13):5034-5039

Price G, Sultemeyer D, Klughammer B, Ludwig M, Badger M (1998) The functioning of the CO_2 concentrating mechanism in several cyanobacterial strains: a review of general physiological characteristics, genes, proteins, and recent advances. Canadian Journal of Botany 76:973-1002

Price GD (2011) Inorganic carbon transporters of the cyanobacterial CO_2 concentrating mechanism. Photosynth Res 109:47–57. doi:10.1007/s11120-010-9608-y

Price GD, Badger MR (1989a) Ethoxyzolamide inhibition of CO_2 uptake in the cyanobacterium *Synechococcus* PCC7942 without apparent inhibition of internal carbonic anhydrase activity. Plant Physiol 89 (1):37-43. doi:10.1104/pp.89.1.37

Price GD, Badger MR (1989b) Ethoxyzolamide inhibition of CO_2-dependent photosynthesis in the cyanobacterium *Synechococcus* PCC7942. Plant Physiology 89 (1):44-50

Price GD, Badger MR (1989c) Expression of Human Carbonic Anhydrase in the Cyanobacterium *Synechococcus* PCC7942 Creates a High CO_2-Requiring Phenotype Evidence for a Central Role for Carboxysomes in the CO_2 Concentrating Mechanism. Plant Physiology 91 (2):505-513

Price GD, Badger MR (1991) Evidence for the role of carboxysomes in the cyanobacterial CO_2-concentrating mechanism. Canadian Journal of Botany 69 (5):963-973. doi:10.1139/b91-124

Price GD, Badger MR, Woodger FJ, Long BM (2008) Advances in understanding the cyanobacterial CO_2-concentrating-mechanism (CCM): functional components, Ci transporters, diversity, genetic regulation and prospects for engineering into plants. J Exp Bot 59 (7):1441-1461. doi:10.1093/jxb/erm112

Price GD, Maeda S, Omata T, Badger MR (2002) Modes of active inorganic carbon uptake in the cyanobacterium, *Synechococcus* sp PCC7942. Functional Plant Biology 29 (2-3):131-149. doi:10.1071/PP01229

Price GD, Pengelly JJ, Forster B, Du J, Whitney SM, von Caemmerer S, Badger MR, Howitt SM, Evans JR (2013) The cyanobacterial CCM as a source of genes for improving photosynthetic CO_2 fixation in crop species. Journal of Experimental Botany 64 (3):753-768. doi:10.1093/jxb/ers257

Price GD, Woodger FJ, Badger MR, Howitt SM, Tucker L (2004) Identification of a SulP-type bicarbonate transporter in marine cyanobacteria. Proc Natl Acad Sci U S A 101 (52):18228-18233

Rae BD, Long BM, Badger MR, Price GD (2013) Functions, compositions, and evolution of the two types of carboxysomes: polyhedral microcompartments that facilitate CO_2 fixation in cyanobacteria and some proteobacteria. Microbiology and Molecular Biology Reviews 77 (3):357-379

Rippka R, Deruelles J, Waterbury J-B, Herdman M, Stanier R-Y (1979) Genetic assignments, strain histories and properties of pure cultures of cyanobateria. J Gen Microbiol 111:1-61

Ritchie RJ (2006) Consistent sets of spectrophotometric chlorophyll equations for acetone, methanol and ethanol solvents. Photosynthesis Research 89 (1):27-41. doi:10.1007/s11120-006-9065-9

Rosing MT, Bird DK, Sleep NH, Bjerrum CJ (2010) No climate paradox under the faint early Sun. Nature 464 (7289):744-747. doi:10.1038/nature08955

Sawaya MR, Cannon GC, Heinhorst S, Tanaka S, Williams EB, Yeates TO, Kerfeld CA (2006) The structure of β-carbonic anhydrase from the carboxysomal shell reveals a distinct subclass with one active site for the price of two. Journal of Biological Chemistry 281 (11):7546-7555

Schaab C, Geiger T, Stoehr G, Cox J, Mann M (2012) Analysis of High Accuracy, Quantitative Proteomics Data in the MaxQB Database. Molecular & Cellular Proteomics : MCP 11 (3):M111.014068. doi:10.1074/mcp.M111.014068

Schägger H, von Jagow G (1991) Blue native electrophoresis for isolation of membrane protein complexes in enzymatically active form. Analytical biochemistry 199 (2):223-231

Schlegel S, Löfblom J, Lee CP, Hjelm A, Klepsch M, Strous M, Drew D, Slotboom DJ, de Gier JW (2012) Optimizing membrane protein overexpression in the Escherichia coli strain Lemo21 (DE3). Journal of molecular biology 423 (4):648-659

Schuergers N, Mullineaux CW, Wilde A (2017) Cyanobacteria in motion. Current opinion in plant biology 37:109-115

Schuurmans RM, Schuurmans JM, Bekker M, Kromkamp JC, Matthijs HC, Hellingwerf KJ (2014) The redox potential of the plastoquinone pool of the cyanobacterium *Synechocystis* species strain PCC 6803 is under strict homeostatic control. Plant physiology 165 (1):463-475. doi:10.1104/pp.114.237313

Schwanhäusser B, Busse D, Li N, Dittmar G, Schuchhardt J, Wolf J, Chen W, Selbach M (2011) Global quantification of mammalian gene expression control. Nature 473 (7347):337

Shibata M, Katoh H, Sonoda M, Ohkawa H, Shimoyama M, Fukuzawa H, Kaplan A, Ogawa T (2002) Genes essential to sodium-dependent bicarbonate transport in cyanobacteria: function and phylogenetic analysis. J Biol Chem 277 (21):18658-18664.

Shibata M, Ohkawa H, Kaneko T, Fukuzawa H, Tabata S, Kaplan A, Ogawa T (2001) Distinct constitutive and low-CO_2-induced CO_2 uptake systems in cyanobacteria: genes involved and their phylogenetic relationship with homologous genes in other organisms. Proc Natl Acad Sci U S A 98 (20):11789-11794.

So AKC, Espie GS, Williams EB, Shively JM, Heinhorst S, Cannon GC (2004) A novel evolutionary lineage of carbonic anhydrase (ε class) is a component of the carboxysome shell. Journal of bacteriology 186 (3):623-630

Soo RM, Hemp J, Parks DH, Fischer WW, Hugenholtz P (2017) On the origins of oxygenic photosynthesis and aerobic respiration in Cyanobacteria. Science 355 (6332):1436-1440

Soo RM, Skennerton CT, Sekiguchi Y, Imelfort M, Paech SJ, Dennis PG, Steen JA, Parks DH, Tyson GW, Hugenholtz P (2014) An expanded genomic representation of the phylum Cyanobacteria. Genome biology and evolution 6 (5):1031-1045

Stanier RY, Bazine GC (1977) Phototrophic Prokaryotes: The Cyanobacteria. Annual Review of Microbiology 31 (1):225-274. doi:doi:10.1146/annurev.mi.31.100177.001301

Strand DD, Fisher N, Kramer DM (2017) The higher plant plastid NAD(P)H dehydrogenase-like complex (NDH) is a high efficiency proton pump that increases ATP production by cyclic electron flow. Journal of Biological Chemistry 292 (28):11850-11860. doi:10.1074/jbc.M116.770792

Supuran CT (2008) Carbonic anhydrases: novel therapeutic applications for inhibitors and activators. Nature reviews Drug discovery 7 (2):168

Supuran CT (2016) Structure and function of carbonic anhydrases. Biochemical Journal 473 (14):2023-2032

Tabita RF, Satagopan S, Hanson TE, Kreel NE, Scott SS (2008) Distinct form I, II, III, and IV Rubisco proteins from the three kingdoms of life provide clues about Rubisco evolution and structure/function relationships. Journal of experimental botany 59 (7):1515-1524. doi:10.1093/jxb/erm361

Tchernov D, Helman Y, Keren N, Luz B, Ohad I, Reinhold L, Ogawa T, Kaplan A (2001) Passive entry of CO_2 and its energy-dependent intracellular conversion to HCO_3^- in cyanobacteria are driven by a photosystem I-generated deltamuH^+. J Biol Chem 276 (26):23450-23455.

Thomas JC, Ughy B, Lagoutte B, Ajlani G (2006) A second isoform of the ferredoxin : NADP oxidoreductase generated by an in-frame initiation of translation. PNAS 103 (48):18368-18373. doi:10.1073/pnas.0607718103

Tsinoremas NF, Kutach AK, Strayer CA, Golden SS (1994) Efficient gene transfer in *Synechococcus* sp. strains PCC 7942 and PCC 6301 by interspecies conjugation and chromosomal recombination. Journal of Bacteriology 176 (21):6764-6768

Tyanova S, Temu T, Sinitcyn P, Carlson A, Hein MY, Geiger T, Mann M, Cox J (2016) The Perseus computational platform for comprehensive analysis of (prote) omics data. Nature methods 13 (9):731

Tyrrell PN, Kandasamy RA, Crotty CM, Espie GS (1996) Ethoxyzolamide Differentially Inhibits CO_2 Uptake and Na^+-Independent and Na^+-Dependent HCO_3^- Uptake in the Cyanobacterium *Synechococcus* sp. UTEX 625. Plant Physiol 112 (1):79-88. doi:10.1104/pp.112.1.79

Umena Y, Kawakami K, Shen JR, Kamiya N (2011) Crystal structure of oxygen-evolving photosystem II at a resolution of 1.9 Ångstrom. Nature 473 (7345):55-U65. doi:10.1038/nature09913

Voruganti S, LaCroix JC, Rogers CN, Rogers J, Matts RL, Hartson SD (2013) The anticancer drug AUY922 generates a proteomics fingerprint that is highly conserved among structurally diverse Hsp90 inhibitors. Journal of proteome research 12 (8):3697-3706

Wagner S, Klepsch MM, Schlegel S, Appel A, Draheim R, Tarry M, Högbom M, Van Wijk KJ, Slotboom DJ, Persson JO (2008) Tuning *Escherichia coli* for membrane protein overexpression. Proceedings of the National Academy of Sciences 105 (38):14371-14376

Waheed A, Okuyama T, Heyduk T, Sly WS (1996) Carbonic anhydrase IV: purification of a secretory form of the recombinant human enzyme and identification of the positions and importance of its disulfide bonds. Archives of biochemistry and biophysics 333 (2):432-438

Wang HL, Postier BL, Burnap RL (2004) Alterations in global patterns of gene expression in *Synechocystis* sp. PCC 6803 in response to inorganic carbon limitation and the inactivation of ndhR, a LysR family regulator. J Biol Chem 279 (7):5739-5751

Waterhouse AM, Procter JB, Martin DMA, Clamp M, Barton GJ (2009) Jalview Version 2—a multiple sequence alignment editor and analysis workbench. Bioinformatics 25 (9):1189-1191

Wenk SO, Schneider D, Boronowsky U, Jager C, Klughammer C, de Weerd FL, van Roon H, Vermaas WF, Dekker JP, Rogner M (2005) Functional implications of pigments bound to a cyanobacterial cytochrome b6f complex. Febs J 272 (2):582-592

Woodger FJ, Badger MR, Price GD (2005) Sensing of inorganic carbon limitation in *Synechococcus* PCC7942 is correlated with the size of the internal inorganic carbon pool and involves oxygen. Plant Physiology 139 (4):1959-1969. doi:10.1104/pp.105.069146

Woodger FJ, Bryant DA, Price GD (2007) Transcriptional regulation of the CO_2-concentrating mechanism in a euryhaline, coastal marine cyanobacterium, *Synechococcus* sp. Strain PCC 7002: role of NdhR/CcmR. J Bacteriol 189 (9):3335-3347. doi:JB.01745-06 [pii]10.1128/JB.01745-06

Xu M, Ogawa T, Pakrasi HB, Mi H (2008) Identification and localization of the CupB protein involved in constitutive CO_2 uptake in the cyanobacterium, *Synechocystis* sp. strain PCC 6803. Plant Cell Physiol 49 (6):994-997. doi:pcn074 [pii] 10.1093/pcp/pcn074

Yachdav G, Kloppmann E, Kajan L, Hecht M, Goldberg T, Hamp T, Hönigschmid P, Schafferhans A, Roos M, Bernhofer M (2014) PredictProtein—an open resource for online prediction of protein structural and functional features. Nucleic acids research 42 (W1):W337-W343

Yeates TO, Crowley CS, Tanaka S (2010) Bacterial microcompartment organelles: protein shell structure and evolution. Annual review of biophysics. doi:10.1146/annurev.biophys.093008.131418

Yeates TO, Kerfeld CA, Heinhorst S, Cannon GC, Shively JM (2008) Protein-based organelles in bacteria: carboxysomes and related microcompartments. Nature Reviews Microbiology 6 (9):681

Zawar P, Javalkote V, Burnap R, Mahulikar P, Puranik P (2016) CO 2 capture using limestone for cultivation of the freshwater microalga *Chlorella sorokiniana* PAZ and the cyanobacterium *Arthrospira* sp. VSJ. Bioresource technology 221:498-509

Zhang P, Battchikova N, Jansen T, Appel J, Ogawa T, Aro EM (2004) Expression and functional roles of the two distinct NDH-1 complexes and the carbon acquisition complex NdhD3/NdhF3/CupA/Sll1735 in *Synechocystis* sp PCC 6803. Plant Cell 16 (12):3326-3340

Zhang P, Battchikova N, Paakkarinen V, Katoh H, Iwai M, Ikeuchi M, Pakrasi HB, Ogawa T, Aro EM (2005) Isolation, subunit composition and interaction of the NDH-1 complexes from *Thermosynechococcus elongatus* BP-1. Biochem J 390 (Pt 2):513-520

Zhu XG, Long SP, Ort DR (2010) Improving photosynthetic efficiency for greater yield. Annual review of plant biology 61:235-261

Zickermann V, Wirth C, Nasiri H, Siegmund K, Schwalbe H, Hunte C, Brandt U (2015) Mechanistic insight from the crystal structure of mitochondrial complex I. Science 347 (6217):44-49. doi:10.1126/science.1259859

APPENDICES

Cyclic electron flow on different carbon sink mutants

Additional to the study discussed in this dissertation, during my time as a PhD and research assistant I collaborated in several side projects. A fruitful one was related to understanding the impacts of carbon sink mutations in *Synechocystis* 6803 photosynthetic performance. Specifically, my efforts were in evaluating changes in cyclic electron transport in the mutants under HC and LC growth conditions, an area of great interest by poorly understood. The results can be found on the published manuscript (Holland *et al.*, 2016). Furthermore, the collaborative study also helped to understand basic metabolic responses, as the importance of glycogen in balancing energetic metabolism in cyanobacteria (Cano *et al.*, 2018). In conclusion, these studies showed that although there is a great potential of manipulating cyanobacteria in an effort of increasing photosynthetic yield, later to be redirected into high-value products and CO_2 mitigation projects, it is important to consider the energetic burden on the cell in search of optimum rates. Summaries of these works are presented here.

Abstract (Holland *et al.*, 2016): Genetic engineering of photosynthetic organisms typically redirects native metabolism towards desirable products, which thereby represent new metabolic sinks. There is limited information on how these modifications impact the evolved mechanisms of photosynthetic energy metabolism and cellular growth.

Two engineered strains of *Synechocystis* sp. PCC 6803 with altered carbon sink capacity were assayed for their photosynthetic and CO_2 concentrating mechanism properties in conditions of high and low inorganic carbon (C_i) availability. In the ΔglgC mutant, glycogen cannot be synthesized and a carbon sink pathway has been effectively removed. The JU547 strain has been engineered by integration of the *Pseudomonas syringae* ethylene forming enzyme and provides a new sink. When cultured under high carbon conditions, ΔglgC displayed diminished photochemical efficiency, a more reduced NADPH pool, delayed initiation of the Calvin-Benson-Bassham cycle, and impairment of linear and cyclic electron flows. It also exhibited a large decrease in photochemical quenching indicative of the accumulation of Q_A^-, normally associated with a reduced PQ pool, but appears instead to be the result of an un- defined dissipative mechanism to spill excess energy. In the case of carbon sink integration, JU547 displayed slightly more oxidized PQ and NADPH pools and increased rates of cyclic electron flow and an enhanced demand for inorganic carbon as suggested by increase in the expression of the bicarbonate transporter, SbtA. Overall, the results highlight the importance of the native regulatory network of autotrophic metabolism in governing photosynthetic performance and provide cogent examples of both predicable and difficult to predict phenotypic consequences upon installation of new pathways in autotrophs.

Abstract (Cano *et al.*, 2018): There is a lack of systematic study on the regulation of high energy metabolites such as ATP levels that drive the metabolism in living organisms. Using light as the energy input, we found that the energy charge (ratio of ATP over ADP+ATP) in the cyanobacterium *Synechocystis* 6803 vary through different growth stages, with a peak upon entry into the rapid growth phase, as well as a positive correlation with light intensity. In contrast, a mutant that can no longer synthesize the main carbon storage compound glycogen showed higher energy charge. The overflow of organic acids in this mutant under nitrogen depletion could also be triggered under high light in nitrogen-replete conditions, with an energy-input level dependency. These findings suggest that energy charge in cyanobacteria is tightly linked to growth and carbon partition, and that energy management is of key significance for their application as photosynthetic carbon dioxide assimilating cell factories.

VITA

Juliana Artier

Candidate for the Degree of

Doctor of Philosophy

Thesis: STRUCTURE-FUNCTION STUDIES OF THE CO_2 UPTAKE COMPLEX IN CYANOBACTERIA

Major Field: MICROBIOLOGY AND MOLECULAR GENETICS

Biographical:

Education:

Completed the requirements for the Doctor of Philosophy in Microbiology & Molecular Biology at Oklahoma State University, Stillwater, Oklahoma in July, 2018.

Completed the requirements for the Master of Science in Genetics and Evolution at Universidade Federal de São Carlos, SP, Brazil in 2010.

Completed the requirements for the Bachelor of Science in Biological Science at Universidade Federal de São Carlos, SP, Brazil in 2008.